The Institute of Paper Chemistry

Appleton, Wisconsin

Doctor's Dissertation

Alkaline Degradation of Amylose: A Kinetic Model

Daniel J. Geddes

June, 1987

ALKALINE DEGRADATION OF AMYLOSE: A KINETIC MODEL

A thesis submitted by

Daniel J. Geddes

B.S. 1980, Western Michigan University

M.S. 1983, Lawrence University

in partial fulfillment of the requirements
of The Institute of Paper Chemistry
for the degree of Doctor of Philosophy
from Lawrence University
Appleton, Wisconsin

June, 1987

TABLE OF CONTENTS

SUMMARY

Amylose has frequently been used as the substrate in studies of alkaline polysaccharide degradation because, unlike other polysaccharides such as cellulose, it is soluble in the reaction medium. Under anaerobic conditions, amylose is degraded by the random cleavage of glucosidic linkages (chain cleavage) and by the stepwise elimination of monomer units from the reducing ends of molecules (peeling). Peeling is important even at room temperature, and can continue to degrade a given molecule until halted by a competing reaction (stopping) or until the molecule is degraded in its entirety (complete peeling). Chain cleavage has widely been stated to be important only at high temperatures (> 140°C), based primarily on cellulose degradation studies, where physical structure plays a role in limiting degradation, or on simple model compound studies, which may not adequately mimic polymer reactions. There is an interaction between the two modes of degradation, because each cleavage reaction opens up a new reducing end group and therefore enhances peeling.

Because of the complex nature of the system, previous studies of amylose degradation have taken overly simplistic views of the process in order to interpret experimental results. The role that complete peeling plays in destroying molecules and reducing ends has either been neglected or overemphasized, and the possibility of low temperature chain cleavage has been overlooked. Past researchers have relied almost exclusively on simple yield loss measurements to follow degradation, and yield data alone do not give a complete picture of the changes that occur.

In the present study, mathematical models were developed to aid in the interpretation of experimental results without resorting to oversimplification. One model, which was based on probabilistic arguments, was used to predict how degradation by peeling should affect amylose molecular weight distributions

(MWDs). Experimentally determined MWDs did not agree with the predictions of the model, in a way that suggested low temperature cleavage was responsible for the differences.

To test for the possibility of low temperature cleavage, the degradation of a high molecular weight amylose in 1M sodium hydroxide was followed at 60, 80, and 100°C by measuring its MWD, yield, and end group composition as a function of time. At all temperatures, significant formation of new reducing end groups and amylose molecules was detected. The results can be explained only by cleavage. The fact that cleavage occurs at low temperatures in amylose but not in crystalline cellulose indicates the importance physical structure has in limiting cellulose degradation.

A second mathematical model was developed to provide insights into how amylose properties (yield, $\overline{DP}_N$, and end group composition) should change over a wide range of peeling, stopping, and cleavage rates. Comparison of experimental observations to model simulations allowed cleavage rates to be estimated. Amylose was found to cleave three orders of magnitude faster per glucosidic linkage than simple disaccharides. This finding reveals the limitations of using small model compounds to study polymer reactions.

The ratio of the peeling rate to the stopping rate was found to increase with increasing temperature. Previous studies have disagreed on how the ratio changes with temperature.

Simulations using the models revealed that complete peeling plays an important, but not dominant, role in degradation. For an amylose with a typical starting MWD, some, but not all, of the molecules will be destroyed by complete

peeling. Under some circumstances, preferential loss of short molecules due to complete peeling can actually cause the average molecular weight to increase during degradation.

INTRODUCTION

One shortcoming of alkaline pulping processes is the loss of pulp strength and yield that occurs as a result of polysaccharide degradation. Interest within the pulp and paper industry in limiting the extent of degradation has lead to extensive study of the reactions of carbohydrates in aqueous alkali. The mechanisms of degradation are understood in general terms, based largely on the study of simple model compounds, such as mono- and disaccharides and their derivatives. There currently exists a need for further research, directed toward applying the insights gained from model compounds to the examination of the degradation of actual carbohydrate polymers.

Undoubtedly, the polysaccharide of greatest importance in papermaking is cellulose. However, there are complications associated with studying cellulose degradation directly. Cellulose is insoluble in aqueous alkali and possesses a variable degree of crystallinity. The degradation of cellulose is therefore controlled not only by the chemical reactions that occur, but also by physical effects such as the rate of diffusion of reagents into and out of the solid cellulose and the variable accessibility of the reactive sites. In order to avoid these complicating physical effects, researchers interested in studying the chemistry of degradation have resorted to using amylose as a polymeric model for cellulose.

Amylose has a structure that is very similar to cellulose. Both compounds are linear polymers of glucose. As shown in Fig. 1, the difference between the two polysaccharides is in the configuration of the glucosidic bonds. In amylose these linkages have the α-(1-4) configuration, while in cellulose they have the β-(1-4) configuration. Unlike cellulose, amylose is soluble in aqueous alkali.

Its degradation therefore proceeds by a series of homogeneous chemical reactions, and is not affected by physical structure.

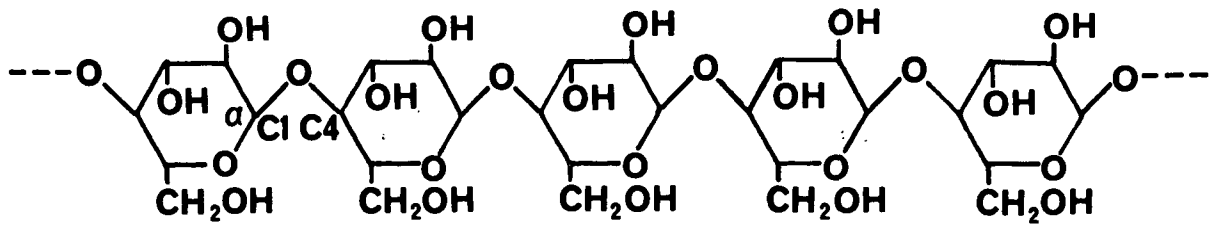

AMYLOSE

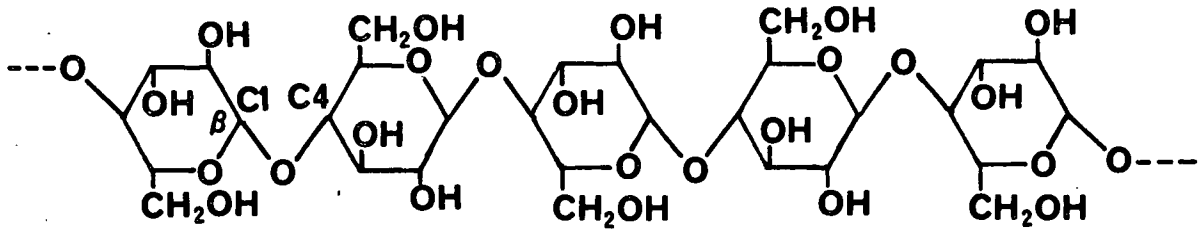

CELLULOSE

Figure 1. Structural formulas of amylose and cellulose.

ALKALINE REACTIONS OF POLYSACCHARIDES

It is generally accepted that polysaccharides are degraded via two pathways in aqueous alkali under anaerobic conditions.[1-4] These are the "peeling" reaction and the "random chain cleavage" reaction. During the alkaline pulping of wood, peeling is responsible for causing undesirable yield losses, and cleavage is responsible for losses in pulp viscosity and strength. The overall degradation process for amylose is shown schematically in Fig. 2.

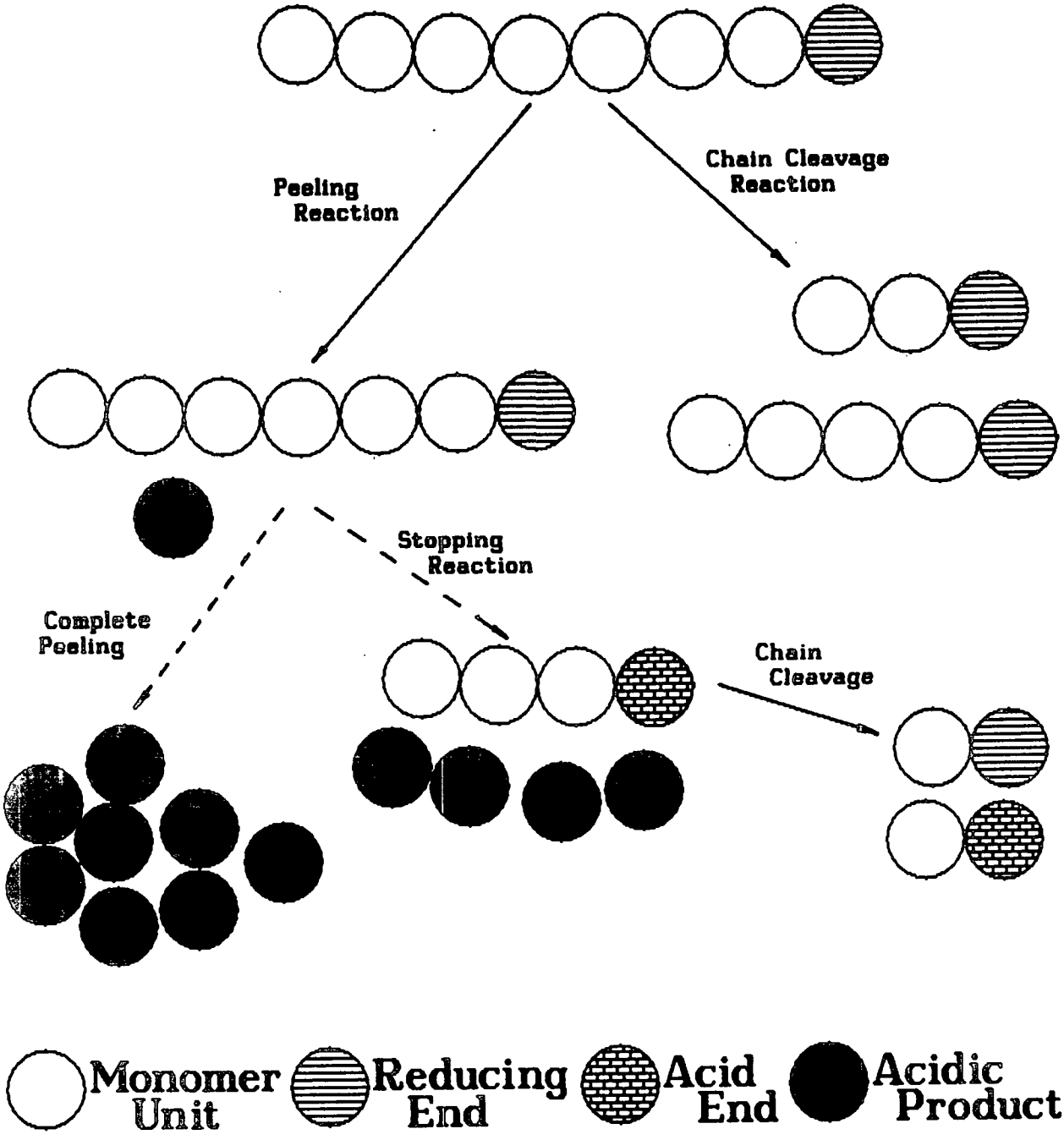

Figure 2. Pathways of amylose degradation in anaerobic alkali.

The peeling reaction occurs at the reducing end of a molecule and eliminates the anhydroglucose unit at that end, converting it into an isosaccharinic acid degradation product. In effect, this destroys a monomer unit, and it is this destruction that primarily causes the yield loss. Besides the isosaccharinic acid, the other product of each peeling reaction is a polysaccharide chain shortened by one monomer unit. Because this shorter chain retains a reducing end, peeling can occur again and again, eliminating successive monomer units, until the process is terminated in one of two ways.

The first way peeling can be terminated is by the "stopping" reaction. Stopping competes with peeling at the reducing end, and transforms the reducing end into a stable metasaccharinic acid end group. The acid end is not reactive toward peeling, and so it stabilizes the remaining amylose chain against further degradation.

The second way the peeling process can be terminated is by "complete peeling." Complete peeling occurs when the peeling reaction makes its way through the entire amylose chain before a stopping reaction takes place, completely degrading all of the anhydroglucose units and destroying the reducing end.

The peeling reaction follows first order kinetics with respect to reducing ends in the presence of excess base,[5,6] and it is reasonable to assume that stopping does as well. Peeling occurs significantly even at room temperature,[7,8] but there is some disagreement in the literature as to whether the ratio of the peeling rate to the stopping rate increases or decreases with increasing temperature. Several studies[9-11] show a decrease in the ratio. Most of these were investigations of cellulose degradation, where physical structure is known to exert an influence.[9,11,12] Other studies[13-16] claim that the ratio increases as temperature is increased.

The random chain cleavage reaction causes the hydrolytic scission of glycosidic linkages. Each occurrence of cleavage forms two short molecules from one long one and opens up one new reducing end which is subject to peeling. Even in the case of a molecule that has undergone the stopping reaction, peeling can be reinitiated in this way. This interaction between cleavage and peeling can make it difficult to interpret the results of a degradation experiment.

The cleavage reaction has been observed to follow first order kinetics with respect to glucosidic bonds.[17] Cleavage is widely believed to occur only at high temperatures. Many authors[2,3,10,18] list a temperature of about 140°C as the minimum temperature for the onset of cleavage. However, this figure has been arrived at based on cellulose degradation studies,[2,3,10] where physical structure plays a role, or based on simple model compound studies,[18] where reaction rates may not extrapolate well to polysaccharide degradation. A recent study by Gentile et al.[9] detected some cleavage in an amorphous hydrocellulose at temperatures as low as 60°C, demonstrating that when the effects of physical structure are reduced, low temperature cleavage becomes a possibility.

PREVIOUS STUDIES OF AMYLOSE DEGRADATION

Several previous studies of amylose degradation are contained in the literature.[13,14,16,19-21] All of these studies were conducted at temperatures below 120°C, and so cleavage was assumed not to occur. Each of the studies will be discussed in this section.

Machell and Richards[21] reacted amylose with 0.5M sodium hydroxide at 100°C and observed behavior consistent with degradation by the peeling and stopping reactions. The soluble degradation products were analyzed by paper chromatography and α- and β-D-glucoisosaccharinic acids were identified. The end groups of the

alkali stable polymer that remained after degradation were tentatively identified as α- and β-D-metasaccharinic acid units by a similar technique. Yield loss was followed by measuring the optical absorbance of the complex formed between the undegraded amylose and iodine. After 20 hours of reaction, the rate of yield loss was very low. The degree of polymerization (DP) of the starting material was estimated to be 450, but no attempt was made to track the DP of the amylose over the course of degradation.

Lai and Sarkanen[14] are the first researchers to actually report rate constants for the peeling and stopping reactions of amylose. They examined the degradation of amylose at temperatures ranging from 56 to 100°C in 0.01-5M sodium hydroxide, measuring yield loss as a function of reaction time. Unfortunately, the equations[10] used to calculate rate constants from the yield loss data suffer from a questionable underlying assumption. The equations were derived by assuming that the number of reducing end groups is unaffected by the peeling reaction. This is equivalent to assuming that molecules never peel completely. Surprisingly, the same study showed that at low alkali concentrations, the ratio of the peeling rate to the stopping rate can be great enough to result in the total degradation of the polymer, presumably by complete peeling. Regardless of the ratio of the peeling to the stopping rate, it seems likely that any amylose prepared from natural sources will contain at least some molecules short enough to peel completely. Because of the apparent contradiction, and because the effect of complete peeling was not thoroughly evaluated, the rate constants reported in this work must be viewed with some degree of skepticism.

In contrast to many cellulose degradation studies, Lai and Sarkanen[14] found that the ratio of the peeling rate to the stopping rate increased with temperature. The initial number average DP ($\overline{DP}_N$) of the starting material was reported to be 820, based on a reducing end group analysis. Neither DP or reducing ends were measured during degradation.

Ziderman and Bel-Ayche[13,19,20,22] have proposed a modification to the classical view of polysaccharide degradation, and tested their hypothesis using amylose as the substrate. They speculated that the ionization and peeling of the original reducing end is slow, while the peeling of subsequent units proceeds at least 1000 times as rapidly. Under the hypothesis, when a given molecule starts to peel it will either rapidly be totally degraded by complete peeling or it will undergo the stopping reaction. Uninitiated molecules, in the meantime, would undergo no reaction at all.

The reason given for the tremendous difference in rate between the peeling of the first and subsequent units is that initiation of peeling requires ionization of the anomeric hydroxyl, while the glucosidic oxygen which is eliminated in each subsequent step is already ionized. It is known, however, that proton exchange occurs rapidly at the anomeric hydroxyl, and so there is no justification to presuming the initiation of peeling to be slower than its propagation.

The kinetic equations of Ziderman and Bel-Ayche[13] account for complete peeling by defining it as a separate degradation process, first order with respect to reducing end groups. The equations contain rate constants for the peeling reaction, the stopping reaction, and complete peeling. Actually, complete peeling is a simple extension of the peeling reaction that occurs when the last remaining monomer unit is converted to degradation products. The need

for a separate rate constant is not at all clear. It is also interesting to note that the kinetic equations are not even consistent with the hypothesis under which they were developed, because they make no distinction between the rate of reaction of the initial reducing end and subsequently generated reducing ends.

Because Ziderman and Bel-Ayche hold that once a molecule begins to peel it almost always peels completely, they maintain that molecules that degrade are simply removed from the molecular weight distribution (MWD) and so the average molecular weight does not change as a result of degradation. Their initial experiments in support of this view measured only yield loss, and the effect of degradation on molecular weight was not examined. However, later work by Arbin et al.[16] showed conclusively that the average molecular weight and the MWD do change during degradation. Indeed, in one of their later studies,[19] Ziderman and Bel-Ayche themselves report that the average molecular weight of amylose can change as a result of degradation. By measuring the viscosity of amylose solutions before and after degradation, they found that the average molecular weight was reduced drastically for an amylose that had an initial $\overline{DP}_N$ of about 1000, but that the molecular weight of a hydroamylose with an initial $\overline{DP}_N$ of 120 was relatively unaffected.

Arbin et al.[16] studied alkaline amylose degradation under both oxidative and anaerobic conditions, with and without the addition of the pulping catalyst anthraquinone. Amylose yield and MWDs were measured over the course of degradation reactions conducted at 80 and 100°C. Under anaerobic conditions without anthraquinone, the yield leveled out at a higher value at 60 than at 100°. By multiplying the leveling-off yield loss by the initial $\overline{DP}_N$ (which was 630),

Arbin calculated that at 60° an average of 290 monomer units were lost per molecule before stopping occurred, and at 100° an average of 400 monomer units were lost. The ratio of the peeling rate to the stopping rate was therefore taken to be 290 at the lower temperature and 400 at the higher temperature. This reasoning neglects the complete peeling process, however, because it assumes that degradation by peeling is always terminated by a stopping reaction.

The shift in MWD found by Arbin for his anaerobic reaction at 80°C are shown in Fig. 3. Over the course of the reaction, the MWD curves were found to retain their shape while shifting as a whole toward lower molecular weights. No theoretical prediction of the effect of peeling and stopping on the MWD of amylose was made. Without such a prediction, it can not be said with certainty whether the observed shifts are consistent with degradation solely by peeling and stopping. Early in the current thesis investigation, an attempt was made to predict, at least approximately, how degradation by peeling and stopping should affect the MWD of amylose. This approximate treatment is covered in the next section to provide background information and to demonstrate the usefulness of mathematical predictions in interpreting the results of polymer degradation experiments. A more thorough treatment of the effects of peeling and stopping is presented in the Results and Discussion section.

Prediction of MWD Shifts Based on a Constant Peeling Length

Under the traditional view of peeling and stopping, the number of monomer units peeled from a molecule before it undergoes the stopping reaction (its "peeling length") is determined by the ratio of the peeling rate (k_p) to the stopping rate (k_s). A simplified prediction of the effect of degradation on the MWD can therefore be made by assuming that the peeling length of each molecule is exactly the same, having a value equal to k_p/k_s. After subtracting this

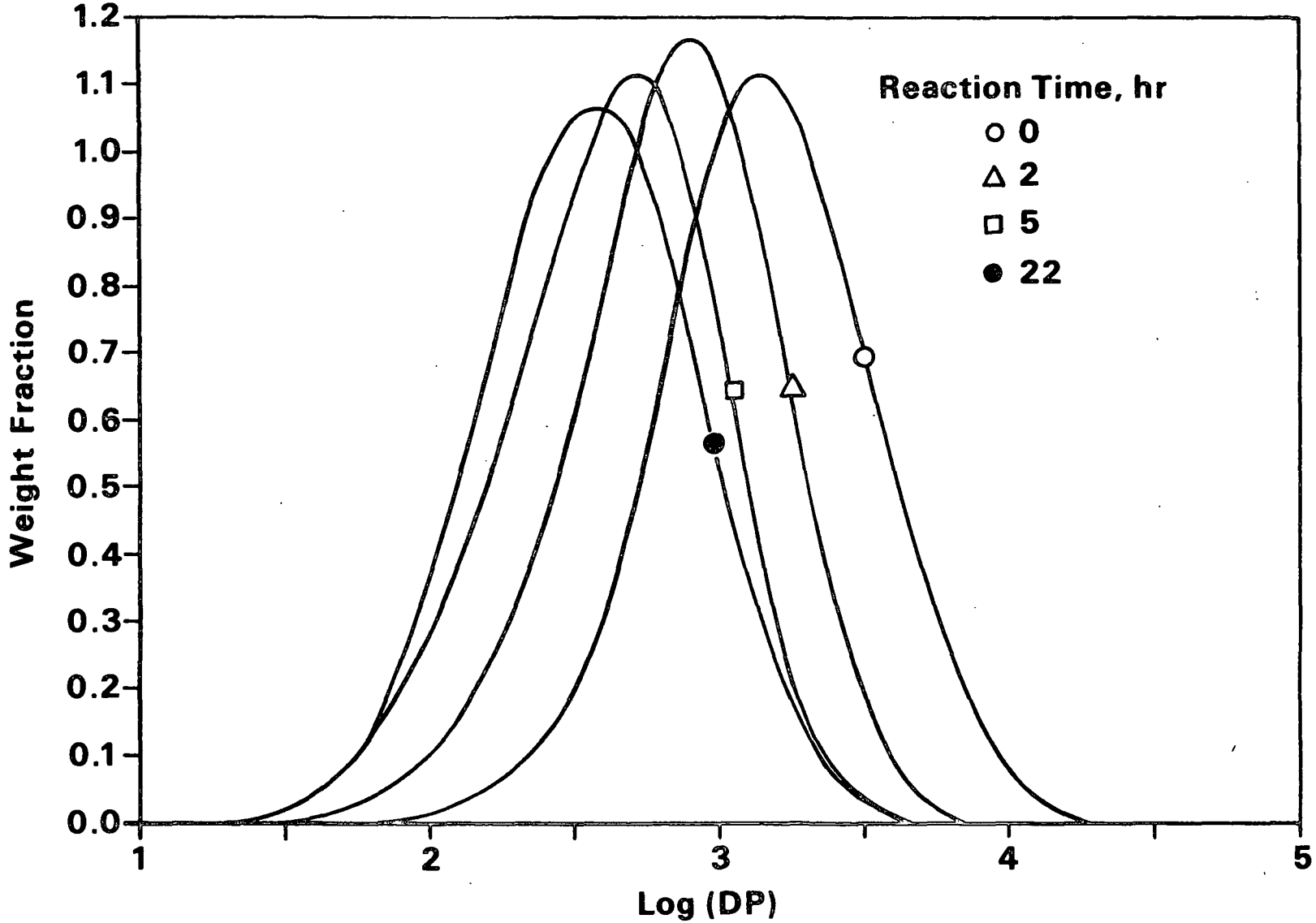

Figure 3. Change in amylose MWD observed by Arbin[16] during degradation at 80°C in 1M sodium hydroxide.

peeling length from each DP present in the initial MWD, the material that remains is the predicted final MWD. Any molecules with a starting length shorter than the peeling length are considered to be completely peeled, and do not appear in the final distribution.

The calculation was performed for $k_p/k_s = 300$, which was close to the value of 290 estimated by Arbin for 80°C. As a starting point for the calculation, a lognormal MWD with the same number and weight average DPs as Arbin's starting material was used. Before performing the subtractions, this distribution was first converted to a number fraction versus linear DP scaling according to the procedure outlined in Appendix I. When the calculation was complete, the resulting distribution was converted back to a weight fraction versus logarithm of DP format.

The initial MWD and the predicted final MWD are shown in Fig. 4. Surprisingly, the calculation predicts that the peak of the MWD should actually shift toward higher molecular weights. This can happen because there is a preferential loss of low DP chains due to complete peeling. In effect, the short chains are destroyed and removed from the MWD, leaving behind the longer chains. The average DP thus increases, according to the calculation.

MWD curves are usually compared after normalizing them so that the area contained by the curves is equal to unity. This is how the MWDs are presented in Fig. 4. The appearance of such plots can be confusing, because they seem to imply that long molecules are formed during degradation. Actually, this is not the case, as demonstrated by Fig. 5. Figure 5 shows the same MWD curves, but the area under the final MWD curve has been adjusted to reflect the yield loss that occurs. On this basis, the final curve is never higher than the initial curve.

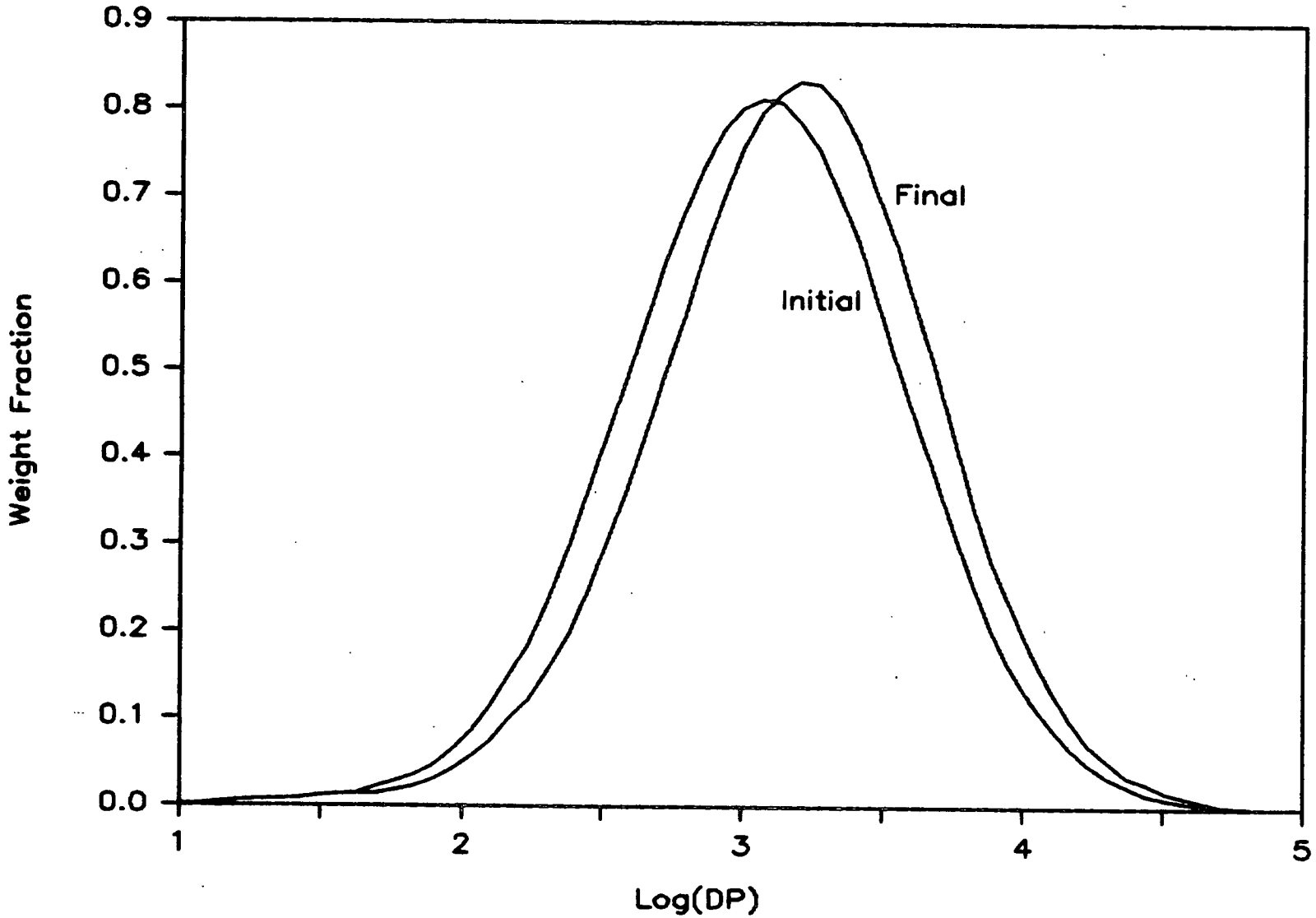

Figure 4. Change in amylose MWD predicted by constant peeling length calculation (curves have been normalized to a constant area).

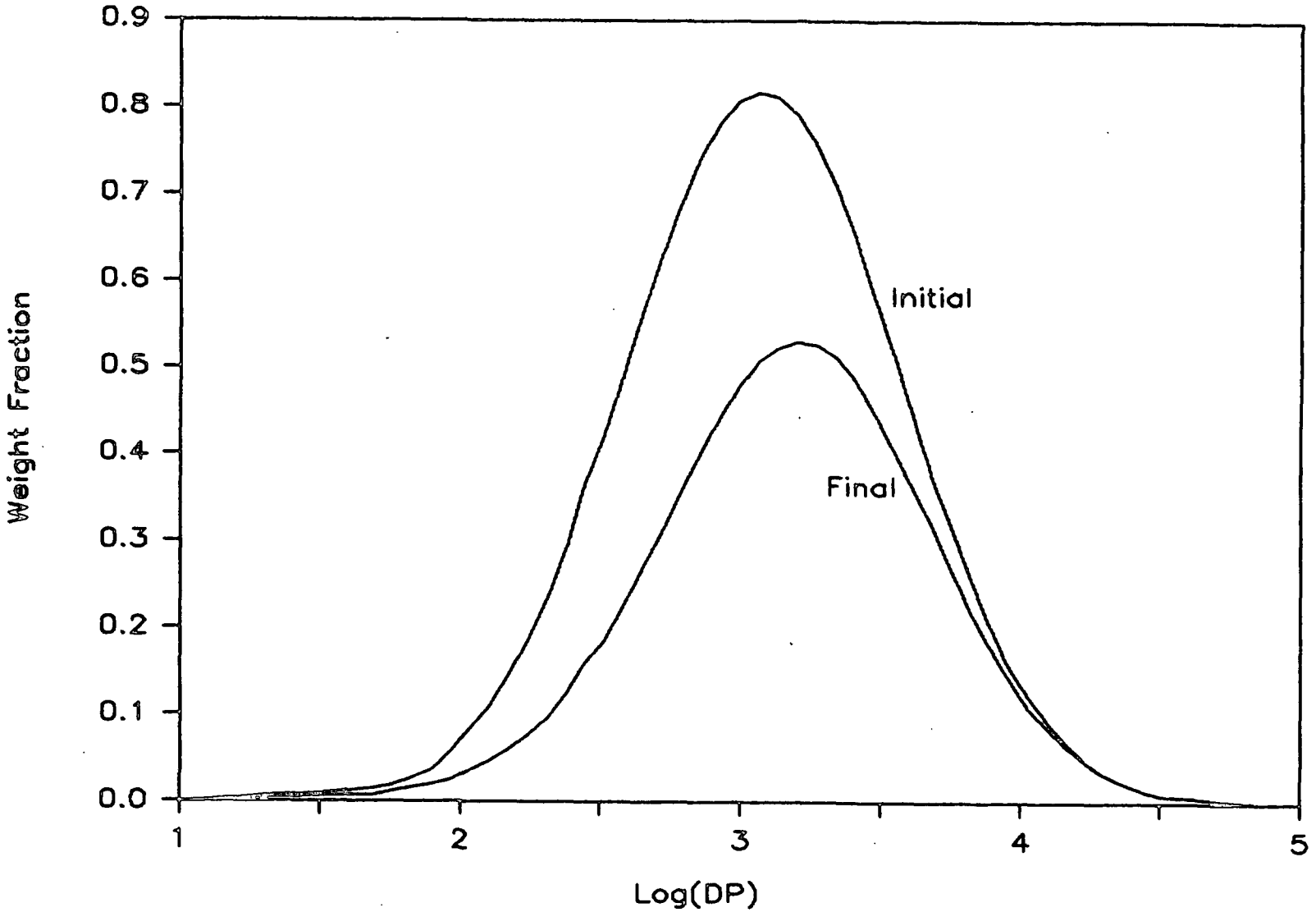

Figure 5. Change in amylose MWD predicted by constant peeling length calculation (final MWD has not been normalized, in order to show the effect of yield loss).

The fact that, in contrast to this prediction, Arbin[16] observed a marked decrease in average DP during degradation suggests that other mechanisms of degradation were active in his experiments. A likely candidate is low temperature chain cleavage, beause the chain cleavage reaction does act to reduce the DP. Because previous studies[13,14,16,19-21] have relied almost exclusively on yield loss measurements to track degradation, low temperature cleavage could have easily gone undetected. Yield loss measurements alone do not provide a detailed enough picture of the degradation process.

This relatively simple computational exercise serves to demonstrate the usefulness of mathematical modeling in the prediction of degradation results. Unlike the degradation of simple model compounds, the progress of polymer degradation cannot always be predicted intuitively. The complexity of polymer systems is best handled by actual numerical predictions based on the hypothesized pathways of degradation.

Contamination of Amyloses with α-(1,6) Branched Material

There is a growing amount of evidence in the literature[23-25] that amyloses prepared from natural sources tend to be contaminated with a material containing α-(1,6) glucosidic linkages in addition to α-(1,4) linkages. This branched polysaccharide may be present even if rigorous steps have been taken to purify the amylose and if the final product has a high "blue value." (The blue value[26] is a measure of the iodine binding capacity of the amylose, and is effective at distinguishing between amylose and the highly branched polysaccharide amylopectin.) Because the presence of α-(1,6) linkages can affect the course of degradation, any study of amylose degradation should include analysis of the substrate to show that it is free of branches. Previous workers[13,14,16,19-21]

have not carefully tested their substrates for branching. Some workers have even used commercial grades of amylose without further purification.[13,14,19]

Summary of the Shortcomings of Previous Amylose Degradation Studies

In formulating the objectives of the current investigation, it was useful to list the items found lacking in previous studies of the anaerobic alkaline degradation of amylose.

All of the previous studies were conducted at low temperatures, and so the chain cleavage reaction was ignored as a potential mechanism of degradation. In light of the poor agreement between the MWD results of Arbin et al.[16] and predictions based on a constant peeling length, and because Gentile et al.[9] observed cleavage at 60°C in amorphous cellulose, neglect of chain cleavage may not have been appropriate.

The progress of degradation was followed primarily by measuring yield loss, and yield measurements alone do not give a complete picture of the overall process. Equations used to convert yield measurements to rate constants have been based on overly simplified views of degradation which do not properly account for the role that complete peeling plays in limiting the number of reducing end groups.

The amyloses used as substrates in previous studies have not been well-characterized. They have not been analyzed for their content of α-(1,6) branch points, and, except for Arbin et al.,[16] previous researchers have not measured the starting molecular weight distribution of their substrates.

No one has attempted to use mathematical modeling techniques to make theoretical predictions of the effects of degradation, and this lack of predictions has caused significant trends in the data to be overlooked.

MATHEMATICAL MODELING OF POLYSACCHARIDE DEGRADATION

Mathematical modeling of amylose degradation is an alternative to calculation of rate constants that promised to aid in the interpretation of experimental results without resorting to oversimplified views of the process. The literature contains some reports of the modeling of the degradation of polysaccharides by ultrasonation,[27,28] acid hydrolysis,[27,29,30] enzymatic hydrolysis,[27] and shearing.[27] All of these are cleavage processes, and the models developed rely on the solution of large systems of differential equations. For a polymer having a wide molecular weight distribution and a high $\overline{DP}_N$, the size of the system of equations can be prohibitively large. This is especially true if the cleavage rate is assumed to depend on the position of the bond within a molecule and on the size of the molecule which contains it. A large part of the effort involved in developing models, therefore, is directed toward devising schemes to simplify the system and reduce the number of equations.

When a molecule is cleaved, its DP is reduced drastically. With one cleavage, its DP can be cut in half. For this reason, for a strictly cleavage-type process, changes in DP do not have to be resolved down to individual monomer units. Typically, large numbers of monomer units can be grouped into larger "quasi-monomeric" units[31] to limit the number of equations. While acceptable for a strictly cleave-type degradation, this brute force lumping approach will not work for degradation by the peeling reaction, because peeling changes the size of a molecule by just one monomer unit at a time.

Although concerned directly with the cleavage of polystyrene by ultrasonation, the work of Glynn et al.[32-34] suggests a second approach to modeling polysaccharide degradation. This method is based on probability theory instead of

on systems of differential equations. The result of each cleavage is determined by two probability distributions, one which gives the probability a given chain will cleave and another which gives the probability pieces of a given size will be formed from the cleavage.

Moo-Young and coworkers[35,36] have modeled the degradation of polysaccharides by exo- and endo-hydrolytic enzymes. The action of exoenzymes is somewhat analogous to the peeling reaction in that degradation occurs only at the end of the molecule. Unlike the peeling reaction, however, attack by exoenzymes is actually a depolymerization and not a degradation. This is because the polymer is converted into monomer or oligomer molecules, and these smaller molecules are not degraded further or destroyed. Endoenzymes operate similarly to the chain cleavage reaction, attacking glycosidic linkages at random throughout the polysaccharide chain. The models developed are based on the kinetics of enzyme action and include no process analogous to the stopping reaction, and so they cannot be used to describe alkaline amylose degradation.

The models of polymer degradation found in the literature cannot be applied to amylose degradation directly, but they can serve as guides to suggest possible approaches to developing new models.

THESIS OBJECTIVE

The objective of this thesis was to investigate the anaerobic alkaline degradation of a well-characterized carbohydrate polymer, using mathematical modeling to assist in the interpretation of the experimental results. The polysaccharide chosen for study was amylose, because it is soluble in aqueous alkali and so its degradation is not limited by its physical structure.

Previous studies have relied primarily on yield loss measurements to track amylose degradation. This investigation was intended to go beyond previous studies by following changes in end group composition and molecular weight distribution in addition to yield during the course of degradation.

Degradation experiments were conducted at several different temperatures. This allowed the effect of temperature on the relative importance of the principal degradation reactions (peeling, stopping, and random chain cleavage) to be evaluated. Particular emphasis was placed on determining whether random chain cleavage occurs at low temperatures, and how the ratio of the peeling rate to the stopping rate is influenced by temperature.

RESULTS AND DISCUSSION

APPROACH

The effect of degradation on complex polymer properties such as the shape and position of the molecular weight distribution and average DP is difficult to predict intuitively. Because of this, previous researchers have been forced to take overly simplistic views of the degradation process. In the current study, simple mathematical models were developed to objectively make such predictions without resorting to oversimplification.

Cleavage has often been assumed not to be an important degradation pathway at low temperatures. A model was developed based on probabilistic arguments to predict the overall shift in MWD that should occur if degradation proceeds only by peeling and stopping. The model results were compared to experimental results to determine whether the experimental observations could be explained without chain cleavage.

To handle the case where chain cleavage is assumed to occur, a more comprehensive model was developed. This model was used to gain insights into how the properties of amylose should behave over a wide range of rates of the principal degradation reactions.

The substrate amylose selected for degradation experiments was high in molecular weight, by design, to make it very sensitive to chain cleavage. Reactions were conducted at temperatures ranging from 60 to 100°C under anaerobic conditions in 1M sodium hydroxide. The amount of cleavage that occurred was characterized by monitoring changes in $\overline{DP}_N$ and total and reducing end group concentrations. The effects of the peeling and stopping reactions were

characterized through yield loss and end group measurements, and also through the $\overline{DP}_N$ data, by comparison to modeling predictions.

MODELING

Two separate mathematical models were developed to predict the effects of alkaline degradation on amylose. The first model uses probabilistic arguments to predict the changes that should occur in the absence of chain cleavage. Previous researchers have assumed cleavage to be insignificant at low temperatures, and this model provided a means to test whether their results are actually consistent with this view. The probabilistic model was also used to evaluate the importance of complete peeling in destroying amylose chains and reducing end groups.

The second model was developed to make predictions in the more comprehensive case where cleavage does play a role in degradation, in addition to peeling and stopping. This comprehensive model is based on the numerical solution of a system of differential equations, and was used to provide insights into how the course of degradation changes when the rates of the three reactions are varied.

Probabilistic Model of Peeling and Stopping

At low temperatures, the degradation of amylose has been assumed to proceed by the peeling and stopping reactions alone. If this is the case, eventually an equilibrium state will be reached when all remaining amylose chains have undergone the stopping reaction and are terminated by stable acidic end groups.

The number of monomer units peeled from an amylose chain (the "peeling length") is determined by the ratio of the first order rate constants for the peeling and stopping reactions, k_P and k_S. Higher ratios tend to cause more

units to peel per chain and lower ratios tend to cause fewer units to peel per chain. A very simple way of visualizing this process is to assume that the peeling length will always exactly equal k_p/k_s. This visualization formed the basis for the "constant peeling length" calculation used to reevaluate Arbin's MWD data which was presented in the Introduction section.

The effect of degradation on the number average DP depends on the total number of monomer units peeled and the number of molecules destroyed by complete peeling. Because the $\overline{DP}_N$ is the average number of monomer units per polymer chain, if the fraction of monomer units lost is greater than the fraction of molecules lost, the $\overline{DP}_N$ will decrease. If an equal percentage of monomers and molecules are destroyed, the $\overline{DP}_N$ will remain constant. Finally, if the fraction of molecules lost is greater than the fraction of monomer units lost, the $\overline{DP}_N$ will increase. The constant peeling length calculation predicted a preferential loss of low DP molecules, and this is equivalent to the loss of molecules being proportionately larger than the loss of monomer units. Either line of reasoning may be used to explain why an increase in $\overline{DP}_N$ was predicted by the calculation.

Actually, it is unlikely that every amylose molecule would lose exactly the same number of monomer units. Instead, there would be some distribution of peeling lengths about the average. Probability theory can be used to mathematically describe this distribution.

In probability theory, a simple experiment that can have only two possible outcomes is called a Bernoulli trial.[37] One possible outcome is termed a "success" and the other a "failure." The probability of success is the same for all trials, and is denoted by the symbol p. The probability of failure is 1-p, and also is constant from trial to trial. The outcome of a given trial is

assumed not to depend on any other trial. An example of a Bernoulli trial is one toss of a fair coin. The possible outcome of this trial are "heads" or "tails," either of which can arbitrarily be viewed as the success.

When multiple Bernoulli trials are combined into more complex probabilistic experiments, various probability distributions can be used to predict the probability of different outcomes. The binomial distribution is perhaps the most commonly encountered. The binomial distribution is used to predict the fraction of successes that will occur in an experiment consisting of a fixed number of trials. For example, the probability of scoring 60 "heads" in 100 tosses of a coin can be determined from the binomial distribution.

Other probability distributions related to the outcomes of Bernoulli trials are encountered less often, but are no less important. In particular, the geometric distribution is useful in answering questions about waiting time. Instead of fixing the number of trials in advance, waiting time experiments require Bernoulli trials to be repeated until the first success is scored. "Waiting time" is the mathematical term for the number of trials which must be conducted in order to score the first success. The geometric distribution can, for example, be used to determine probability that ten tosses of a coin will be required before the first "head" is scored.

Mathematically, the geometric distribution can be described by the equation[37]

$$P(X=x) = p \cdot (1-p)^{x-1} \qquad (1)$$

where $P(X=x)$ is the probability that the waiting time X will have the specific value x ($x= 1, 2, 3, \ldots$). The mean value of X is $1/p$.

During the degradation of amylose by the peeling and stopping process, only two chemical reactions are occurring at the reducing ends. The completion of one reaction can therefore be viewed as a Bernoulli trial. If peeling is viewed as a "failure" and stopping is viewed as a "success," then the distribution of peeling lengths becomes equivalent to the distribution of the number of Bernoulli trials which must be conducted before the first success is scored. This is a geometric distribution, where the probabilities of success and failure are determined by the relative rates of the two reactions. For example, if $k_P/k_S = 300$, then for each 300 occurrences of the peeling, one occurrence of the stopping reaction can be expected, and the probability of success would be 1/301. In general the probability of success would be given by

$$p = k_S/(k_S + k_P) \approx k_S/k_P \qquad (2)$$

where the approximation is appropriate for small ratios of k_S to k_P.

If the peeling length is given the symbol P_L, then by analogy to Eq. (1) the probability of the peeling length being equal to any value m is given by

$$P(P_L=m) = (k_S/k_P) \cdot (1-k_S/k_P)^m \qquad (3)$$

The exponent on the right hand side of Eq. (3) is m instead of m-1 because unlike a mathematical waiting time which must have a value of at least 1, the peeling length can have a value of 0. This is because stopping can occur on the first trial. If it does, the amylose chain is not shortened, but instead its reducing end is simply converted into an acid end group.

Given an initial distribution of molecular weights, then, the final distribution can be determined. In practice, this was accomplished by using a computer program. This computer program is described and listed in Appendix II.

The program reserves two separate arrays of memory, one for the initial distribution (which remains unchanged) and one for the final distribution (which accumulates as the calculation proceeds). The calculation starts with the highest DP present, DP_{MAX}. The fraction of molecules of length DP_{MAX} that peel to each shorter DP is determined from Eq. (3), by considering each peeling length from 0 up to DP_{MAX} in order. The fraction of molecules that have $P_L > DP_{MAX}$ are destroyed by complete peeling, and so do not appear in the final distribution.

Next, the calculation continues with molecules with a starting length one unit shorter than DP_{MAX}. Eventually all of the possible starting DPs are treated in the same way, and the calculation is complete. The equilibrium yield loss is then determined from the fraction of monomer units that peeled, and the final $\overline{DP}_N$ is calculated from the accumulated MWD.

Molecular weight distributions are often plotted as continuous functions on a weight fraction versus logarithm of DP basis. Direct application of Eq. (2) requires the distribution to be tabulated on a number fraction basis, with linear scaling of the DP. The interconversion between these distributions is explained in Appendix I.

Early simulation runs on the computer revealed that only every tenth DP and peeling length had to be considered to give acceptable results. This reduced computation time considerably.

Comparison of Model Predictions to Arbin's[16] Experimental Results

The probabilistic model was used to reevaluate the MWD data acquired previously by Arbin et al.[16] Figure 3 showed the shifts in MWD he observed during the alkaline degradation of amylose at 80°C. The initial MWD of Arbin's starting material was approximately lognormal in shape. As was done for the

constant peeling length calculation, for modeling a truly lognormal starting distribution was used.

Table 1 compares Arbin's experimental results to the predictions of the simulation for several values of k_p/k_s. In all cases, the model predicts an increase in $\overline{DP}_N$. This is due to the fact that proportionally more molecules are destroyed than monomer units. The results presented in Table 1 show that the fraction of molecules lost due to complete peeling (indicated by the decrease in the relative total end group concentration) is always greater than the fraction of monomer units lost (indicated by the decrease in yield).

Table 1. Comparison of probabilistic model predictions to the experimental results of Arbin et al.[16]

Description	$\overline{DP}_N$	Relative Total End Group Concentration	Yield, wt.%
Arbin's Results			
Starting material	630	--	100.0
Final material	254	--	56.8
Model Results			
Starting material	630	1.000	100.0
Final material for			
k_p/k_s = 100	635	0.903	91.0
k_p/k_s = 200	663	0.752	79.1
k_p/k_s = 300	687	0.651	71.1
k_p/k_s = 400	708	0.578	64.9
k_p/k_s = 500	726	0.521	60.0
k_p/k_s = 600	742	0.475	55.9
k_p/k_s = 700	757	0.437	52.5
k_p/k_s = 1000	834	0.354	44.5

One basis for comparing the model to experimental results is to choose the value of k_p/k_s that gives the closest match to the yield loss measured by Arbin. When k_p/k_s = 600, a final yield of 55.9% is predicted. This is fairly close to

the experimentally observed value of 56.8%. The potential importance of complete peeling is demonstrated by the model's prediction that 52.5% of all molecules would peel completely at this value of k_p/k_s. The initial MWD and final MWD predicted for k_p/k_s = 600 are plotted in Fig. 6.

This probabilistic treatment of peeling and stopping represents a substantial refinement over assuming a constant peeling length. However, the trends predicted by both calculations agree. Degradation by peeling and stopping alone should have caused an increase, and not a decrease in the average molecular weight. Arbin's observation of a decreasing $\overline{DP}_N$ cannot be explained by peeling and stopping alone, and so it is likely that random chain cleavage played a role.

Modeling of the Degradation of a High DP Amylose

The amylose used as the substrate in the experimental part of this thesis was purposely tailored to be a sensitive detector of chain cleavage. Chain cleavage has the greatest effect on high DP molecules, because these molecules contain more glucosidic bonds that can be attacked by cleavage. The substrate amylose had a higher $\overline{DP}_N$ than that used in previous studies, and the peak of its MWD was offset toward high molecular weights.

The MWD of this substrate was used as the starting point for additional modeling work. The computer program used to complete this portion of the modeling work is described and listed in Appendix II. The objective of this modeling was to predict how the substrate amylose should be affected by peeling and stopping, for comparison to the results of new degradation experiments. Table 2 shows simulation results for several values of k_p/k_s. Once again, increases in DP are predicted exclusively. In the actual degradation experiments, the yield losses observed typically were about 50%. For k_p/k_s = 2500,

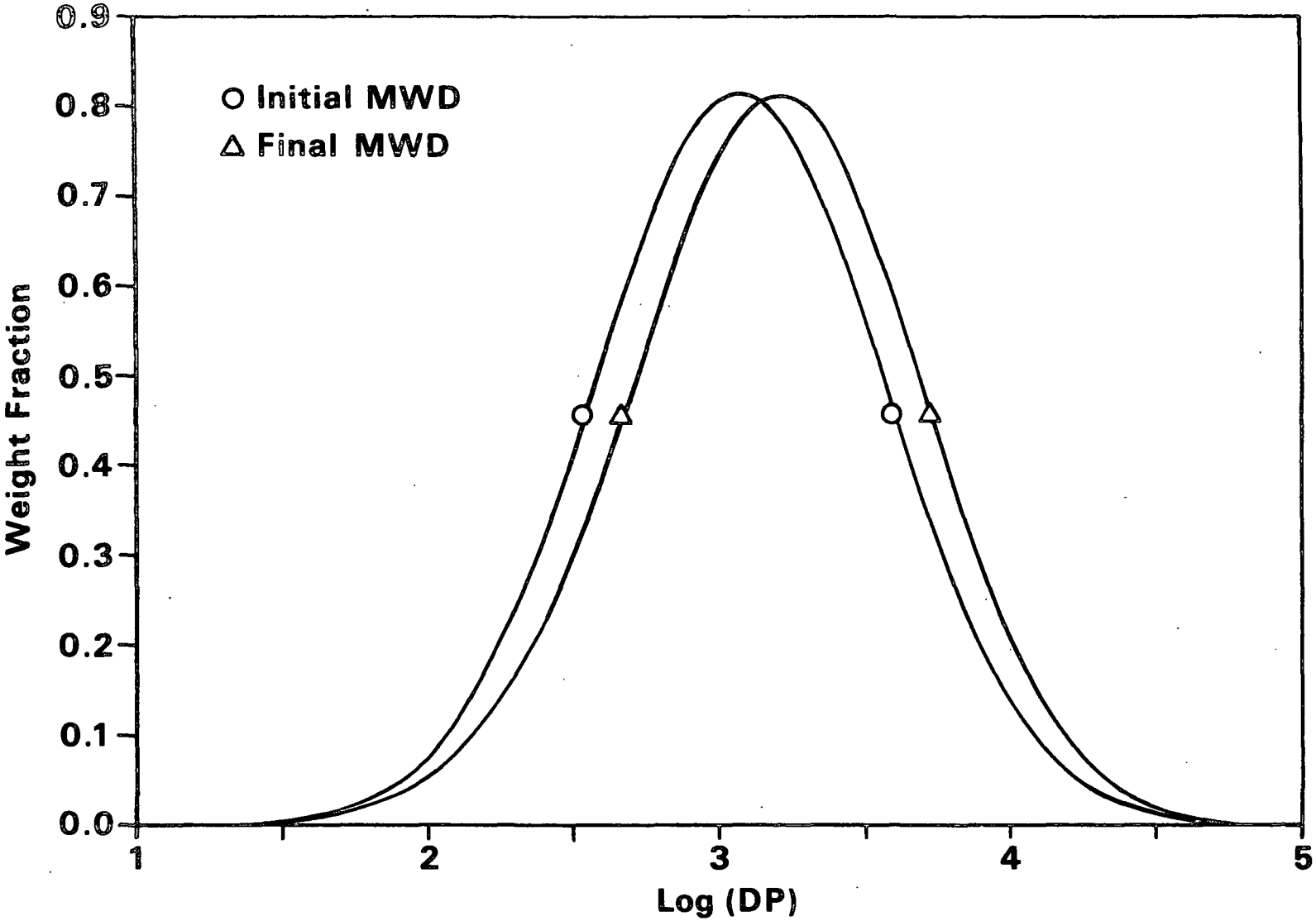

Figure 6. Change in amylose MWD predicted by probabilistic model for Arbin's[16] starting material for k_p/k_S = 600.

the predicted equilibrium yield was 51.9%, and the shift in MWD that would result is shown in Fig. 7. Once again, the importance of complete peeling is demonstrated by the model's prediction that 64% of all the original amylose molecules and reducing ends would be destroyed by complete peeling at this value of k_P/k_S.

Table 2. Probabilistic model predictions for a high DP starting material.

Description	$\overline{DP}_N$	Relative Total End Group Concentration	Yield, wt.%
Starting material	1840	1.000	100.0
Final material for			
k_P/k_S = 300	2039	0.808	88.7
k_P/k_S = 500	2167	0.704	82.2
k_P/k_S = 1000	2383	0.553	70.9
k_P/k_S = 1500	2520	0.464	63.0
k_P/k_S = 2000	2615	0.404	56.9
k_P/k_S = 2500	2687	0.359	51.9
k_P/k_S = 3000	2742	0.324	47.9
k_P/k_S = 3500	2787	0.296	44.4

The predictions listed in Table 2 can be compared to those in Table 1 to demonstrate the influence that the shape and position of the starting MWD can have on degradation. For the high DP material, much higher k_P to k_S ratios are required to give yield losses equal to those seen with Arbin's starting material. This is because at a higher average DP there are fewer reducing ends in a given weight of amylose.

Comprehensive Model

A second mathematical model was developed for the case where cleavage occurs in addition to peeling and stopping. This model involves solving a system of differential equations to predict changes in amylose yield, $\overline{DP}_N$, and end group composition during the course of degradation.

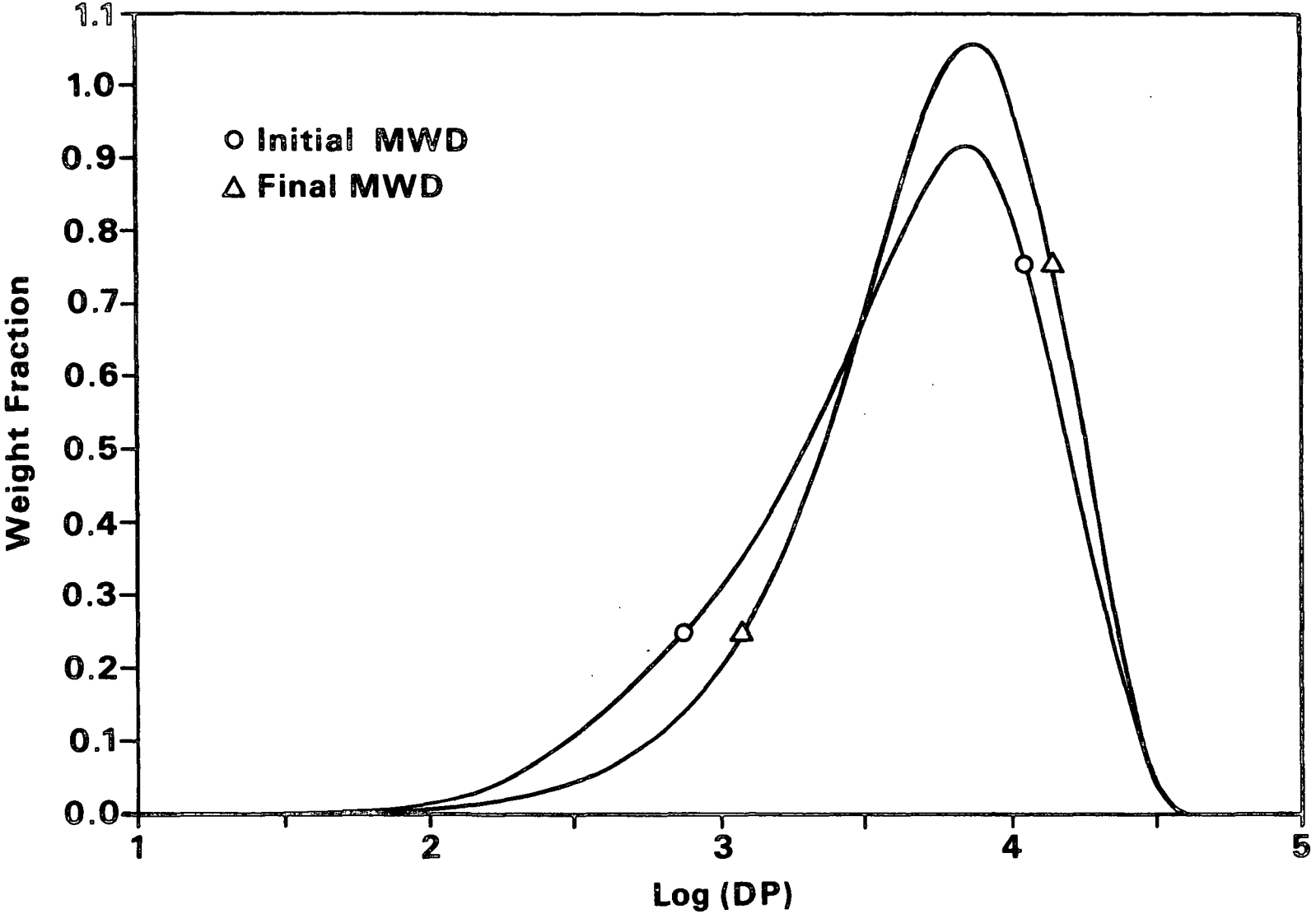

Figure 7. Change in amylose MWD predicted by probabilistic model for a high DP starting material for k_p/k_S = 2500.

Figure 8 illustrates the pathways by which a molecule of arbitrary length n can be formed or lost when all three chemical reactions are operating. Molecules with acid ends must be treated separately from molecules with reducing ends because they are stabilized toward peeling. In the following discussion, the molar concentration of molecules of length n with reducing ends is designated by $[N_{R,n}]$, and the concentration of molecules of length n with acid ends is designated by $[N_{A,n}]$. As in the probabilistic model, the peeling and stopping reactions are treated as being first order with respect to reducing end groups, with rate constants k_P and k_S. The chain cleavage reaction is treated as being first order with respect to glucosidic bonds, and its rate constant is given the symbol k_{CC}.

The equations describing degradation can be developed step by step, by breaking the overall process into three subprocesses. The subprocesses are 1) peeling and stopping, 2) cleavage of molecules with reducing ends, and 3) cleavage of molecules with acid ends. In the following discussion, the differential equations describing the contributions of the individual subprocesses will be subscripted PS, CR, and CA, respectively.

First, consider the ways that peeling and stopping can produce or consume molecules. A molecule n units long with a reducing end is formed whenever a molecule one monomer unit longer peels. The same type of molecule may be lost by stopping, in which case it is converted to an acid-ended molecule of the same length, or by peeling, in which case it retains its reducing end but is shortened by one monomer unit. Thus, the rate of production of molecules with reducing ends is

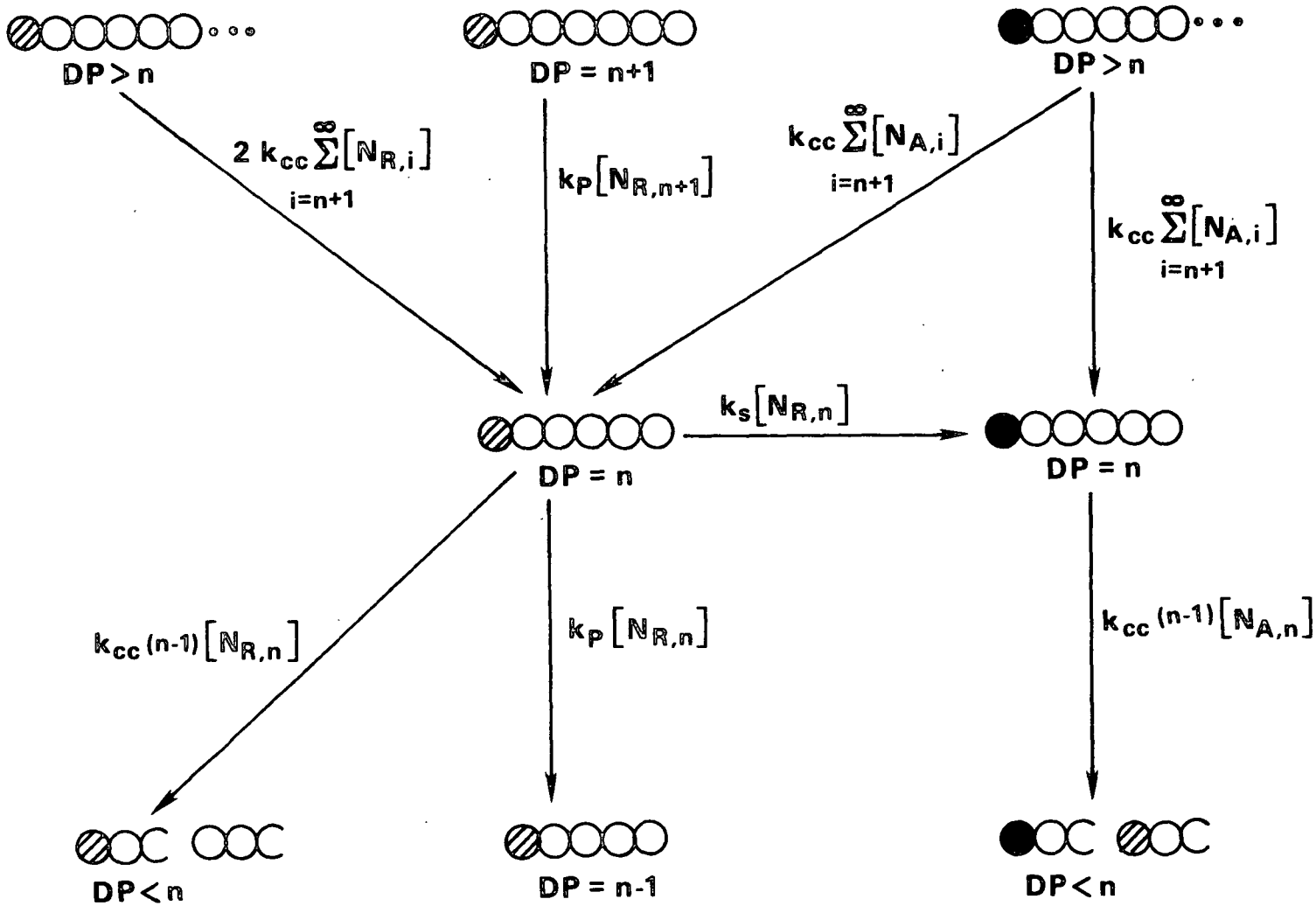

Figure 8. Pathways of production and consumption of amylose molecules of length n (● = acid end, ⊖ = reducing end).

$$\left[\frac{d[N_{R,n}]}{dt}\right]_{PS} = k_p[N_{R,n+1}] - k_s[N_{R,n}] - k_p[N_{R,n}] \tag{4}$$

and the rate of appearance of acid-ended molecules is

$$\left[\frac{d[N_{A,n}]}{dt}\right]_{PS} = k_s\,[N_{R,n}] \tag{5}$$

Next, consider the effect of cleavage of molecules with reducing ends. A molecule of length n forms anytime a longer molecule cleaves n units from either end. A molecule of length i (where $i > n$) contains i-1 glucosidic bonds. The total rate of cleavage per molecule is determined by the product of the rate per glucosidic bond (k_{CC}) and the number of bonds per molecule (i-1). If all bonds are equally reactive, then on average only two out of (i-1) cleavages result in the formation of a molecule of length n. This is because only two of the bonds are exactly n units from either end of the molecule. Since all higher DPs can form molecules of length n by cleavage, the contribution of each higher DP must be determined and the results summed. A molecule of length n is consumed by cleavage whenever any of its bonds is broken. The rate of production of molecules with reducing ends can therefore be written as

$$\left[\frac{[N_{R,n}]}{dt}\right]_{CR} = k_{CC} \sum_{i=n+1}^{\infty} \left[\frac{2}{(i-1)} \cdot (i-1)[N_{R,i}]\right] - k_{CC}(n-1)[N_{R,n}]$$

$$= 2k_{CC} \sum_{i=n+1}^{\infty} [N_{R,i}] - k_{CC}(n-1)[N_{R,n}] \tag{6}$$

The concentration of acid-ended molecules is not affected by cleavage of molecules with reducing end groups.

Finally, consider the contributions made by the cleavage of molecules with acid end groups. Each cleavage results in the formation of two shorter molecules, one with an acid end and one with a reducing end. Using the same reasoning as above, the production rate for molecules of length n with reducing ends is

$$\left[\frac{d[N_{R,n}]}{dt}\right]_{CA} = k_{CC} \sum_{i=n+1}^{\infty} [N_{A,i}] \tag{7}$$

and the rate of production of molecules with acid ends is

$$\left[\frac{d[N_{A,n}]}{dt}\right]_{CA} = k_{CC} \sum_{i=n+1}^{\infty} [N_{A,i}] - k_{CC}(n-1)[N_{a,n}] \tag{8}$$

The overall degradation process is described by summing Eq. (4), (6), and (7) for molecules with reducing ends to give

$$\frac{d[N_{R,n}]}{dt} = \left[\frac{d[N_{R,n}]}{dt}\right]_{PS} + \left[\frac{d[N_{R,n}]}{dt}\right]_{CR} + \left[\frac{d[N_{R,n}]}{dt}\right]_{CA} = \tag{9}$$

$$-[k_P+k_S+k_{CC}(n-1)]\,[N_{R,n}] + k_P\,[N_{R,n+1}] + k_{CC}\left[2\sum_{i=n+1}^{\infty}[N_{R,i}] + \sum_{i=n+1}^{\infty}[N_{A,i}]\right]$$

and Eq. (5) and (8) for molecules with acid ends to give

$$\frac{d[N_{A,n}]}{dt} = \left[\frac{d[N_{A,n}]}{dt}\right]_{PS} + \left[\frac{d[N_{A,n}]}{dt}\right]_{CA} =$$

$$-k_{CC}(n-1)[N_{A,n}] + k_S[N_{R,n}] + k_{CC}\sum_{i=n+1}^{\infty}[N_{A,i}] \tag{10}$$

One set of two equations [Eq. (9) and (10)] is required for each DP present in the distribution. For an amylose isolated from natural sources, the MWD

can extend up to a DP of 40,000 or more. Modeling of the degradation of such a substrate would require the solution of a system of 80,000 coupled differential equations.

Because the goal of the modeling work was to obtain a qualitative understanding of polysaccharide degradation, it was possible to gain significant insights into the degradation process without shouldering the heavy burden of solving these very large systems of equations. This was accomplished by working with a monodisperse starting distribution, which reduced the problem to a size easily handled by simple numerical integration techniques. The actual numerical method used was Euler's method.[38] This method allowed the summation terms in Eq. (9) and (10) to be accumulated efficiently, and was sufficiently accurate, provided small time steps were used. The computer program which was written to implement the model is described and listed in Appendix II.

The end product was a powerful but simple model that can be used to probe the effects of varying the rate constants singly or in combination. The starting DP chosen for modeling was 1600. This was reasonably close to the $\overline{DP}_N$ of the substrate amylose used in the experimental investigation, which was 1840. Simulations with the model have shown that moderate changes in the starting DP have little effect on the results.

In order to use the model, values were needed for the rate constants k_P, k_S, and k_{CC}. Starting values for these constants were estimated from data found in the literature.

Green and coworkers[5] studied the peeling reaction of cellobiose using a fast flow reactor. They determined the half-life of cellobiose in 0.02 to 2M NaOH at temperatures ranging from 60 to 120°C. The rate of reaction was not affected by

alkali concentration as long as the concentration was at least 0.5M. Conversion of their half-life data into rate constants and interpolation through the use of the Arrhenius equation[39] gives rate constants of 0.068 min^{-1} at 60°C, 0.74 min^{-1} at 80°C, and 6.30 min^{-1} at 100°C.

Ziderman and Bel-Ayche[40] measured rate constants for the peeling of maltose and cellobiose in dilute (< 0.1M) NaOH. The rate constants ranged from 0.0035 min^{-1} at 67°C to 0.783 min^{-1} at 97°C. The conditions yielding the latter value were the closest to those used in the current project, except for the alkali concentration, which was 0.1M instead of 1.0M.

Gentile et al.[9] report an initial peeling rate of 0.67 min^{-1} for amorphous hydrocellulose in 1.0M NaOH at 80°C. Crystalline cellulose degraded under identical conditions had an initial peeling rate of 0.47 min^{-1}.

Based on the above references, in round numbers an approximate starting value for k_p over the range of 60 to 100°C was taken to be 1.0 min^{-1}.

The ratio of the peeling rate to the stopping rate, k_p/k_s, is given in or can be inferred from a number of references. In the study by Ziderman and Bel-Ayche,[40] this ratio ranged from about 3 to more than 66.7 for cellobiose. In an earlier study by MacLeod and Schroeder,[6] which used cellobiose and similar alkali concentrations but lower temperatures (25 and 45°C), the ratio was so high that no product of the stopping reaction could be detected.

Several polysaccharide degradation studies report k_p to k_s ratios. None of these results account properly for complete peeling, and most do not consider chain cleavage. However, the ratios reported still may be useful in providing ball park estimates. Based on yield loss measurements, Young and Liss[41] report

a ratio of 224 for amylose, and ratios ranging from 25 to 103 for galacto- and glucomannans at 100°C in 1M sodium hydroxide. Samuelson and Wennerblom[42] and Franzon and Samuelson[12] give ratios ranging from 40 to 65 for cellulose at pulping temperatures, based on osmotically determined DP losses. Using similar reasoning, Arbin[16] suggested ratios of 290 and 400 for amylose at 80 and 100°C. Gentile et al.[9] determined rate coefficients directly from the rate of loss of the reducing end groups, the rate of yield loss, and the rate of appearance of acidic end groups. The ratios he measured for cellulose ranged from 23 to 291.

Based on the references cited, in round numbers, the starting guess used for the k_P/k_S ratio was 100. The central value used for k_S in modeling experiments was therefore 0.01 min^{-1}.

All simple model compound studies indicate that cleavage should be practically undetectable at 60 to 100°C. Of all low temperature degradation studies using polysaccharides as substrates, only Gentile et al.[9] report values for k_{CC}, for an amorphous cellulose substrate. These workers measured k_{CC}s of up to 1.45 x 10^{-7} min^{-1} at 60°C and 9.83 x 10^{-7} min^{-1} at 80°C. The rate constants are calculated on the basis of the rate of formation of total end groups and do not account for the loss of end groups by complete peeling, and thus are probably too low.

Based mostly on Gentile's results and comparison of initial modeling experiments to experimental $\overline{DP}_n$ results, a starting value for the cleavage constant was chosen to be 1.0 x 10^{-5} min^{-1}.

Degradation was simulated by using the starting values for the rate constants reported above (k_P = 1.0, k_S = 0.01, and k_{CC} = 1 x 10^{-5} min^{-1}). Each of the rates was then varied by one order of magnitude in either direction to

allow a wide range of behaviors to be examined. The system of equations was solved for each combination of rate constants, and the results were plotted in such a way to allow the effects of the individual constants to be determined.

The changes in relative reducing end group concentration predicted by the model are shown in Fig. 9. The relative concentration is the concentration at any time divided by the initial concentration. Cleavage rate has a large influence on the results, because faster cleavage produces more reducing end groups. Reducing ends are consumed by two processes, stopping and complete peeling, and this is reflected in the results. Increasing k_S tends to limit the number of reducing ends by speeding their conversion to acid ends. Increasing k_P also limits reducing ends, by promoting complete peeling. Complete peeling is also enhanced at high k_{CC}, because rapid cleavage produces short chains which tend to degrade completely.

The predicted relative total (reducing + acid) end group concentrations are shown in Fig. 10. The relative total end group concentration is equivalent to the relative number of amylose molecules per unit volume. Production of new amylose chains during the first part of the reaction is determined by k_{CC}. In fact, the initial slopes of the curves depend primarily on k_{CC} and are not influenced much by k_P or k_S. This provides a powerful tool for evaluating experimental results, because it allows the cleavage rate to be gaged easily regardless of variations in the peeling and stopping rates.

Unlike the reducing end group concentration, which could be diminished by either chemical stopping or complete peeling, the total end group concentration can be reduced only by complete peeling. As demonstrated by the curves in Fig. 10, high stopping rates reduce the consumption of molecules by stabilizing

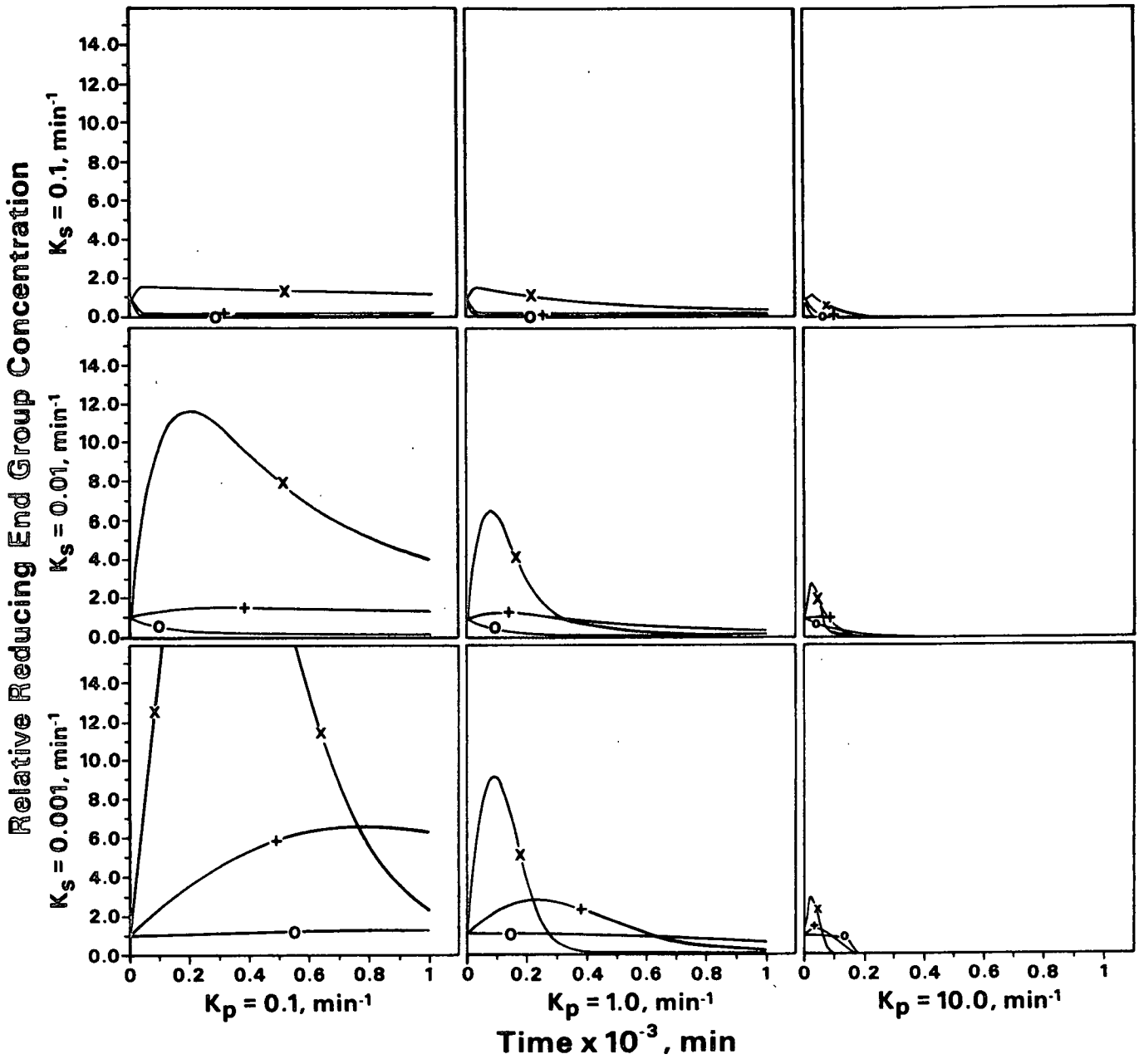

Figure 9. Relative reducing end group concentrations predicted by comprehensive model. (k_{CC}: 0 = 10^{-6} min^{-1}, + = 10^{-5} min^{-1}, X = 10^{-4} min^{-1}.)

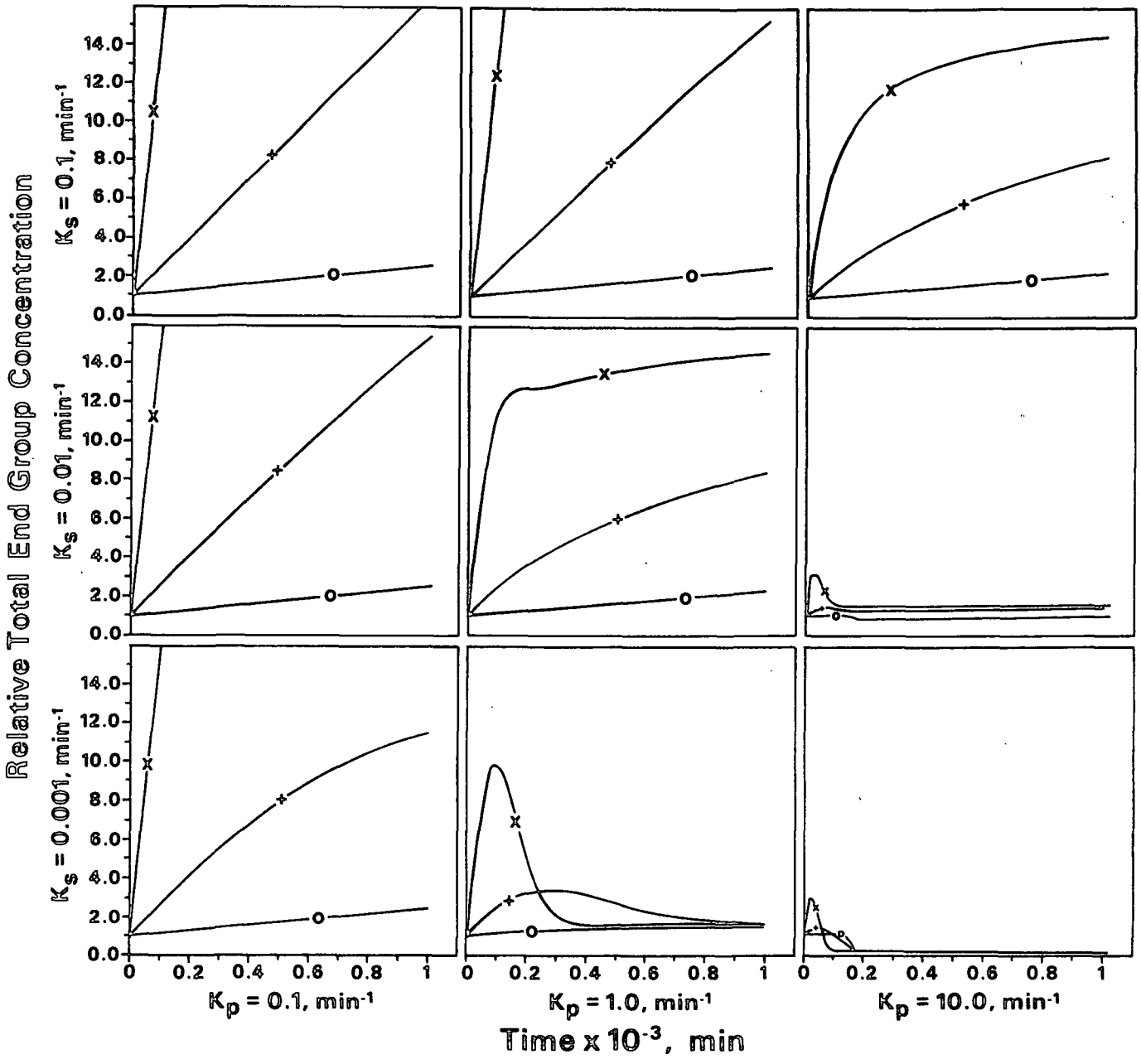

Figure 10. Relative total end group concentrations predicted by comprehensive model. (k_{CC}: 0 = 10^{-6} min^{-1}, + = 10^{-5} min^{-1}, X = 10^{-4} min^{-1}.)

the active end groups. High peeling rates, on the other hand, enhance consumption. High k_{CC}s promote complete peeling later in the reaction, by forming short chains.

Taken together, the end group predictions clearly demonstrate that complete peeling plays an important role in controlling the course of amylose degradation. The effect of complete peeling is evident even at high cleavage rates.

The predicted course of yield loss is shown in Fig. 11. High values of k_{CC} cause a rapid loss of yield. This is not because cleavage causes yield loss directly, but because cleavage creates reducing ends and so it enhances peeling. Yield loss also increases as the k_P to k_S ratio is increased, and peeling becomes more favored relative to stopping. The plots demonstrate the danger of following amylose degradation by measuring yield loss alone. For any given reaction time, the same amount of yield loss can be caused by many different combinations of peeling, stopping, and chain cleavage rates.

Figure 12 shows the predicted $\overline{DP}_N$ results. Except at the very large k_P to k_S ratios prevailing in the lower right hand corner of the figure, the curves are pretty much independent of k_P and k_S and depend mostly on k_{CC}. This was not surprising in the light of the probabilistic model results, which showed peeling and stopping alone do not tend to decrease molecular weight. The peculiar dip in the curves observed at high k_P to k_S ratios merits further discussion, because it plays a key role in the interpretation of experimental results.

At very high k_P/k_S, the peeling process does make a contribution to DP loss. As molecules are rapidly shortened by peeling, very few molecules have a chance to undergo the stopping reaction. Those that do will tend to be

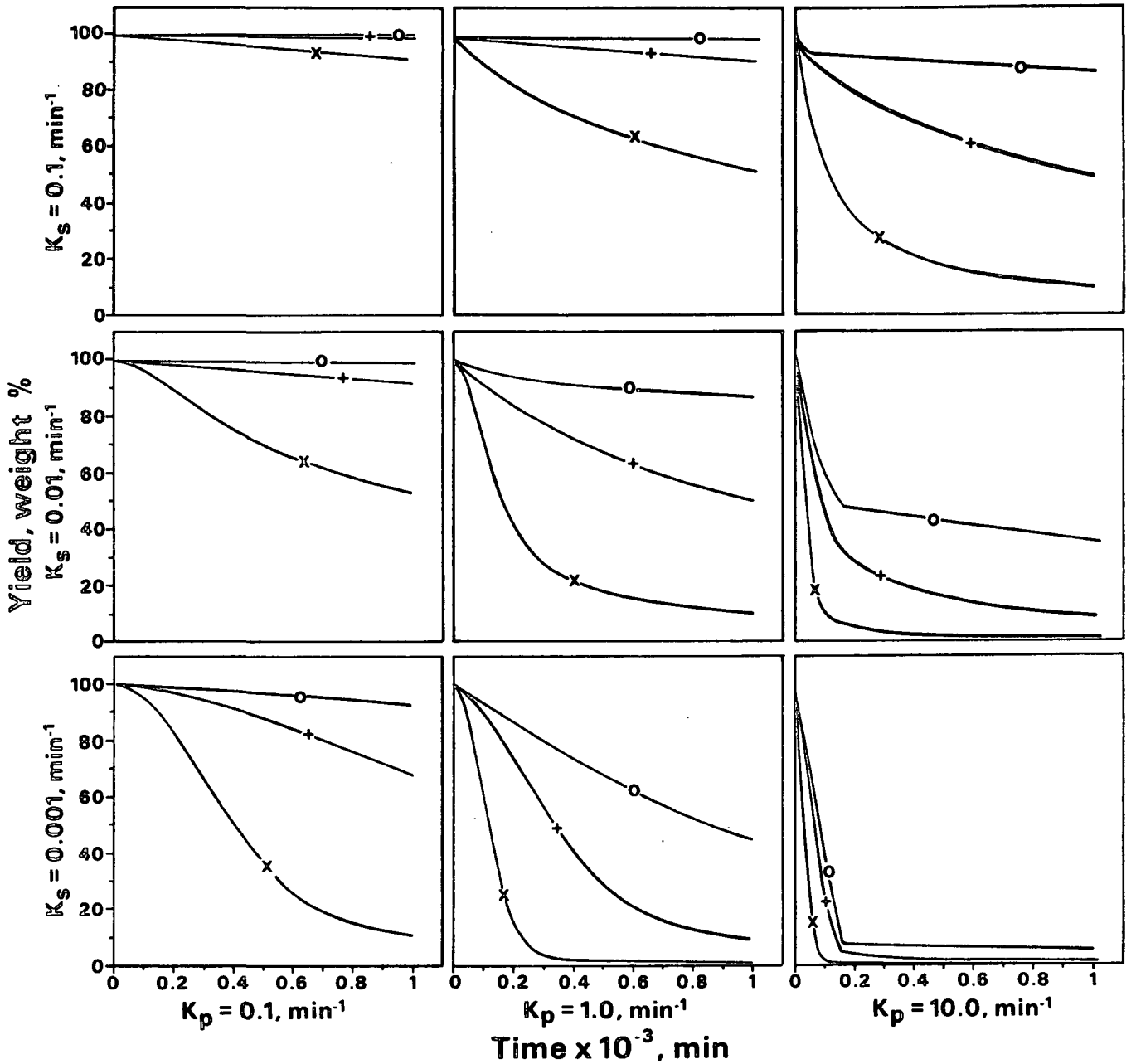

Figure 11. Yields predicted by comprehensive model. (k_{CC}: 0 = 10^{-6} min^{-1}, + = 10^{-5} min^{-1}, X = 10^{-4} min^{-1}.)

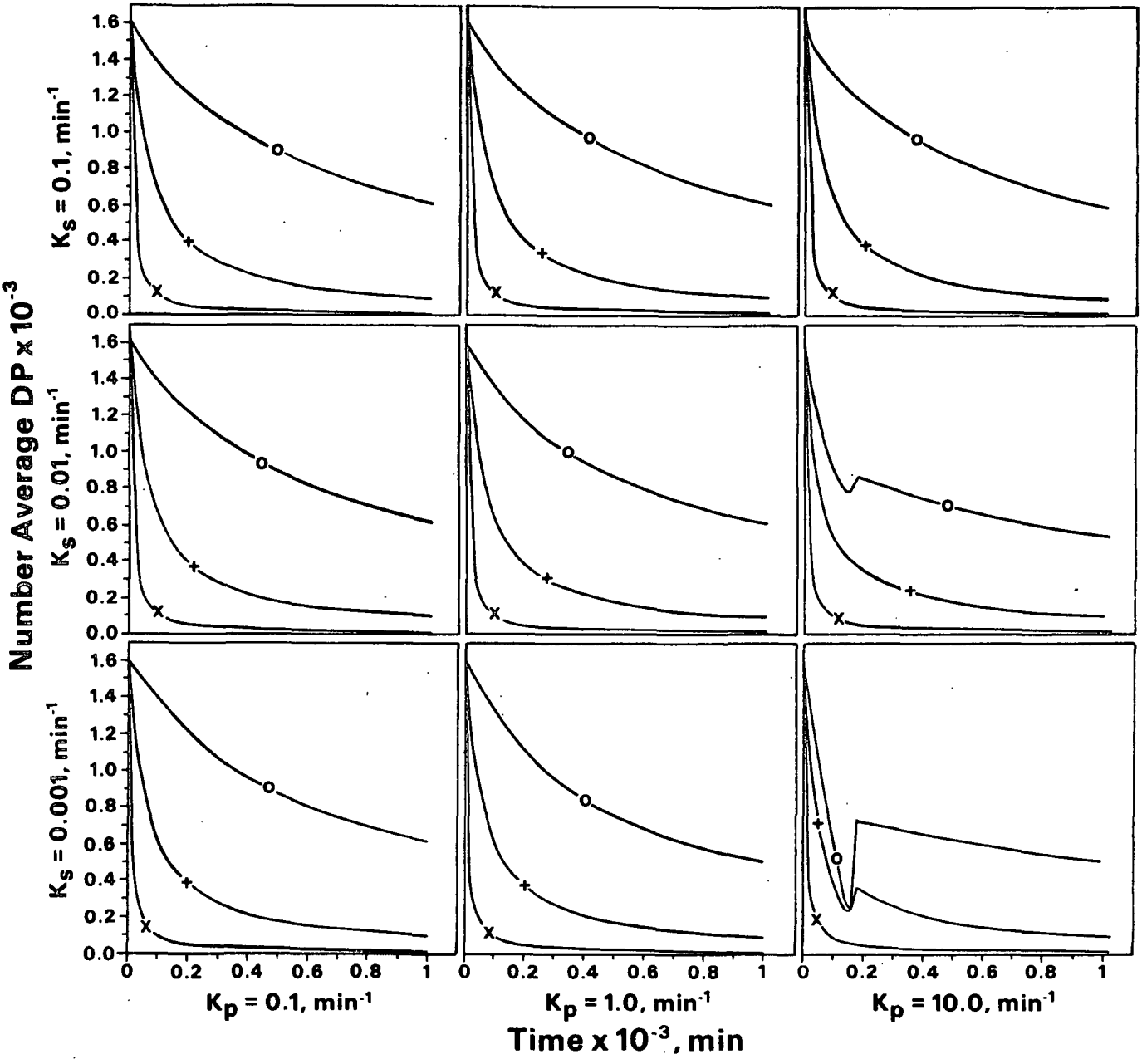

Figure 12. $\overline{DP_N}$s predicted by comprehensive model. (k_{CC}: 0 = 10^{-6} min^{-1}, + = 10^{-5} min^{-1}, X = 10^{-4} min^{-1}.)

longer than the average, because molecules with reducing ends continue to peel toward lower molecular weights. Eventually, a point in time is reached where most of the molecules with reducing ends are destroyed by complete peeling, and the acid-ended molecules begin to dominate the MWD. It is at this point that the upward slope in the $\overline{DP}_N$ curve is located. Figure 13 shows the correspondence between the $\overline{DP}_N$ curve and the end group curves for the case where k_P = 10 min^{-1}, k_S = 0.001 min^{-1}, and k_{CC} = 1 x 10^{-5} min^{-1}. It can be seen that the dip in the $\overline{DP}_N$ curve does occur near where the reducing end and acid end concentration curves cross.

The dip in the $\overline{DP}_N$ curves appears only at high ratios of k_P to k_S when the cleavage rate is moderate or slow. Starting from any curve in Fig. 12 that possesses the feature, movement toward lower values of k_P/k_S tends to reduce the depth of the valley, and if the change is great enough, the dip is eliminated entirely. This happens because cleavage starts to dominate the DP loss process. Movement toward higher cleavage rates has exactly the same effect.

Comparison of Models

The predictions of the two modeling approaches were compared for one arbitrary combination of rate constants to check the consistency of the solutions obtained. A monodisperse starting distribution was used, with an average DP of 1800. The cleavage rate was set equal to zero in the comprehensive model, and a value for k_P/k_S of 1200 was input to both models. The results are listed in Table 3. Agreement between the models was excellent. This adds additional confidence to the results of each model, since two very different methods were used to arrive at the same equilibrium values.

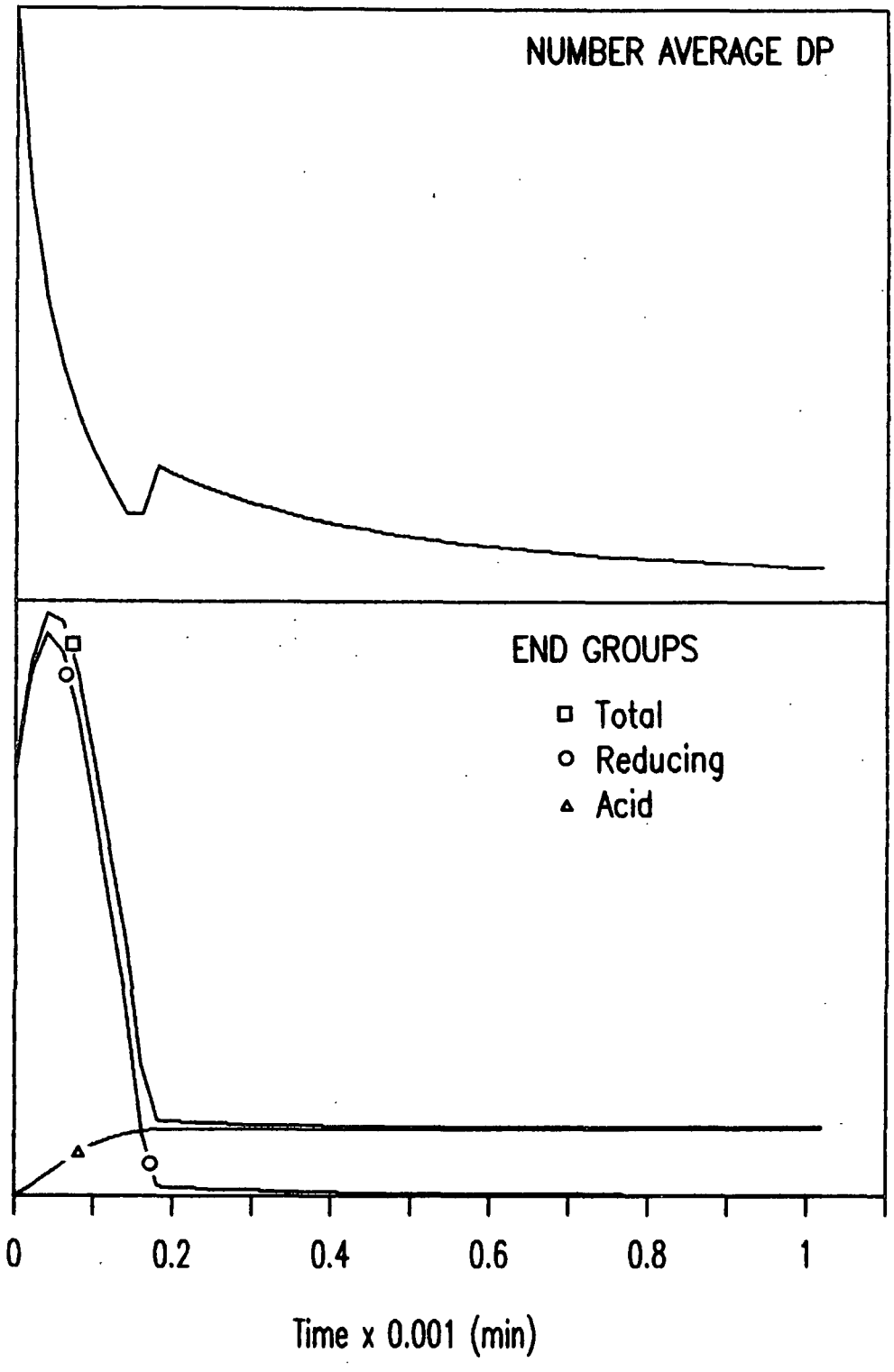

Figure 13. $\overline{DP}_N$ and end group concentrations predicted by comprehensive model for k_p = 10.0 min^{-1}, k_S = 0.001 min^{-1}, and k_{CC} = 10^{-5} min^{-1}.

Table 3. Comparison of probabilistic model results to comprehensive model results.

Description	$\overline{DP}_N$	Relative Total End Group Concentration	Yield, wt. %
Starting material	1800	1.000	100.0
Final material predicted by			
Probabilistic model	1122	0.780	48.6
Comprehensive model	1117	0.777	48.2

DEGRADATION EXPERIMENTS

Selection of Amylose Substrate

An objective of the current study was to determine whether the random chain cleavage reaction plays a role in the low temperature alkaline degradation of amylose. The chain cleavage reaction has a greater effect on long molecules than on short molecules, because long molecules contain more glucosidic linkages that can be broken. Therefore, a substrate tailored to be a sensitive detector of chain cleavage should be high in molecular weight.

An enzymatic synthesis of a high DP amylose was attempted, using the same method developed to synthesize gel permeation chromatography (GPC) calibration standards. The synthesis, which is mentioned in Appendix III, was unsuccessful, forcing a search for an alternative source of the substrate.

A commercially available amylose was found which had an average DP higher than that reported in any previous amylose degradation study. The amylose was found to be contaminated with a branched polysaccharide, but this was easily removed by a simple purification procedure. The purified product had a $\overline{DP}_N$ of

1840 (as determined by GPC) and a MWD with its peak offset toward high molecular weights, making it an ideal detector of chain cleavage.

Alkaline Degradation Reactions

Degradation experiments were conducted under conditions similar to those used by Arbin[16]. Amylose (1% w/v) was treated with 1M sodium hydroxide under anaerobic conditions at temperatures of 60, 80, and 100°C in a Teflon-lined reactor. The amylose was kept separate from the alkali solution during the heat-up period, in a special capsule. When the alkali reached the desired temperature, the capsule was blown open by pressurizing it, and the amylose was released into solution. The reactor is described in the Experimental section. An anaerobic environment was maintained during the loading of the reactor and preparation of reaction solutions by working in a glove bag filled with prepurified nitrogen.

At the desired time intervals, reaction solution was removed from the reactor by means of a sampling line. A portion of the solution was analyzed directly for its amylose content, and the remainder of the amylose in the sample was recovered by precipitation. The MWD of the recovered product was determined by GPC, and reducing and total end group contents were measured.

Comparison of Experimental MWDs to Probabilistic Predictions

The experimentally determined MWD curves at selected time intervals for reactions at 60°, 80°, and 100°C are shown in Fig. 14. At all temperatures, the distribution was found to shift toward lower molecular weights and become more symmetrical as degradation proceeded. These observations are in direct conflict with the predictions of the probabilistic model of the peeling and stopping process. The model predicted (see Fig. 7) that the distribution should remain

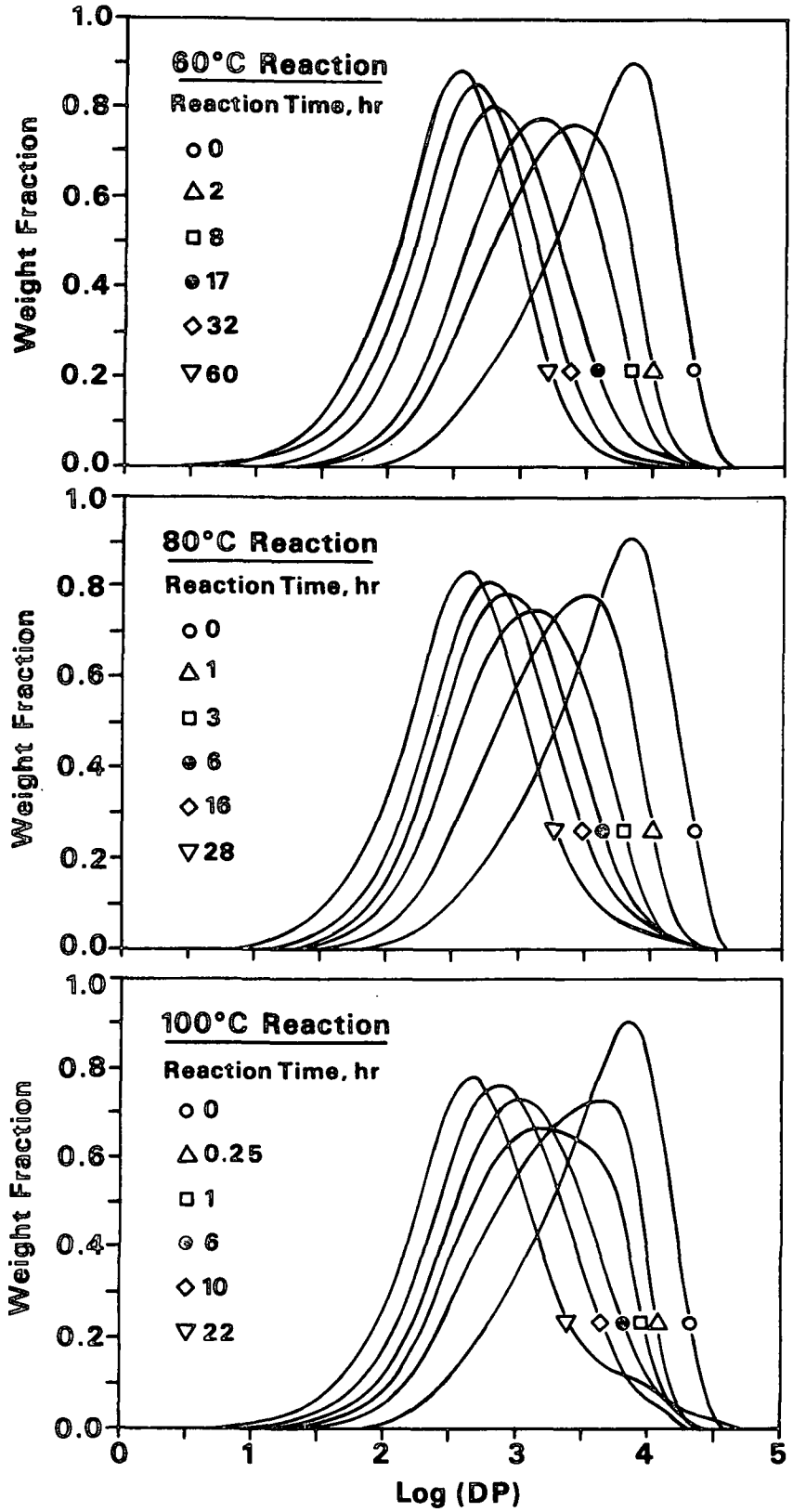

Figure 14. MWDs of amylose during degradation in 1.0M sodium hydroxide at 60°, 80°, and 100°C.

assymetrical, and that the peak of the distribution should shift slightly upward, toward higher molecular weights.

As was true for Arbin's observations, the poor agreement between the model and the experimental results suggests that the results cannot be explained by the peeling and stopping reactions alone. The decreasing molecular weight observed experimentally seemed to be indicative of low temperature cleavage. Additional evidence was gathered to show that cleavage was indeed occurring at low temperatures. This evidence is presented in the next section.

Chain Cleavage

A characteristic of the cleavage reaction is that it causes an increase in the number of amylose chains and in the number of reducing end groups. This is because every time a molecule is cleaved two small chains are formed from one long one, and a new reducing end group is opened up. The peeling and stopping process, on the other hand, can only decrease the numbers of amylose chains and reducing ends. Amylose molecules are destroyed by complete peeling. A reducing end is destroyed whenever a molecule is peeled completely or when a stable acid end group is formed by the stopping reaction.

A direct way to determine whether cleavage is an active pathway of degradation, then, is to examine how the total and reducing end group concentrations change with time. An increase in either or both quantities would indicate cleavage is occurring.

The total end group concentrations measured for the degradation experiments are shown in Fig. 15. Only the data from the first part of the reactions are shown, to allow comparison of the results to the model predictions, and to allow the initial part of the curves to be distinguished. The complete data are

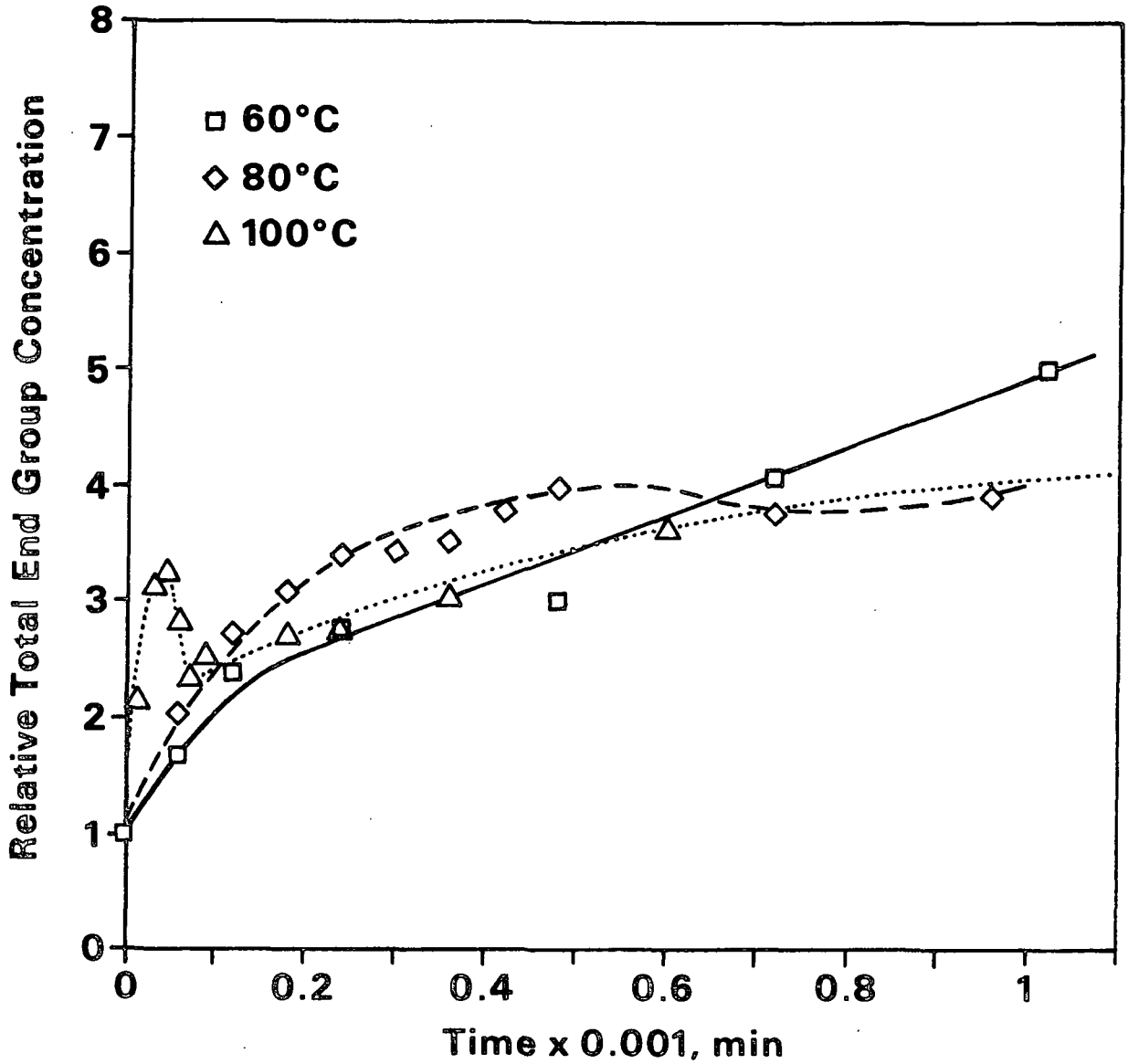

Figure 15. Total end group concentration during degradation of amylose in 1.0M sodium hydroxide at 60°, 80°, and 100°C.

listed in Appendix IV. The results are presented on a relative basis, by dividing the concentration at any time by the initial concentration. Relative concentrations greater than unity indicate that there are more amylose chains present than there were at the beginning of the reaction. At all temperatures, the relative end group concentration was observed to increase, indicating that cleavage did occur.

Figure 16 shows the relative concentration of reducing end groups over the course of the same reactions. Each of the curves increases to a height greater than unity at some point in time, demonstrating that new reducing ends were formed. Again, cleavage is indicated. The total end group results and the reducing end group results provide two relatively independent pieces of evidence to prove cleavage does indeed occur at temperatures at least as low as 60°C.

The experimental yield loss results are shown in Fig. 17. The 80 and 100° curves demonstrate that the yield can appear to be leveling off even in a system that has been shown to include chain cleavage. Previous researchers have mistakenly believed such leveling could occur only in the absence of chain cleavage. The leveling begins late in the reaction, when most of the molecules have stable acid end groups which protect them from peeling. The effect of cleavage is also moderated late in the reaction, because the average DP has been reduced to the point that there are not many bonds per molecule to be attacked. Even when a molecule is split by an occasional cleavage reaction, the new reducing ends tend to be rapidly destroyed because of the short chain lengths prevailing, limiting the amount of yield loss.

The initial slopes of the total end group curves in Fig. 15 increase in the order of increasing temperature. This indicates that the rate of cleavage

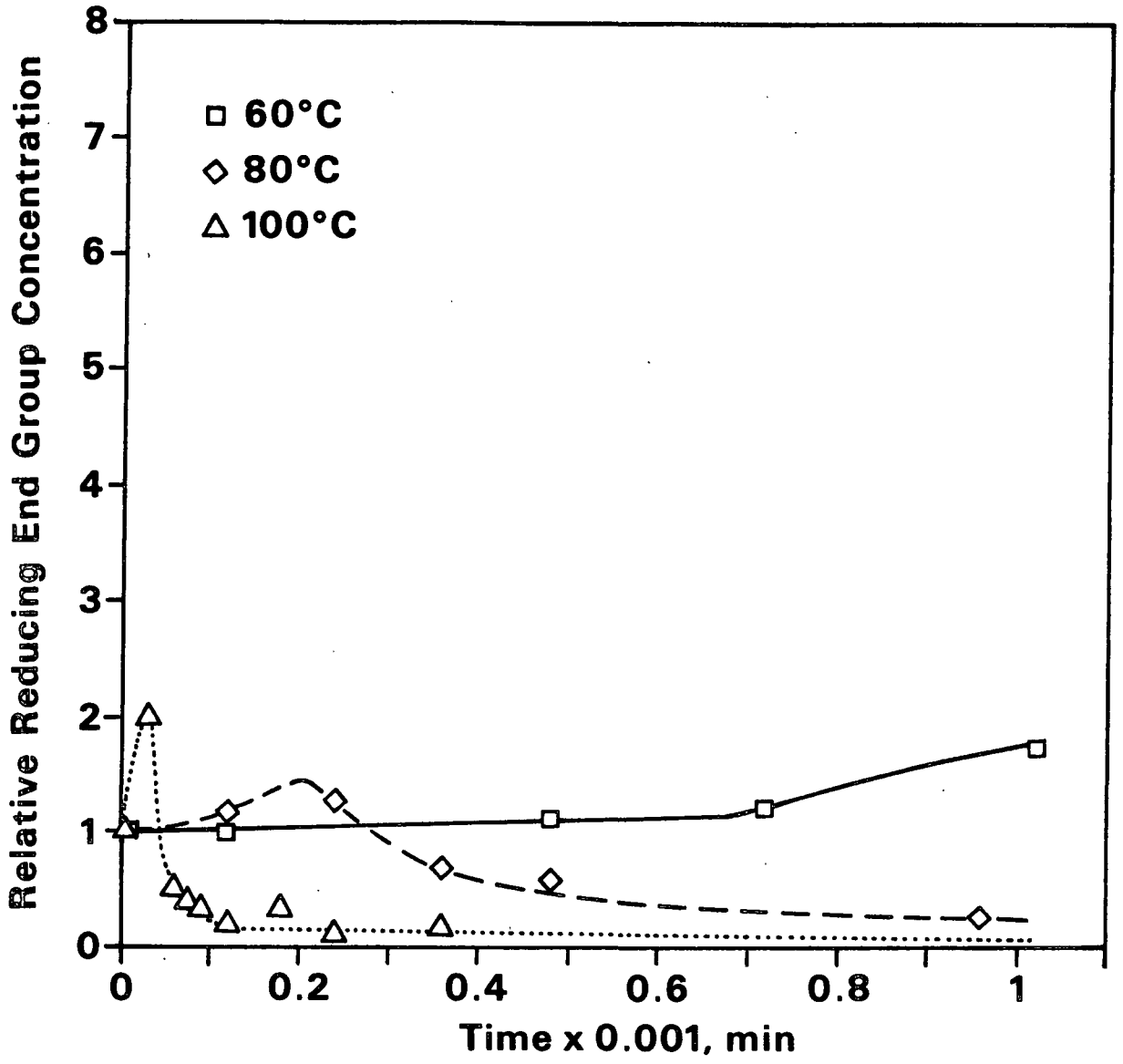

Figure 16. Reducing end group concentration during degradation of amylose in 1.0M sodium hydroxide at 60°, 80°, and 100°C.

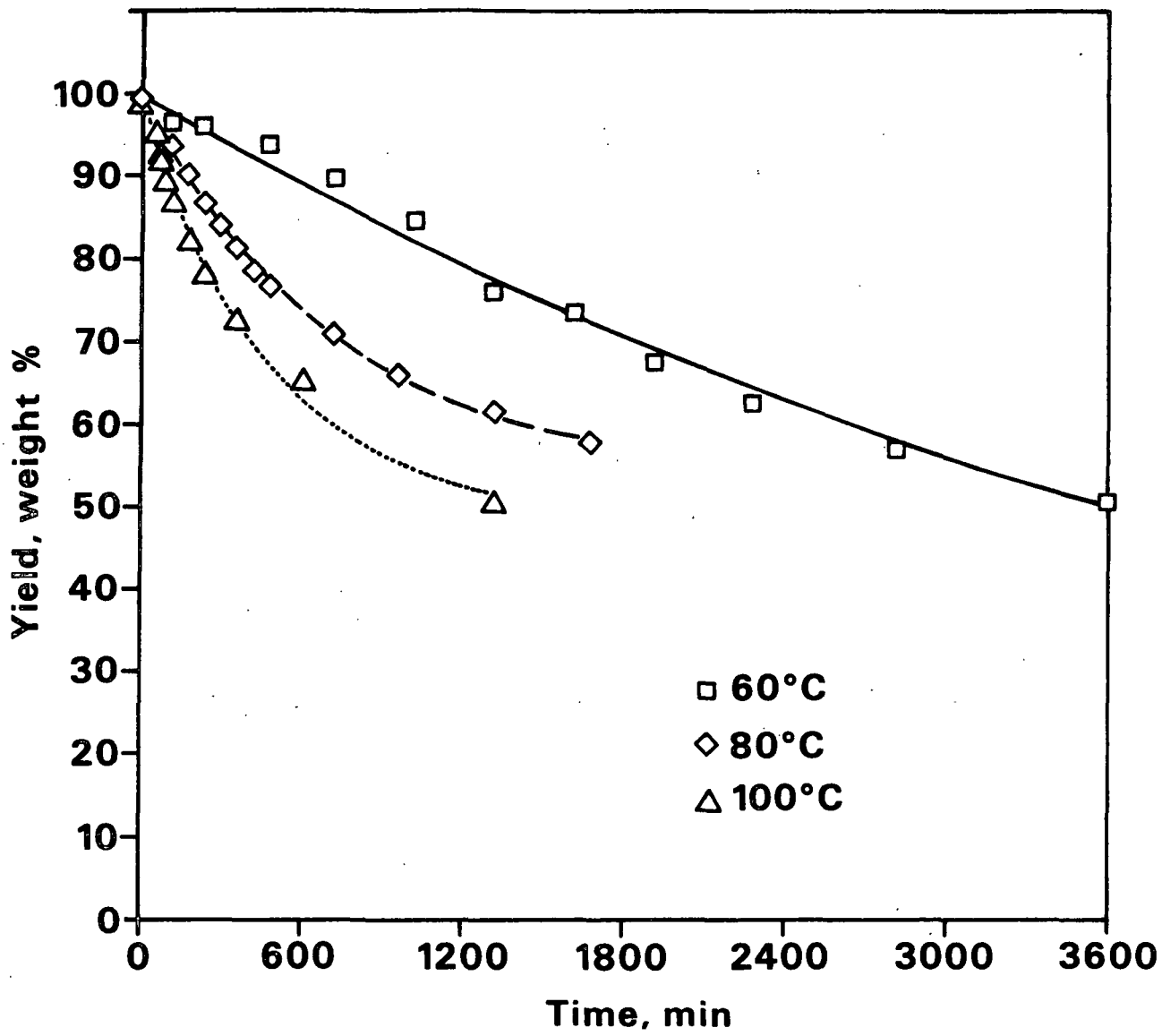

Figure 17. Amylose yield during degradation in 1.0M sodium hydroxide at 60°, 80°, and 100°C.

increases with increasing temperature, as is expected for a chemical reaction. Comparison of these slopes to the comprehensive model predictions (Fig. 10) suggests that the cleavage rates ranged from roughly 0.5×10^{-5} min^{-1} at 60° to 5.0×10^{-5} at 100°.

The cleavage rates estimated for amylose can be compared to rates obtained from disaccharide degradation studies. A recent study[43] of the high temperature (170-200°C) degradation of 1,5-anhydromaltitol was used to determine rate constants and an activation energy for the cleavage of α-(1,4) glucosidic bonds. Extrapolation of these results by the Arrhenius relation[39] indicates that the rate constant should be about 3×10^{-8} min^{-1} at 100°C. Thus, the apparent rate of cleavage for amylose is more than three orders of magnitude faster than the rate for simple model compounds.

Peeling and Stopping

The $\overline{DP}_N$ results for the degradation reactions are presented in Fig. 18. As expected, the fastest loss in $\overline{DP}_N$ occurred at the highest temperature, where cleavage was fastest. The peculiar dip in the 100°C curve provides a clue to interpreting the relative importance of the peeling and stopping reactions. This type of behavior was noted in simulations with the comprehensive model (Fig. 12) only at high ratios of the peeling rate to the stopping rate. In the simulations, the feature occurred when the number of molecules with acid ends became greater than the number of molecules with reducing ends. Figure 19 shows the 100° experimental $\overline{DP}_N$ and end group results plotted on the same time scale. Just as with the modeling results, the dip in the experimental $\overline{DP}_N$ curve is found at the point where the reducing end group and acid end group concentration curves cross. Recall that the model predicted that the dip will disappear at higher cleavage rates or at lower k_P to k_S ratios.

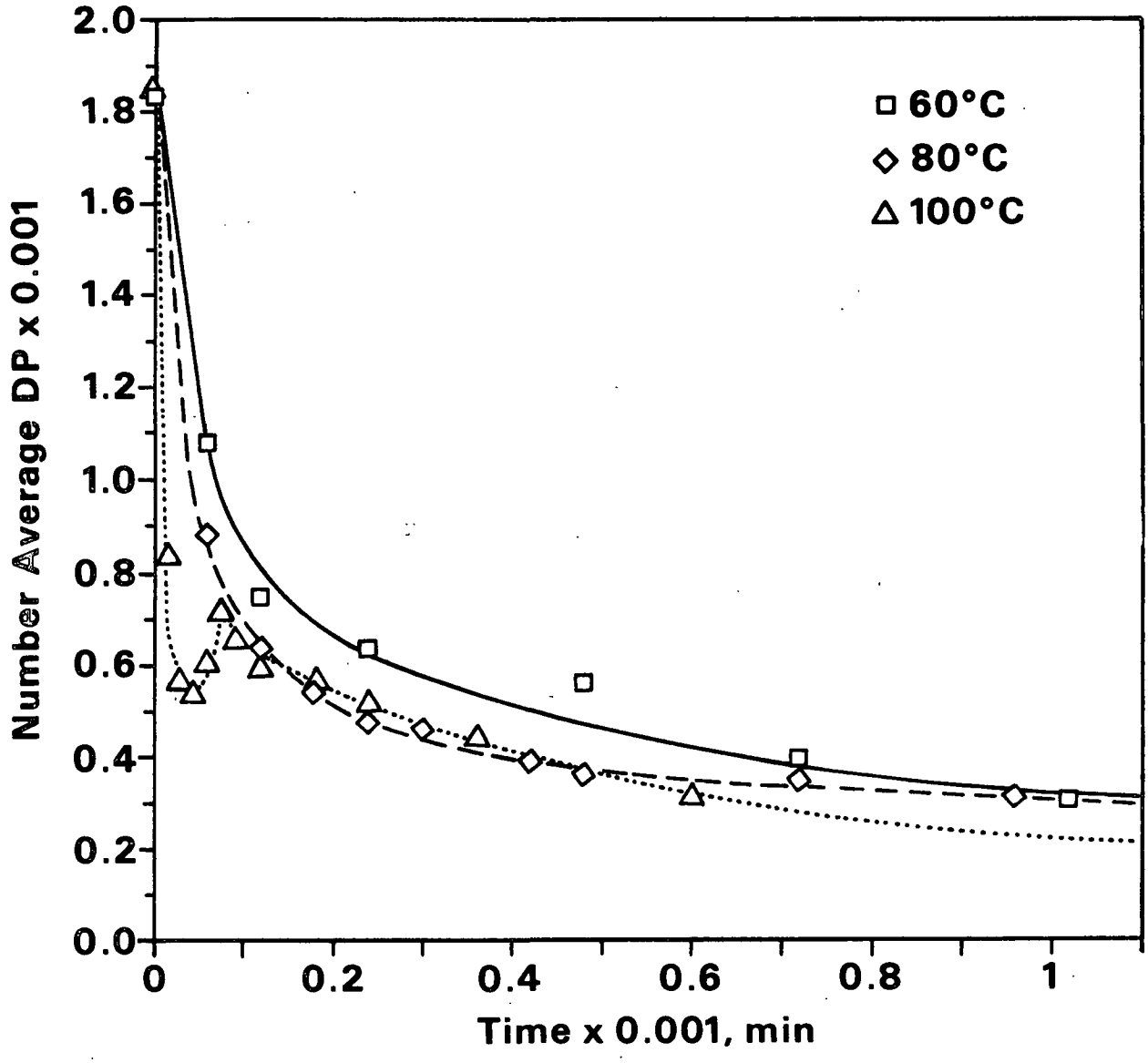

Figure 18. Amylose $\overline{DP}_N$ during degradation in 1.0M sodium hydroxide at 60°, 80°, and 100°C.

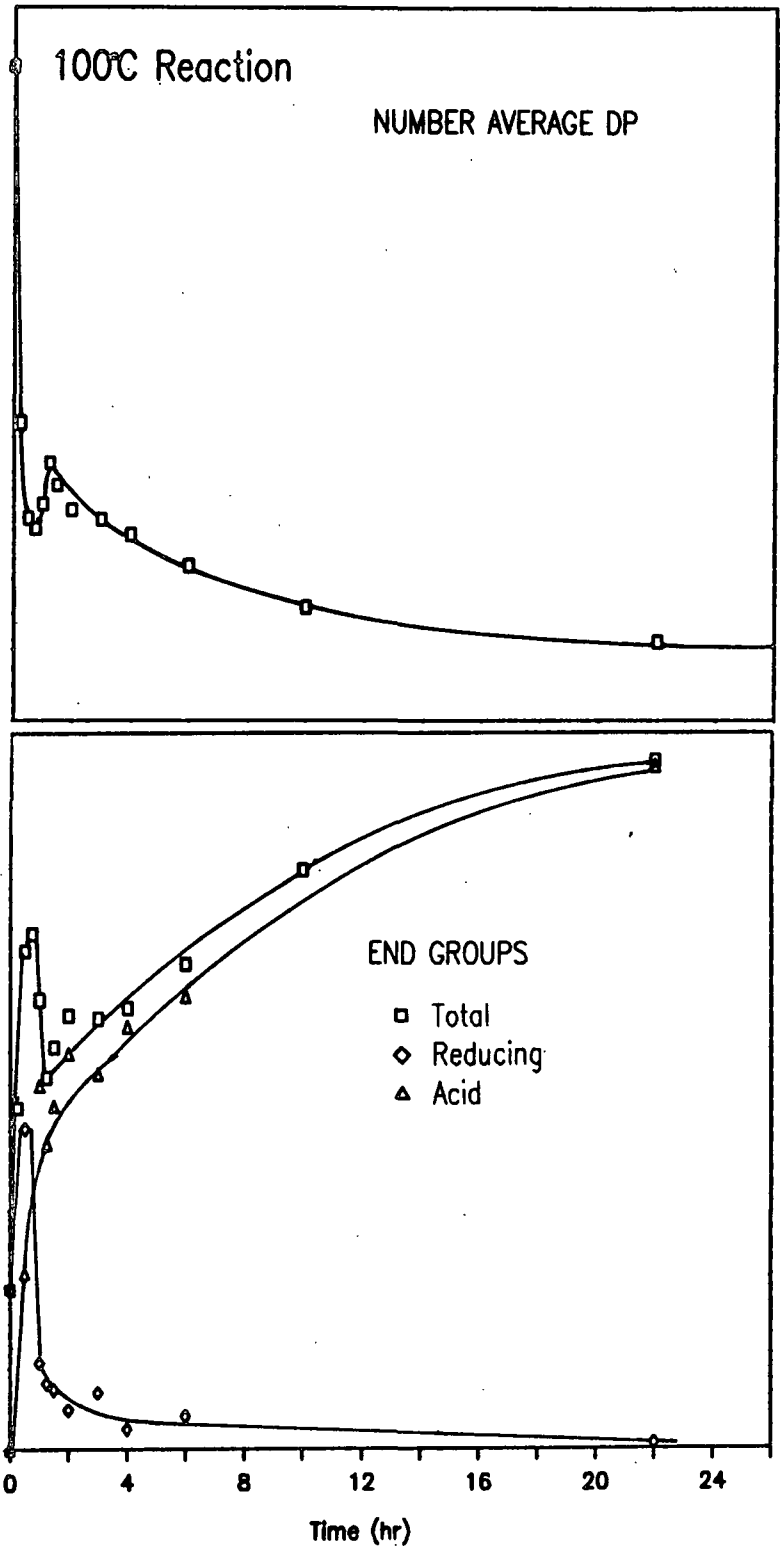

Figure 19. $\overline{DP}_N$ and end group concentrations during degradation of amylose in 1.0M sodium hydroxide at 100°.

In the experimental results, the dip feature disappears at lower temperatures. Because cleavage was slower at lower temperatures, this disappearance can be explained only by a decrease in the k_P to k_S ratio. Thus, it must be true that k_P/k_S increases with increasing temperature.

A greater importance of peeling relative to stopping at higher temperatures is consistent with other aspects of the experimental results. The total end group concentration at 1000 minutes in Fig. 15 is higher for the 60° reaction than for the 100° reaction. Since cleavage actually was producing new chains more rapidly at 100°, this behavior can only be explained by an increased importance of complete peeling at the higher temperature. More complete peeling occurs at higher values of k_P/k_S. The enhanced importance of complete peeling at higher temperatures can also explain the trends observed in reducing end group concentration (Fig. 16).

Reproducibility of Results

The 80°C degradation reaction was replicated to determine the reproducibility of the results. For each reaction, the quantities that are measured most directly are yield, $\overline{DP}_N$, and reducing end group concentration.

Figure 20 compares the yield results of the two reactions. There was very good agreement between the two sets of numbers.

Figure 21 shows the $\overline{DP}_N$ results for the two reactions. This quantity also displayed very good reproducibility.

Figure 22 compares the reducing end group concentration results. The same trends were observed in both reactions, but a moderate amount of statistical scatter is evident. This is not surprising, because of the large number of

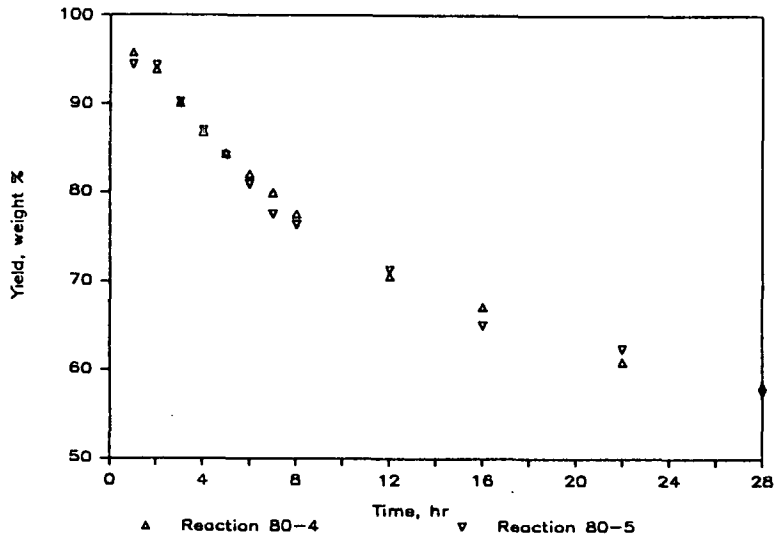

Figure 20. Yield results for duplicate 80°C reactions.

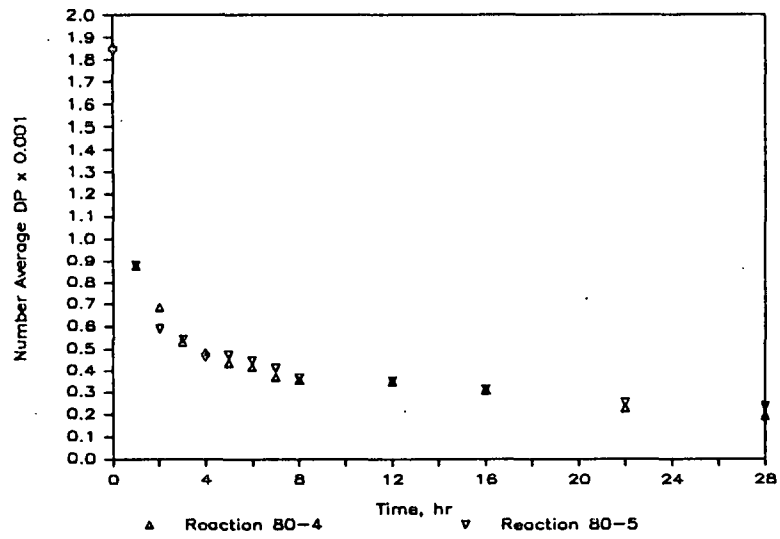

Figure 21. $\overline{DP_N}$ results for duplicate 80°C reactions.

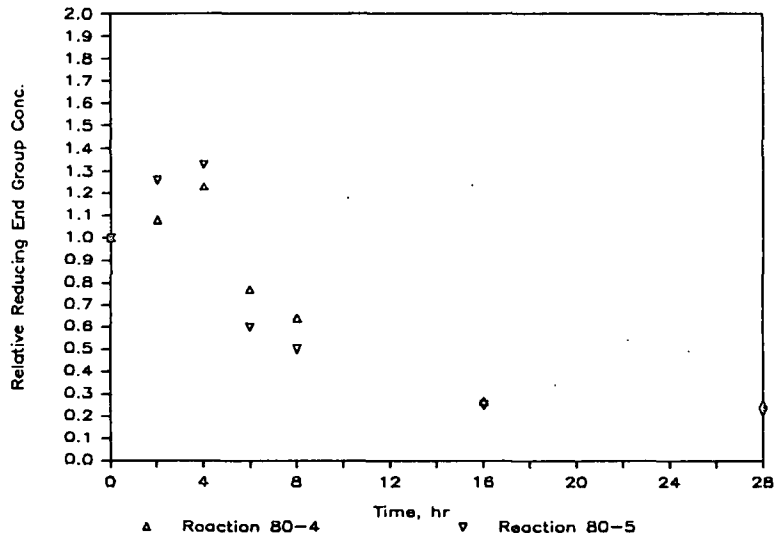

Figure 22. Reducing end group results for duplicate 80°C reactions.

individual measurements that go into each end group analysis. The quality of the results is sufficient to show that reducing ends are formed during degradation.

LIMITATIONS OF THE COMPREHENSIVE MODEL

The mathematical models of amylose degradation were developed with the objective of providing insights to aid in the interpretation of experimental data. In particular, the comprehensive model was used to examine what broad trends should be expected in the experimental results for various combinations of peeling, stopping, and chain cleavage rates. Some of the trends observed using the model were also seen in degradation experiments. The experimental results could be explained by comparison to the corresponding model cases. In this way, the model successfully achieved its objective.

The comprehensive model was not meant to serve as an engineering-type model, capable of predicting the precise value of each property at any given time, under any set of reaction conditions. In fact, the model has very limited usefulness in such a role, largely because of the assumption of a monodisperse starting material.

For example, it was possible to roughly match the model end group concentration and $\overline{DP}_N$ curves to the experimental curves. For the same combinations of rate constants that give a good match in end group concentrations, the model predicts larger yield losses than those observed experimentally. This discrepancy may be related to the fact that the experimental starting material was polydisperse. The polydisperse material contains some amylose chains of shorter lengths that are more likely than average to peel completely. Complete peeling destroys the reducing end before extensive yield loss can occur, and thus limits yield loss.

CONCLUSIONS

Complete peeling plays an important role in the alkaline degradation of soluble polysaccharides. For an amylose of moderate to high $\overline{DP}_N$ prepared from natural sources, some (but not all) of the molecules will peel completely. Preferential destruction of short molecules by complete peeling can actually cause the average molecular weight of a polysaccharide to increase during degradation, if chain cleavage is slow or nonexistent. Previous kinetic analyses have assumed that complete peeling does not occur,[14] that almost all molecules peel completely,[13] or that degradation by the peeling and stopping reactions must lead to a decrease in the average molecular weight of amylose.[16]

The random chain cleavage reaction occurs at significant rates at temperatures as low as 60°C for amylose in 1M sodium hydroxide. This finding is consistent with the report of low temperature cleavage in amorphous cellulose by Gentile *et al.*[9] Amylose, which is totally soluble in aqueous alkali, is more reactive toward cleavage than even amorphous cellulose, indicating that physical structure plays a very important role in limiting the degradation of cellulose. The glucosidic bonds of amylose cleave more than 1000 times faster than those of the simple model compound 1,5-anhydromaltitol, demonstrating the limitations of using simple compounds as models for polysaccharides. The rate of the chain cleavage reaction increases with temperature.

The ratio of the peeling rate to the stopping rate increases as temperature increases. This finding agrees with many previous studies,[13-16] and conflicts with others.[9-11]

Simple mathematical modeling techniques are useful in assisting in the interpretation of the complex process of polysaccharide degradation.

The initial $\overline{DP}_N$ and shape of the MWD of an amylose can exert an influence on the course of its degradation. Longer molecules are more susceptible to cleavage, and complete peeling becomes more important at low molecular weights. Puzzling observations reported in the literature can be explained by this finding. For example, it is no longer surprising that Ziderman and Bel-Ayche[19] observed drastic changes in the average DP of a high molecular weight amylose but little change in the average DP of a low molecular weight hydroamylose.

EXPERIMENTAL

PURIFICATION OF REAGENTS

Anhydrous Pyridine[44]

Potassium hydroxide (150 g) was mixed with reagent grade pyridine (1000 mL), and the mixture was refluxed for three hours. The pyridine was then fractionally distilled, and the first 200 mL were discarded. The next 600 mL was collected into amber glass bottles, which were tightly capped for storage.

Distilled Tetrahydrofuran

Reagent grade tetrahydrofuran (1500 mL) was fractionally distilled over lithium aluminum hydride.[44] The first 100 mL of distillate was discarded, and the next 1000 mL was collected into a round bottom flask. The purified reagent was used within 24 hours after distillation.

WASHING OF AMYLOSE

Many of the experimental techniques described below involved washing amylose or its derivatives with various solvents to remove impurities or by-products. Unless otherwise noted, this washing was accomplished by mixing the solvent with the amylose, stirring, centrifuging the mixture, and then removing the supernatant by suction.

ENZYMATIC SYNTHESIS OF AMYLOSE MOLECULAR WEIGHT STANDARDS

Background information about the development of this procedure is given in Appendix III.

Maltoheptaose, α-disodium glucose 1-phosphate, dithiothreitol, and rabbit phosphorylase *a* were purchased from Sigma Chemical Company (St. Louis, MO).

All reagent solutions used in the synthesis reactions were made up in β-glycerophosphate buffer (pH 6.80, 0.100M) which contained dithiothreitol (0.015M) and EDTA (0.001M).

Four synthesis reactions were conducted, numbered 1 through 4. Reaction 1 was designed to produce the lowest DP material, and Reaction 4 was designed to produce the highest.

Phosphorylase solution (17 units/mL, 25 mL) was placed in each of four flasks, and precisely measured volumes of maltoheptaose solution (4.65 mM) were added (25.42 mL for Reaction 1, 3.372 mL for Reaction 2, 0.5247 mL for Reaction 3, and 0.0804 mL for Reaction 4). The enzyme/maltoheptaose mixtures were incubated at 30°C for at least 45 minutes prior to initiating the reactions.

Buffer (25 mL) and α-disodium glucose 1-phosphate solution (0.125M, pH 6.80, 100 mL) were added to the four reaction vessels. The enzyme/maltoheptaose solutions were transferred quantitatively to the vessels, and additional buffer was used to bring the total volume up to a constant level (250.0 mL). The vessels were sealed, flushed with argon, and placed in a water bath at 30°C. Throughout the reactions, a gentle mixing was maintained by means of magnetic stirrers.

Periodically, samples were withdrawn from the vessels to check the progress of the reactions by inorganic phosphate analysis according to the method of Fiske and SubbaRow.[45] Additional enzyme was added as a concentrated solution (425 units/mL) after 46 hours to Reaction 2 (1.0 mL), Reaction 3 (1.0 mL), and Reaction 4 (2.0 mL) and again after 70 hours to Reaction 3 (1.0 mL) and Reaction 4 (1.0 mL).

The reactions were stopped when phosphate analysis showed that the desired conversion of glucose 1-phosphate to amylose had been reached. This occurred at

28 hours for Reaction 1, (33% conversion), 46 hours for Reaction 2 (40% conversion), 145 hours for Reaction 3 (46% conversion), and 188 hours for Reaction 4 (36% conversion). The syntheses were terminated by refluxing the reaction mixtures for 10 minutes under nitrogen, and the denatured enzyme was removed by filtering the hot solutions through a glass fiber disk.

The filtrate was poured into absolute ethanol (1500 mL), and the precipitate was allowed to settle overnight. The supernatant was removed by centrifugation and the precipitate was washed nine times with aqueous ethanol (50% v/v, 2 x 1500 mL, 7 x 900 mL), once with absolute ethanol (900 mL), and once with anhydrous ethyl ether (500 mL), and filtered on to a glass fiber disk from pentane (250 mL). The final products were dried under vacuum over phosphorus pentoxide at 30°C (yields: 0.66 g of Product 1, 0.83 g of Product 2, 0.94 g of Product 3, and 0.74 g of Product 4). Elemental analyses for nitrogen and phosphorus were used to verify that the products were essentially free of protein and phosphates.

The number average degree of polymerization of the products was determined by reducing end group analysis. The calculated $\overline{DP}_N$ for Product 1 was 41.4, for Product 2 was 366, for Product 3 was 2550, and for Product 4 was 6100. All products were shown to be free of α-(1,6) branch points by the fact that there were no changes in the MWDs after treatment with isoamylase (Fig. 23). The details of the branching analysis are described below.

ANALYSIS OF AMYLOSE FOR α-(1,6) BRANCHING

The debranching procedure described by Kobayashi et al.[23] was modified to allow recovery of the product so that the carbanilate derivative could be prepared and analyzed by gel permeation chromatography. Isoamylase was purchased

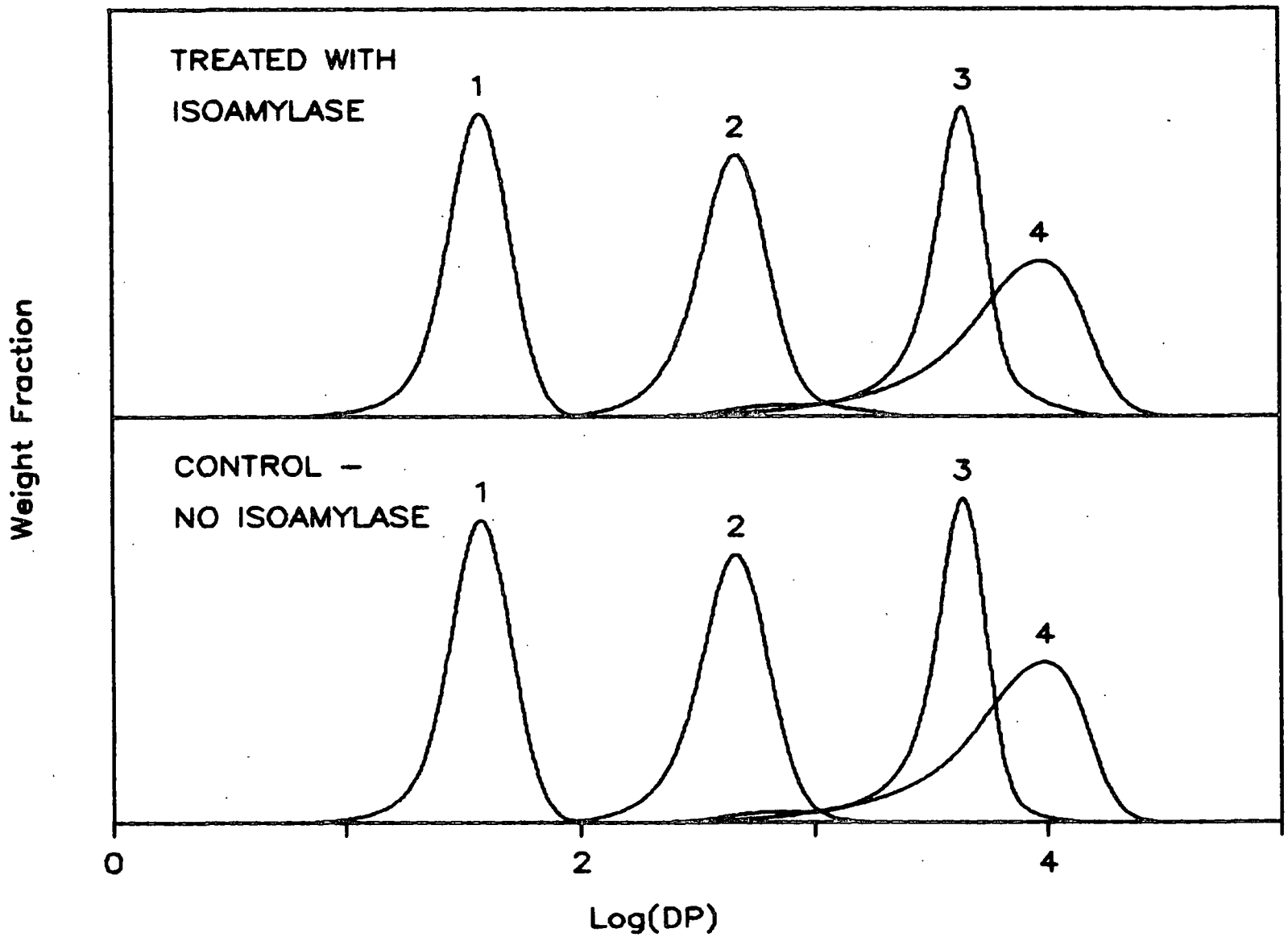

Figure 23. MWDs of enzymatically synthesized amyloses before and after treatment with isoamylase.

from Sigma Chemical Company (St. Louis). Before use, the enzyme (5000 units, 3500 units/mg protein) was washed of ammonium sulfate by diluting it with acetate buffer (pH 3.80, 0.1M, 5 mL) and concentrating it (to 0.5 mL) twice in a collodion bag apparatus. The resulting solution was diluted to a known volume (5.0 mL) with additional buffer and stored under refrigeration.

For each sample evaluated, two sample solutions were made. Amylose (30 mg) was dissolved in dimethyl sulfoxide (2.00 mL) and mixed with acetate buffer (2.00 mL) and water (3.00 mL). Isoamylase solution (0.590 mL) was added to one of the solutions (treated) and an equal volume of buffer was added to the other (control).

The samples were incubated at 40°C for 24 hours in a water bath. The polysaccharides were precipitated by pouring the solutions into absolute ethanol (50 mL), washed three times with absolute ethanol (100 mL), once with anhydrous ethyl ether (50 mL), and once with pentane (50 mL), and dried under vacuum at 30°C over phosphorus pentoxide.

All of the samples were carbanilated and analyzed by GPC using the same procedure as is described below for $\overline{DP}_N$ determination. A sample was judged to be free from α-(1,6) branches if no differences were detected between the control and treated sample chromatograms. Amylopectin was subjected to the analysis to verify the reliability of the technique. As demonstrated by Fig. 24, amylopectin was debranched by the treatment.

PREPARATION OF SUBSTRATE AMYLOSE

Amylose (48 g, Potato Type III, Lot 75F-3854, Sigma Chemical Co.) was dissolved in dimethyl sulfoxide (8.64 L), and ethanol (3.84 L) was added slowly

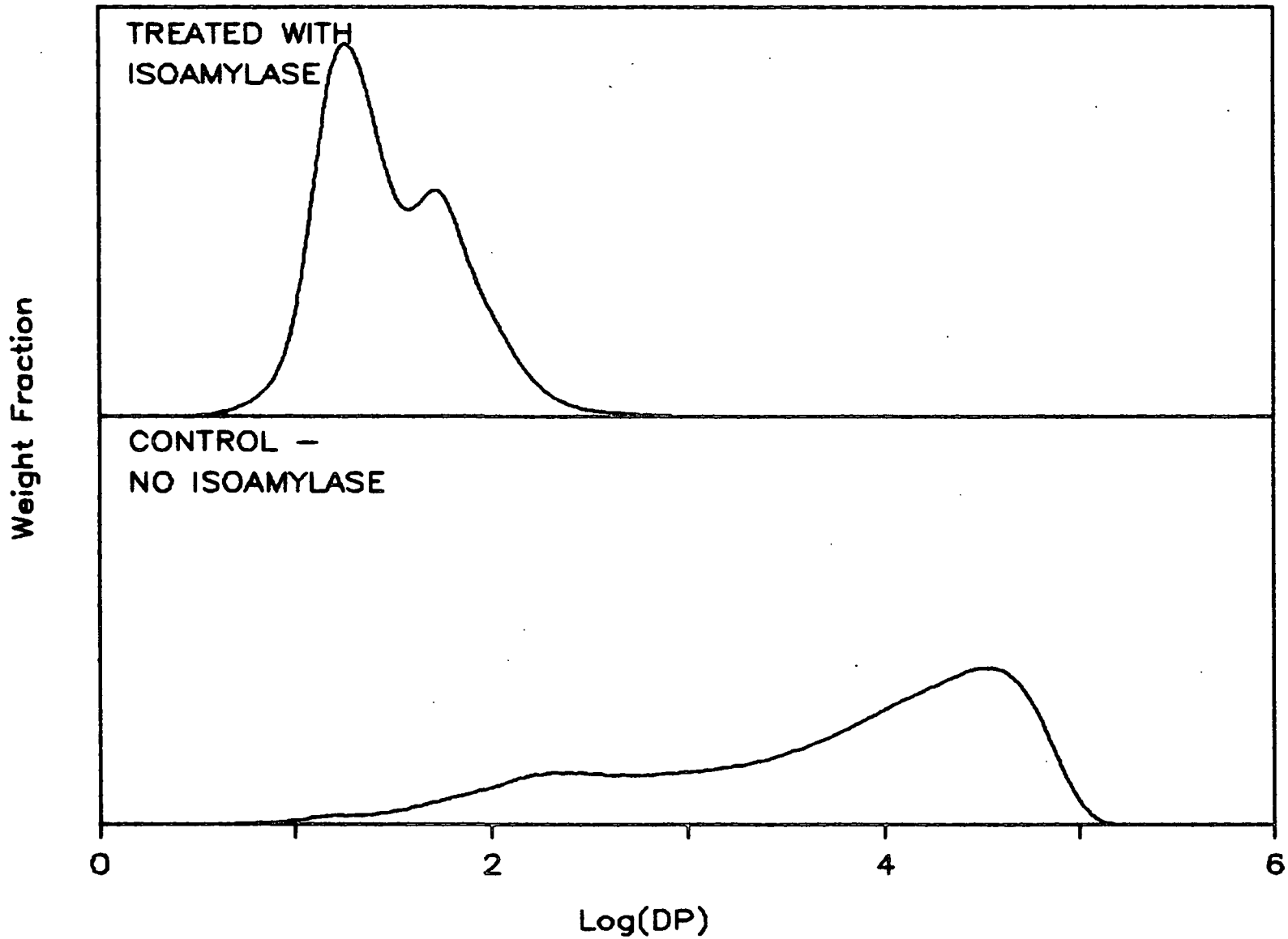

Figure 24. MWD of amylopectin before and after treatment with isoamylase.

with stirring. A small amount of undissolved material was removed by centrifugation, and additional ethanol was added until the solution became noticeably cloudy. The cloudy precipitate was removed by centrifugation and discarded.

The remaining amylose was precipitated by adding absolute ethanol (10.0 L) to the supernatant, and washed three times with absolute ethanol (3.5 L), once with anhydrous ethyl ether (1.0 L), and once with pentane (1.0 L). The precipitate was dried under vacuum over phosphorus pentoxide at 40°C.

The dry powder was made into a slurry with cold water and added to a flask of vigorously boiling water (the total volume of water used was 1800 mL). After refluxing for 45 minutes under nitrogen, any undissolved material was removed by centrifugation of the hot mixture. The supernatant was reheated to near boiling, and n-butanol (120 g) was added. The hot flask was wrapped with paper towelling for insulation and left to cool slowly overnight. The resulting grainy white crystals were washed with saturated aqueous n-butanol (1500 mL), and then redispersed in boiling water and crystallized a second time. The recrystallized material was washed once with saturated aqueous n-butanol (1000 mL), five times with ethanol (1000 mL), twice with anhydrous ethyl ether (1000 mL), and once with pentane (1000 mL). The final product was dried under vacuum over calcium sulfate at 40°C (yield: 19.10 g, 39.8%).

The branching analysis described above was used to monitor the amount of branched impurity during the purification. Figure 25 demonstrates that essentially all of the branched material was eliminated by the procedure described. Branched material was evident in the raw amylose because of the low DP peak that developed upon treatment with isoamylase. This peak was virtually nonexistent when the purified amylose was treated with the enzyme.

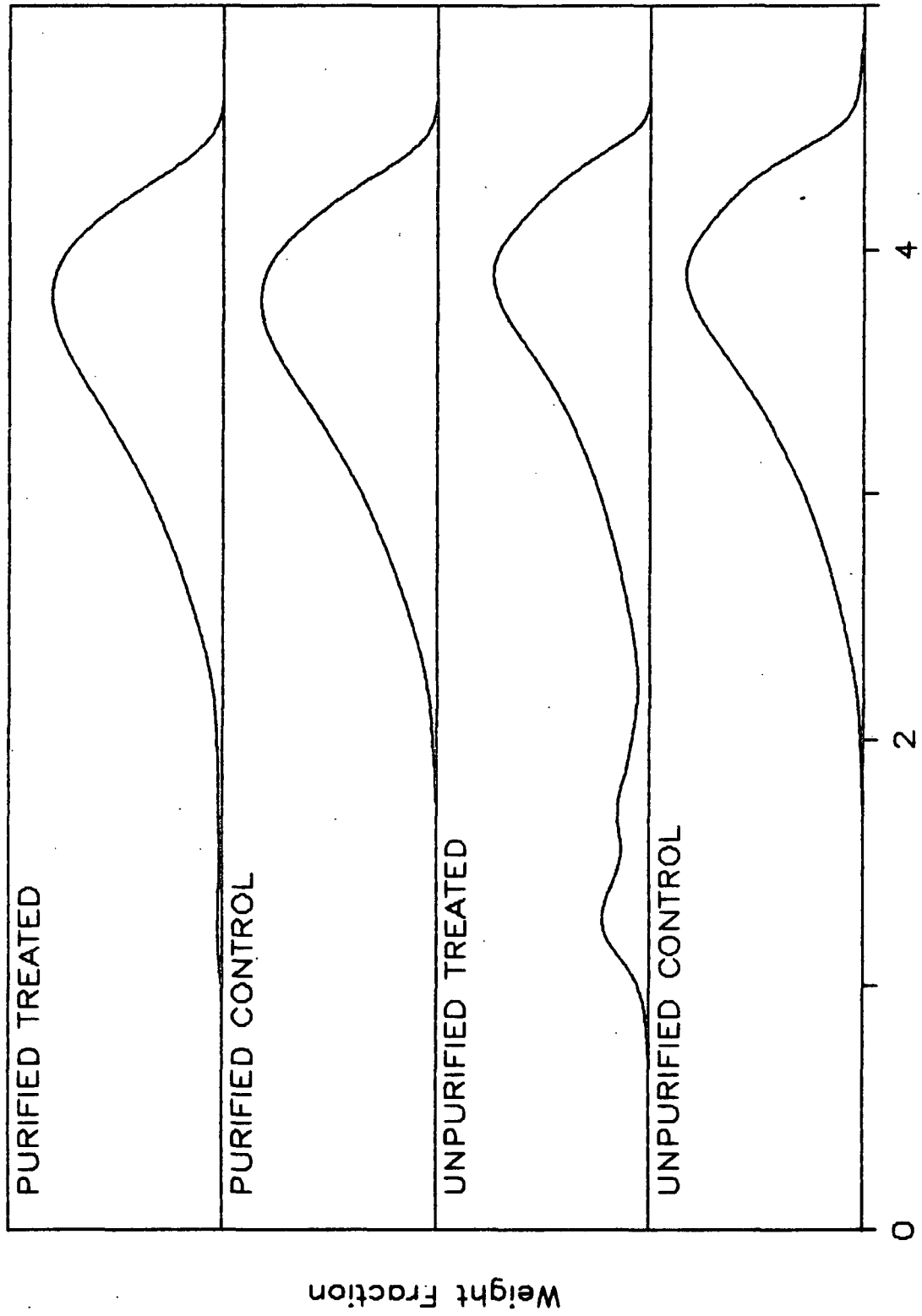

Figure 25. MWD of unpurified and purified substrate amylose, before and after treatment with isoamylase.

MEASUREMENT OF $\overline{DP}_N$ AND MWD

Carbanilation

Anhydrous pyridine (4 mL) and phenyl isocyanate (0.25 mL) were added to amylose samples (10 mg) in glass hypo vials. The vials were flushed with nitrogen and sealed. After 48 hours at 80°C, the excess phenyl isocyanate was expended by adding methanol (0.125 mL), and the carbanilate solutions were diluted with dioxane (8 mL). When accurate yield determinations were to be made, the solutions were filtered through a Whatman GF/C glass fiber filter disk to remove any unreacted polysaccharide. The carbanilates were precipitated into a mixture of water (20 mL), methanol (40 mL), and acetic acid (0.4 mL). The precipitates were washed once with a mixture of water (11.5 mL), methanol (21.5 mL) and acetic acid (0.2 mL), once with a mixture of water (32 mL) and acetic acid (0.2 mL), and twice with water (65 mL). Final drying was accomplished by freeze drying.

Gel Permeation Chromatography

Gel permeation chromatography was performed at 21.1°C on a Jordi-Gel Mixed Bed (High MW) column (Jordi Associates, Mills, MA) using distilled tetrahydrofuran as the mobile phase. The detector was a Perkin-Elmer LC-55 B UV spectrophotometer, set to measure absorbance at 235 nm. The injector loop volume was 200 µL, and the flow rate was 1.50 mL per minute. Elution volumes were measured relative to a low molecular weight, total permeation standard, methyl N-phenyl carbamate.[46] Sample (0.5-5.0 mg) was dissolved in distilled tetrahydrofuran (5 mL), and methyl N-phenyl carbamate solution (2.5% w/v in stabilized tetrahydrofuran, 3 µL) was added. Before injection, all carbanilate solutions were filtered through 0.45 µm nylon or Teflon syringe filters.

The column was calibrated using the enzymatically prepared amylose molecular weight standards and maltoheptaose, according to the dispersion-compensated method of McCracken.[47,48] Chromatograms were collected and stored digitally using an IBM PC microcomputer and a Tecmar Labmaster analog to digital converter (Tecmar, Inc., Solon, Ohio). Molecular weight averages were computed from the chromatograms using the microcomputer.

REACTION PROCEDURE

Preparation of Sodium Hydroxide Solution

Oxygen-free water was prepared by refluxing distilled water (1400 mL) under prepurified nitrogen for fifteen minutes. A stream of nitrogen was bubbled through the water as it cooled, and the flask containing the liquid was tightly stoppered and transferred to a glove bag.

The glove bag was loaded with the necessary equipment and chemicals and sealed. The bag was filled with prepurified nitrogen and evacuated three times before being filled with nitrogen a final time.

In order to prepare a sodium hydroxide solution that would be 1.0M at the reaction temperature, it was necessary to correct the room temperature concentration for the expansion of the solution with temperature. It was assumed that the percentage expansion would be the same for sodium hydroxide as for pure water. Thus, the proper room temperature concentration, $[NaOH]_{RT}$, was determined by the relation

$$[NaOH]_{RT} = 1\underline{M} \times \frac{d_{20}}{d_T} \qquad (11)$$

where d_{20} and d_T are the densities (in g/cm^3) of water at 20°C and at the

reaction temperature, respectively. One liter of this solution should weigh (in grams)

$$1.0410 \times \frac{d_{20}}{d_T} \times 1000 \qquad (12)$$

where 1.0410 is the density of 1M NaOH at 20°C (g/cm^3).[49]

One 1N Acculute sodium hydroxide vial (Anachemia Chemicals, Inc., Champlain, NY) was opened, emptied into a beaker, and rinsed three times with oxygen-free water. The solution was diluted with additional oxygen-free water to the proper weight of one liter at temperature, determined from Eq. (12). Some of the solution was removed for checking the molarity and the rest was placed in a tightly stoppered flask and left in the glove bag. The molarity was checked by three titrations against potassium acid phthalate (ca. 3 g, weighed analytically), and was always found to be within 0.5% of the desired concentration.

Reactor Loading

The amylose degradation reactions were conducted in a Teflon-lined stainless steel reactor equipped with a magnetic stirrer, a platinum resistance temperature detector, an ice-cooled sampling line, and a gas-tight Teflon capsule attached to a pressurization port. The reactor is shown schematically in Fig. 26.

A solid disk of Teflon was forced into the top of the amylose capsule. This disk served as a piston to push the amylose out into the reactor when the capsule was pressurized. Teflon thread seal tape was wrapped around the perimeter of the disk to ensure an air-tight seal with the walls of the capsule. The capsule and disk were dried for 12 hours in a vacuum oven at 105°C.

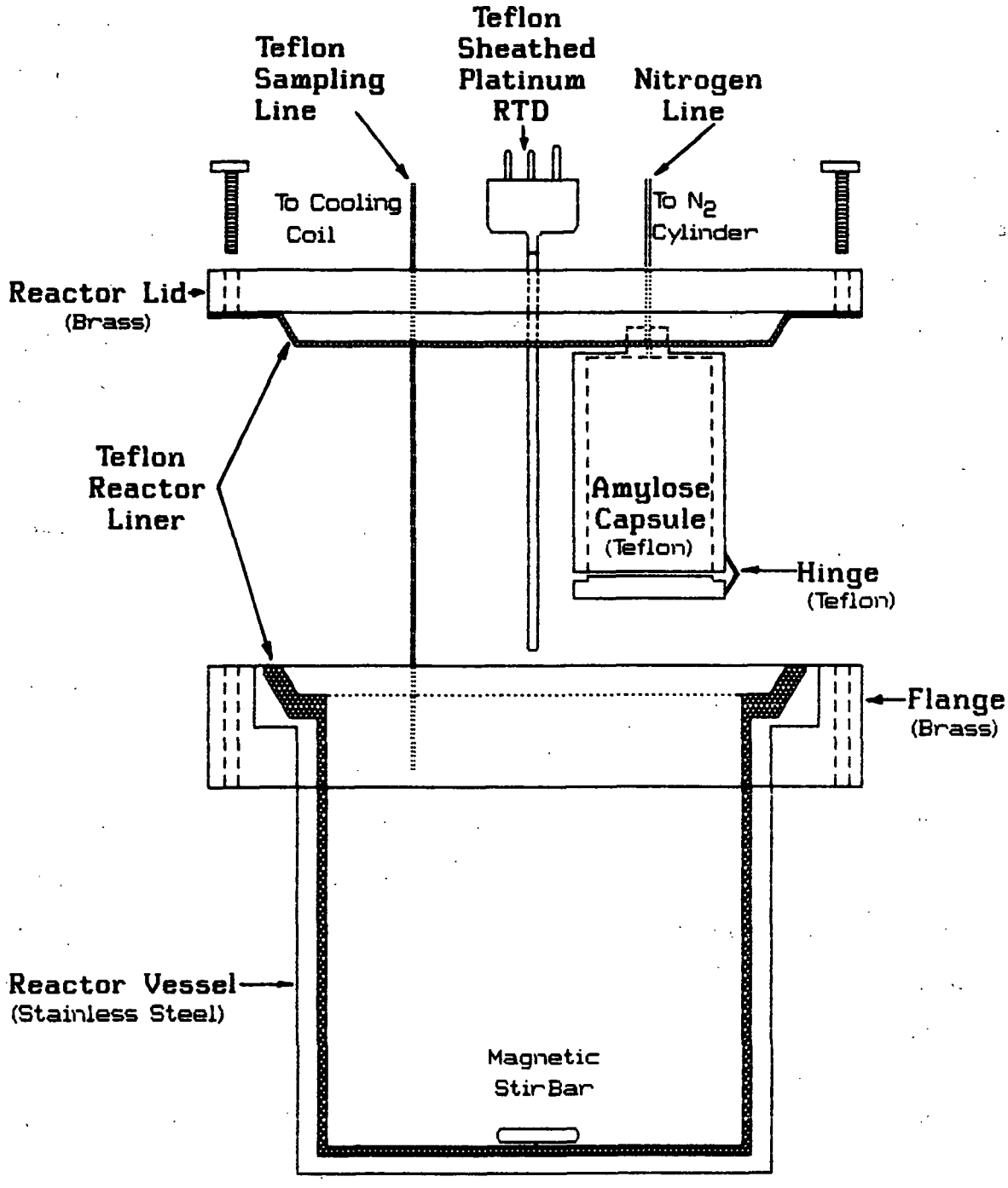

Figure 26. Reactor.

Substrate amylose (ca. 2.5 g) was weighed into the capsule and dried in a vacuum oven over calcium sulfate for 12 hours at 100°C. During drying, a stream of dry air was continuously fed into the oven. The capsule and its contents were then reweighed to determine the dry weight of the amylose. In a glove bag under nitrogen, the proper amount of sodium hydroxide solution to give a 1% w/v amylose solution at the reaction temperature was weighed into the Teflon reactor liner. The liner was lowered into the reactor shell, and a one inch long magnetic stir bar was dropped into the liquor. Next, the capsule was screwed into its place in the lid, and the reactor was tightly sealed while it was still in the glove bag.

Sample and nitrogen lines were attached to the reactor, and it was lowered into the oil bath. The oil bath had a volume of about 7.5 gallons and was heated with Vycor immersion heaters (Corning Glass Works, Corning, NY). Its temperature was controlled to within 0.1°C with a Model 4201 RTD Temperature Controller (Omega Engineering, Inc., Stamford, CT). The bath was equipped with a mechanically driven magnetic stirrer.

During the heat-up period, the magnetic stirrer turned at 500 rpm. When the contents reached the desired temperature, the reactor was pressurized with prepurified nitrogen (to 150 psig) through the capsule line. Upon pressurization, the reactor was shaken and pounded to ensure that the amylose fell into solution. The rotation rate of the magnetic stirrer was then decreased to 345 rpm.

At the desired sampling intervals, solution (ca. 2.0 mL) was first withdrawn to purge the sample line. Then reaction solution (15-20 mL) was withdrawn through the ice-cooled sample loop into a chilled graduated cylinder. Four aliquots (0.200 mL each) were withdrawn from the reaction solution for yield determination and placed into 8 mL screw cap vials. The vials were stored under

refrigeration until the degradation reaction was completed. The remainder of the sample was approximately neutralized with concentrated hydrochloric acid and precipitated into absolute ethanol (200 mL). The degraded amylose was recovered from the precipitate, as described below.

Recovery of Degraded Amyloses

The degraded amyloses which had been precipitated into alcohol were recovered by washing them four times with absolute ethanol (200 mL), once with ethyl ether (100 mL), and once with pentane (50 mL). After most of the pentane was removed by suction, the remaining slurries were transferred to 8 mL screw cap vials. The vials were centrifuged and additional pentane was removed. The vials were then placed in a vacuum oven at 40°C over desiccant for two days.

Yield Analysis

Yield was determined by hydrolyzing the amylose and measuring the resulting glucose concentration by the hexokinase method.[16,50] Hydrochloric acid (1M, 1.0 mL) was added to each of the vials containing samples withheld for yield determination, and the vials were capped and placed in a pressure cooker. The cooker was kept at 120°C for one hour, and then allowed to cool to room temperature. Sodium hydroxide solution (2M, 0.4 mL) was added to approximately neutralize the solutions. Next, the hydrolyzates were diluted to a controlled volume (10.0 mL) with Trizma buffer (0.05M, pH 7.60, Sigma Chemical Co.).

The contents of one assay vial (Sigma Chemical No. 16-UV) were dissolved in water (50.0 mL). Portions of the resulting enzyme solution (1.00 mL) were then pipetted into disposable microcuvettes, and initial optical absorbance readings were measured against water at a wavelength of 340 nm. Sample solution (0.100

mL) was added to each cuvette, and the final absorbance was recorded after at least five minutes had elapsed. The change in absorbance, ΔA, was calculated as the difference between the final and initial absorbance readings, and the glucose concentration in the hydrolyzate was computed by

$$G_H = \frac{\Delta A \times V_T \times M_G}{A_{NADH} \times V_H} = 0.3186\ \Delta A \qquad (13)$$

where G_H = glucose concentration in hydrolyzate (mg/mL)

V_T = total volume of liquid in cuvette (1.10 mL)

M_G = weight of one µmol of glucose (0.18016 mg)

A_{NADH} = optical absorbance of a 1 µmol/mL solution of NADH (6.22)

V_H = volume of hydrolyzate in cuvette (0.10 mL).

The yield of amylose was then calculated according to

$$Y = \frac{G_H \times V_{TH}}{V_S \times C_A} \times \frac{M_{AG}}{M_G} \times \frac{d_T}{d_{20}} \times 100 \qquad (14)$$

where Y = amylose yield (weight %)

V_{TH} = total volume of diluted hydrolyzate (10.0 mL)

M_{AG} = weight of one µmol of anhydroglucose (0.16214 mg)

d_T = density of water at reaction temperature (g/cm^3)

V_S = volume of reaction solution hydrolyzed (0.200 mL)

C_A = initial amylose concentration at reaction temperature (10.0 mg/mL)

d_{20} = density of water at 20°C (g/cm^3)

The four aliquots withheld at each sampling time were analyzed separately, and the results were averaged.

The amylose yield curves obtained in this way did not extrapolate exactly to 100% at the beginning of the reaction. Arbin[16] also observed this trend, and attributed it to amylose sticking to the sides of the capsule and to inaccuracies in the moisture content determination. In order to objectively correct the yield curves to a zero-time yield of 100%, a nonlinear curve of the form

$$Y_F = (P_1 - P_3) \times \exp(P_2 \times t) + P_3 \qquad (15)$$

was fit to the raw yields,

where Y_F = yield predicted by the fitted equation (weight %)

t = time (min)

P_1 = parameter for predicted yield at time zero (weight %)

P_2 = parameter for exponential decay rate (min^{-1})

P_3 = parameter for predicted leveling-off yield (weight %)

The computer program BMDP AR was used to fit the curves.[51] The parameters calculated for the successful degradation reactions are listed in Table 4.

Table 4. Curve fitting results for yield data.

Reaction	P1	P2	P3
60°	103.3	-0.01155	0.00
80° (80-4)	105.5	-0.08127	56.44
80° (80-5)	107.3	-0.08767	58.37
100°	94.6	-0.12990	46.15

Yields were corrected by dividing the yield at each sampling time by P_1. The corrected yields are listed in Appendix IV, along with the smoothed corrected yields calculated by correcting the values predicted by Eq. (15). The smoothed

yields were used in subsequent calculations of end group concentrations, because the function fit the data well and helped to correct for statistical scatter in the results.

END GROUP ANALYSIS

Reducing End Groups

The method used for reducing end group determination is based on that of Manners et al.,[52] but the procedure given here includes several modifications necessary for applying the technique to amyloses of high DP. Sorbitol dehydrogenase and nicotinamide adenine dinucleotide (NAD) were purchased from Boehringer Mannheim Biochemicals (Indianapolis).

Amylose (40 mg) was dissolved in dimethyl sulfoxide (1.0 mL) and sodium borohydride solution (50 mg sodium borohydride in 0.5 mL water and 1.5 mL dimethyl sulfoxide) was added. After shaking for 48 hours at room temperature, excess borohydride was destroyed with hydrochloric acid (2.2M, 0.50 mL), and the samples were poured into absolute ethanol (10-12 mL). The resulting precipitates were washed three times with absolute ethanol (10-12 mL), once with anhydrous ethyl ether (10-12 mL), and dried from pentane (2-5 mL) under vacuum at 40°C over calcium sulfate.

The reduced amyloses were hydrolyzed with trifluoracetic acid (2M, 15 mL) at 120°C for one hour. The hydrolyzates were dried by vacuum evaporation (40-50°C), and residual acid was removed by three evaporations (40-50°C) to dryness from water (5.0 mL). In order to remove traces of borate which interfered with the glucitol assay, it was necessary to evaporate (30-40°C) the product to dryness four times from methanol (5 mL). This removed the borate as methyl

borate. The final mixtures of glucose and glucitol were dried under vacuum at 40°C over calcium sulfate.

The dry hydrolyzates were dissolved in pyrophosphate buffer (pH 9.50, 0.1M, 2-4 mL) and the pH of the resulting solutions was adjusted to 9.50 ± 0.02 with sodium hydroxide solution (2.0M). Duplicate aliquots (0.1 mL) were removed for glucose analysis by the hexokinase method.[50] Further volumetric dilution with pyrophosphate buffer was then done on materials with a high reducing end group content, such as the low DP calibration standards, to bring the glucitol concentration into the proper range (2-15 mg/L) for analysis.

Immediately before conducting the glucitol analysis, a stock assay solution was prepared by combining pyrophosphate buffer (20.00 mL) with NAD solution (20 mM, 4.00 mL) and water (15.00 mL). Stock solution (1.00 mL) and sample (0.50 mL) were added to a spectrophotometer cell, and an initial absorbance reading was taken at 340 nm. Sorbitol dehydrogenase solution (160 U/mL, 25 µL) was then added and the final absorbance was recorded after 40 minutes elapsed. The glucitol concentration was calculated from the change in absorbance, assuming that one mole of NAD is reduced to NADH per mole of glucitol present, using a molar extinction coefficient[52] for NADH at 340 nm of 6.22×10^6 cm^2.

When solutions containing glucose but no glucitol were analyzed, a small change in absorbance was noted. Therefore, it was necessary to correct the absorbance readings of unknown samples before calculating glucitol concentrations. A correction curve was prepared for each set of assays by concurrently analyzing several glucose solutions of known concentration (0 to 30 g/L) and plotting absorbance versus concentration.

Duplicate glucitol determinations were done on each hydrolyzate solution. The average number of monomers per reducing end ($\overline{DP}_R$) was determined from the molar concentrations of glucose and glucitol according to the relation

$$\overline{DP}_R = \frac{[\text{Glucose}] + [\text{Glucitol}]}{[\text{Glucitol}]} \qquad (16)$$

For the enzymatically synthesized amylose molecular weight standards, $\overline{DP}_R$ is equivalent to $\overline{DP}_N$, because the standards contain one reducing end per molecule. Each standard was assayed in triplicate, and the average mean deviation between replicates was 2.7%. Maltoheptaose was analyzed by the method and had a calculated $\overline{DP}_R$ of 7.03, demonstrating the accuracy of the technique.

For degraded amyloses, the relative concentration of reducing ends, $[N_R]_{REL}$ could be calculated by

$$[N_R]_{REL} = \frac{Y_t}{100} \times \frac{\overline{DP}_{R,0}}{\overline{DP}_{R,t}} \qquad (17)$$

where Y_t is the weight percent yield at time t and $\overline{DP}_{R,0}$ and $\overline{DP}_{R,t}$ are the $\overline{DP}_{Rs}$ at the start of the reaction and at time t, respectively.

Total and Acid End Groups

The relative molar concentration of total end groups, $[N_T]_{REL}$ was calculated from the yield and the number average degree of polymerization, according to the equation

$$[N_T]_{REL} = \frac{Y_t}{100} \times \frac{\overline{DP}_{N,0}}{\overline{DP}_{N,t}} \qquad (18)$$

where $\overline{DP}_{N,0}$ and $\overline{DP}_{N,t}$ are, respectively, the $\overline{DP}_N$ at the start of the reaction and the $\overline{DP}_N$ at time t.

The acid end group concentration, $[N_A]_{REL}$, determined relative to the initial total end group concentration, was calculated as the difference between the total ends and acid ends,

$$[N_A]_{REL} = [N_T]_{REL} - [N_R]_{REL} \quad (19)$$

ACKNOWLEDGMENTS

The author would like to thank the members of his thesis advisory committee - Dr. L. R. Schroeder, Dr. R. A. Halcomb, and Dr. M. A. Johnson - for their interest and participation in this research project.

The many contributions of staff members are also acknowledged, in particular: Leon Straub, Marvin Filz, Paul Van Rossum, and Glen Winkler. For their ongoing assistance throughout the course of the project, the author is grateful to the computer center staff: Mike Gabrielski, Sue Pociask, and Joanne Klinkert. The help of fellow students too numerous to mention has also been greatly appreciated.

Most importantly, the author would like to thank his wife, Cindy, and his sons, Danny and Luke, for their love, encouragement, and patience.

Finally, for providing the opportunity to pursue such an interdisciplinary line of research, the author gratefully acknowledges The Institute of Paper Chemistry and its member companies.

LITERATURE CITED

1. Meller, A., Holzforschung 14:78-89(1960).

2. Rydholm, S., Pulping Processes. New York, Interscience 1965:596-605.

3. Janes, R. L. In MacDonald and Franklin's Pulp and Paper Manufacture. 2nd ed., Vol. I: The Pulping of Wood, p. 33-73, McGraw-Hill, New York, 1969.

4. Sjostrom, E., Wood Chemistry: Fundamentals and Applications, Academic Press, New York, 1981.

5. Green, J. W.; Pearl, I. A.; Hardacker, K. W.; Andrews, B. D.; Haigh, F. C., Tappi 60(10):120-125(1977).

6. MacLeod, J.; Schroeder, L. R., J. Wood Chem. Technol. 2:187-205(1982).

7. MacLaurin, D. J.; Green, J. W., Can. J. Chem. 47:3957-64(1969).

8. MacLaurin, D. J.; Green, J. W., Can. J. Chem. 47:3947-55(1969).

9. a) Gentile, V.; Schroeder, L. R.; Atalla, R. A., ACS Symp. Ser. (In press).
   b) Gentile, V. Effects of Physical Structure on the Alkaline Degradation of Hydrocellulose. Doctoral Dissertation. Appleton, WI, The Institute of Paper Chemistry, June, 1986.

10. Haas, D. W.; Hrutford, B. F.; Sarkanen, K. V., J. Appl. Polym. Sci. 11:587-600(1967).

11. Lai, Y.; Sarkanen, K. V., Cellulose Chem. Technol. 1:517-27(1967).

12. Franzon, O.; Samuelson, O., Svensk Papperstid. 60:872-7(1957).

13. Ziderman, I.; Bel-Ayche, J., J. Appl. Polym. Sci. 22:1151-8(1978).

14. Lai, Y.; Sarkanen, K. V., J. Polymer Sci. C28:15-26(1969).

15. Richards, G. N.; Sephton, H. H., J. Chem. Soc. 1957:4492-9(1957).

16. a) Arbin, F. L. A.; Schroeder, L. R.; Thompson, N. S.; Malcolm, E. W., Cellulose Chem. Technol. 15:523-34(1981).
   b) Arbin, F. L. A. The Effect of Oxygen and Anthraquinone on the Alkaline Depolymerization of Amylose. Doctoral Dissertation. Appleton, WI, The Institute of Paper Chemistry, June, 1980.

17. Brandon, R. E.; Schroeder, L. R.; Johnson, D. C., Cellulose Technology Research, ACS Symp. Ser. 10:125-146(1975).

18. Best, E. V. Kinetics of Hot Alkaline Cleavage of the Glycosidic Bonds of Methyl-a-D-glucoside and Methyl-a-cellobioside. Doctoral Dissertation. Appleton, WI, The Institute of Paper Chemistry, June, 1968.

19. Ziderman, I.; Bel-Ayche, J., J. Appl. Polymer Sci. 23:3427-30(1979).

20. Ziderman, I.; Weiss, N., J. Appl. Polymer Sci. 23:1883-7(1979).

21. Machell, G.; Richards, G. N., J. Chem. Soc. 1958:1199-1204(1958).

22. Ziderman, I.; Bel-Ayche, J., J. Appl. Polymer Sci. 22:711-18(1978).

23. Kobayashi, S.; Schwartz, S. J.; Lineback, D. R., J. Chromat. 319:205-14 (1985).

24. Takeda, Y.; Shirasaka, K.; Hizukuri, S., Carbohyd. Res. 132:83-92(1984).

25. Hizukuri, S.; Takeda, Y.; Yasuda, M.; Suzuki, A., Carbohyd. Res. 94:205-13(1981).

26. Bourne, E. J.; Haworth, W. N.; Macey, A.; Peat, S., J. Chem Soc. 1948:924(1948).

27. Ederer, H. J.; Basedow, A. M.; Ebert, K. H., In Ebert, Deuflhard, and Jager's Modelling of Chemical Reaction Systems: Proceedings of an International Workshop, Heidelberg, September 1-5, 1980. p. 189-215, Springer-Verlag, New York, 1981.

28. Basedow, A. M.; Ebert, K. H., Polymer Bull. (Berlin) 1:299-306(1979).

29. Basedow, A. M.; Ebert, K. H.; Ederer, H. J., Macromolecules 11:774-81 (1978).

30. Ebert, K. H.; Ederer, H. J.; Emmert, J., Polymer Bull. (Berlin) 6:471-76 (1982).

31. Heymach, J.; Jost, B., J. Polymer Sci. C25:145-53(1969).

32. Glynn, P. A. R.; van der Hoff, B. M. E., J. Macromol. Sci., Chem. A7:1695-719(1973).

33. Glynn, P. A. R.; van der Hoff, B. M. E.; Reilly, P. M., J. Macromol. Sci., Chem. A6:1653-64(1972).

34. van der Hoff, B. M. E.; Glynn, P. A. R., J. Macromol. Sci., Chem. A8:429-49(1974).

35. Suga, K.; van Dedum, G.; Moo-Young, M., Biotechnol. Bioeng. 17:433-39 (1975).

36. Wheatley, M. A.; Moo-Young, M., Biotechnol. Bioeng. 19:219-233(1977).

37. Bhattacharyya, G. K.; Johnson, R. J., Statistical Concepts and Methods. New York, John Wiley & Sons, 1977:140-64.

38. Carnahan, B.; Luther, H. A.; Wilkes, J. O., Applied Numerical Methods, New York, John Wiley & Sons, 1969:344.

39. Benson, S. W., The Foundations of Chemical Kinetics. New York, McGraw-Hill, 1960:66-8.

40. Ziderman, I.; Bel-Ayche, J., J. Appl. Polymer Sci. 32:3255-61(1986).

41. Young, R. A.; Liss, L., Cellulose Chem. Technol. 12:399-411(1978).

42. Samuelson, O.; Wennerblom, A., Svensk Papperstid. 57:827-30(1954).

43. Leege, J. A Characterization of the Thermodynamic Functions of Activation for 1,5-Anhydromaltitol. Master's Research Report. Appleton, WI, The Institute of Paper Chemistry, 1987.

44. Perrin, D. D.; Armarego, W. L. F.; Perrin, D. R., Purification of Laboratory Chemicals. 2nd ed. New York, Pergamon Press, 1980.

45. Sigma Technical Bulletin No. 670, The Colorometric Determination of Inorganic Phosphorus. St. Louis, Sigma Chemical Co., 1974.

46. Schroeder, L. R.; Haigh, F. C., Tappi 62:103-5(1979).

47. McCracken, F. L., J. Appl. Polymer Sci. 21:191-8(1977).

48. Ring, G. J. F.; Stratton, R. A.; Schroeder, L. R., J. Liq. Chromatogr. 6:401-24(1983).

49. Dean, J. A., Lange's Handbook of Chemistry. 11th Ed., New York, McGraw-Hill, 1973:10-106.

50. Sigma Procedure No. 16-UV, Glucose: Quantitative Enzymatic (Hexokinase) Determination. St. Louis, Sigma Chemical Co., 1983.

51. Ralston, M., In Dixon's BMDP Statistical Software. Berkeley, CA, University of California Press, 1983:305-314.

52. Manners, D. J.; Masson, A. J.; Sturgeon, R. J., Carbohyd. Res. 17:109-14 (1971).

53. Hastings, N. A. J.; Peacock, J. B., Statistical Distributions: A Handbook for Students and Practitioners. New York, John Wiley & Sons, 1975:84-9.

54. Banks, W.; Greenwood, C. T.; Khan, K. M., Carbohyd. Res. 17:25-33(1971).

55. Bailey, J. M.; Whelan, W. J., J. Biol. Chem. 236:969-73(1961).

56. Husemann, E.; Fritz, B.; Lippert, R.; Pfannemuller, B., Makromol. Chem. 26:199-213(1958).

57. Pfannemuller, B., Naturwissenschaften 62:231-3(1975).

58. Whelan, W. J.; Bailey, J. M., Biochem. J. 58:560-9(1954).

59. Graves, D. J.; Wang, J. H. In Boyer's The Enzymes. 3rd ed., Vol. 5, p. 435-82, New York, Academic Press, 1971.

60. Flory, P. J., J. Am. Chem. Soc. 62:561-5(1940).

61. Brown, D. H.; Cori, C. F., In Boyer, Lardy, and Myrback's The Enzymes. 2nd ed., Vol. 5, p. 207-28, New York, Academic Press, 1961.

62. Bourne, E. J., In Williams' Biochemical Transformations of Starch and Cellulose., p. 3-16, Cambridge, Cambridge University Press, 1953.

63. Pfannemuller, B.; Burchard, W., Makromol. Chem. 121:1-17(1969).

64. Kasvinsky, P. J.; Madsen, N. B.; Fletterrick, R. J.; Sygusch, J., J. Biol. Chem. 253:1290-6(1978).

65. Kasvinsky, P. J.; Madsen, N. B., J. Biol. Chem. 251:6852-9(1976).

66. Cleland, W. W., Biochemistry 3:480-2(1964).

APPENDIX I

CONVERSION OF MWDs FROM WEIGHT FRACTION VERSUS LOG(DP) SCALING TO NUMBER FRACTION VERSUS DP SCALING

A MWD can be plotted as either the differential distribution or as the integral distribution. Differential distributions provide information on the relative amount of polymer of each DP. Integral distributions give the cumulative fraction of polymer up to and including a given DP.

With either format, it is possible to vary the scales of the plot. The DP scale (x-axis) can be logarithmic or linear, and the relative amount scale (y-axis) can be based either on the relative weight or on the relative number of polymer molecules.

The type of MWD that is provided most directly by GPC is the differential distribution, on a weight amount basis, with logarithmic scaling of the DP axis. For the purpose of modeling, the relative number of molecules of each size was needed, and so it was necessary to convert the MWD to a number amount basis, with linear scaling of the DP. The conversion was accomplished in two steps. First, the logarithmic scale was transformed into a linear one, and then the weight fractions were converted to number fractions.

The height of a differential distribution at any point depends on whether the DP scale is linear or logarithmic. On a linear scale the distance between adjacent DPs is constant, but on a logarithmic scale the distance between adjacent DPs is large at low molecular weights, and very small at high molecular weights. This compression of the scale at high DPs magnifies the importance of high molecular weights when the MWD is plotted on a logarithmic scale (See Fig. 27).

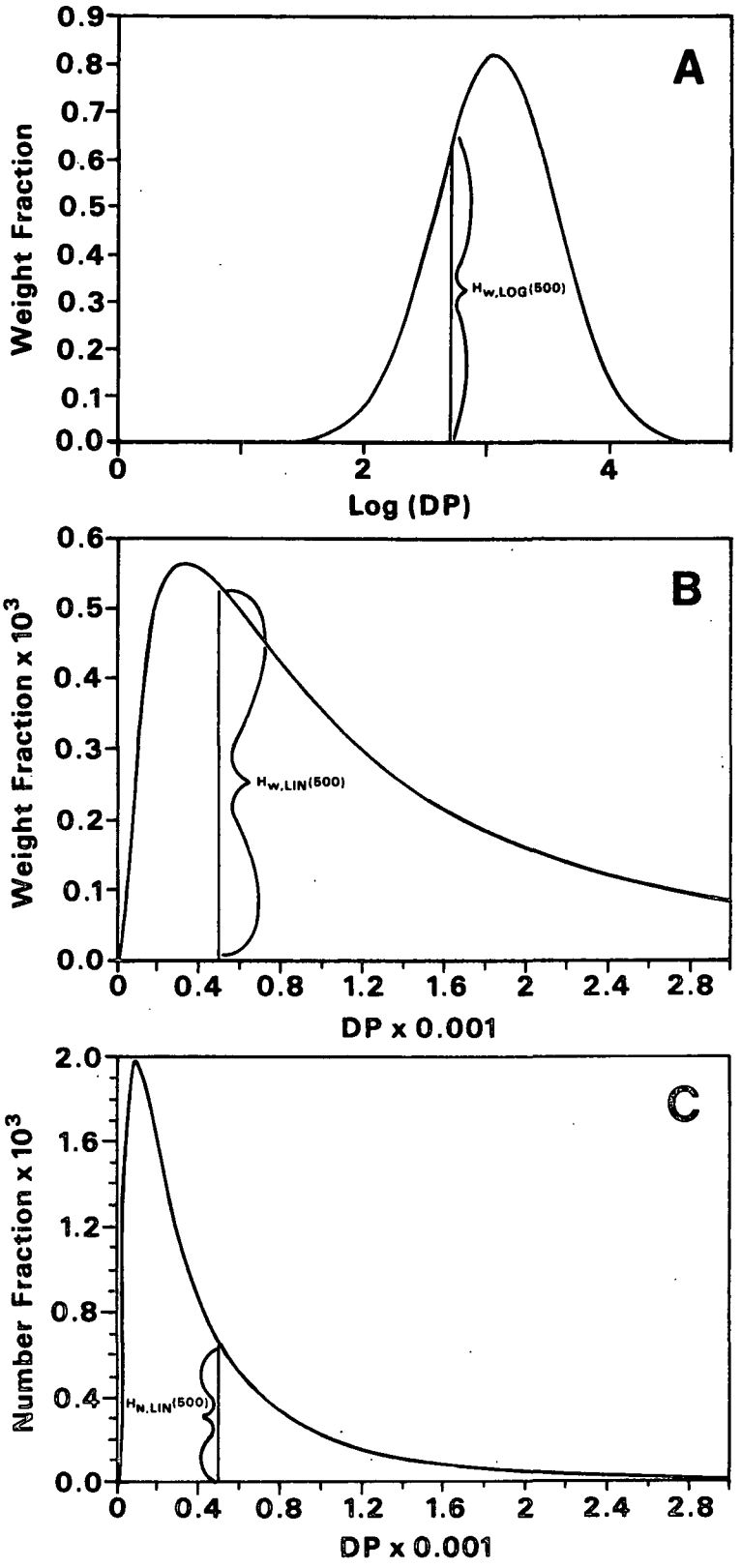

Figure 27. Differential lognormal molecular weight distribution.
A. Plotted on weight fraction versus log(DP) basis.
B. Plotted on weight fraction versus DP basis.
C. Plotted on number fraction versus DP basis.

Unlike the differential curves, the heights of the integral distribution curves at a given DP do not depend on the type of DP scale (see Fig. 28). The total weight of polymer up to and including a particular DP is the same for a linear scale as for a logarithmic one. Therefore, the conversion scheme can be developed using the integral distributions as a starting point.

The integral distribution function on a linear scale can be given the symbol F(x), where x is an arbitrary DP. Similarly, the integral distribution function on a logarithmic scale can be given the symbol G(y), where y = log(x). At any given x it must be true that

$$F(x) = G(y). \tag{20}$$

The differential distributions may be arrived at by differentiating Eq. (20) with respect to x:

$$\frac{d\,F(x)}{d\,x} = \frac{d\,G(y)}{d\,y} \cdot \frac{d\,y}{d\,x} \tag{21}$$

Since y = log(x), dy/dx = 1/x. Substituting this result into Eq. (20) gives

$$\frac{d\,F(x)}{d\,x} = \frac{d\,G(y)}{d\,y} \cdot \frac{1}{x} \tag{22}$$

Thus, at any given molecular weight x, the logarithmically scaled distribution can be converted to the linearly scaled distribution by dividing the ordinate by x. After all DPs have been converted, it is necessary to normalize the resulting distribution so that the area it encloses is equal to unity.

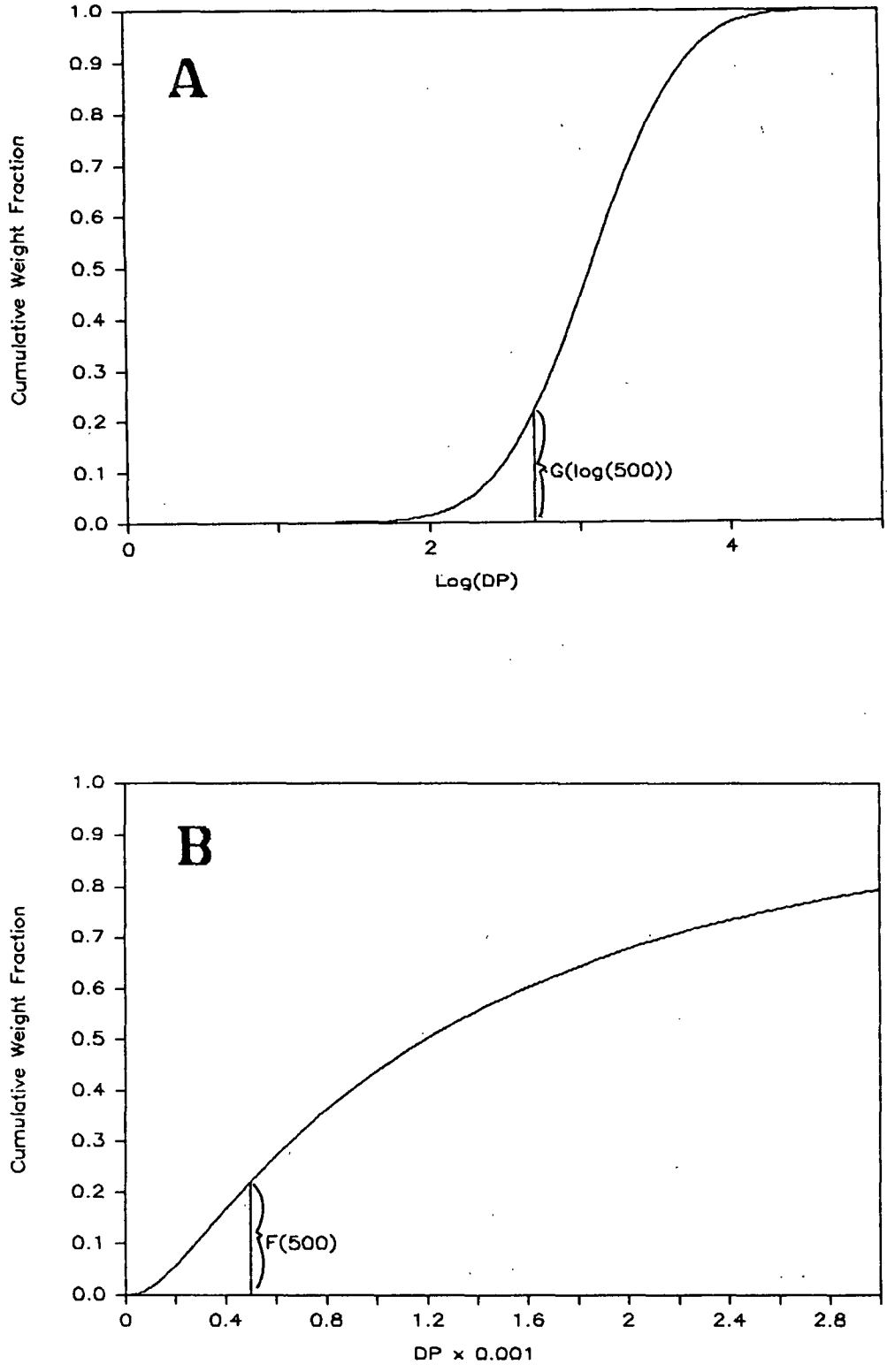

Figure 28. Integral lognormal molecular weight distribution.
A. Plotted on logarithmic DP scale.
B. Plotted on linear DP scale.

Converting the polymer fractions from a weight basis to a number basis is straightforward. The number of moles of a given size of molecule can be determined by dividing the weight of the molecules by their molecular weight. Since the DP is the molecular weight divided by a constant, if only relative amounts are important, the weights can be divided by the DP instead. Conversion from weight fractions to number fractions thus involves another division by the DP. Once again, the area contained by the distribution curve must be normalized to unity.

To summarize, if $H_{W,LOG}(I)$, $H_{W,LIN}(I)$, and $H_{N,LIN}(I)$ are the respective ordinates of the weight fraction versus log(DP) distribution, the weight fraction versus DP distribution, and the number fraction versus DP distribution at DP=I, then conversion between the distributions can be accomplished by the relation

$$\frac{H_{W,LOG}(I)}{I^2} = \frac{H_{W,LIN}(I)}{I} = H_{N,LIN}(I) \qquad (23)$$

The conversion is completed by normalizing the resulting distribution. Figure 27 shows a lognormal MWD plotted in all three formats.

APPENDIX II

COMPUTER PROGRAMS

A. Probabilistic Modeling of Effect of Peeling and Stopping on Arbin's[16] Starting Material

Listed below is the FORTRAN 77 program used to model the effect of peeling and stopping on a lognormal MWD with approximately the same shape as the starting material used by Arbin et al.[16]

The important constants are input to the program by changing the parameter statement that appears near the beginning of the program. STEP is the interval between DPs actually used in the calculation. For example, if STEP=10, then every tenth DP and peeling length is included in the calculation. DPMIN and DPMAX are the minimum and maximum DPs considered. IMAX is DPMAX/STEP. MEDIAN and SHAPE are the parameters which specify the position and dispersion of the lognormal distribution.[53] Increasing MEDIAN raises the $\overline{DP}_N$ and increasing SHAPE raises the polydispersity. Finally, KPOKS is the value of k_p/k_s input to the model.

The program outputs its results into two files. One file contains the tabulated MWDs for plotting, and the other contains a table of results comparing the properties of the final material to the starting material.

Computer Program PEEL/MODEL/V3/LOGNORMAL:

```
$RESET FREE
      INTEGER DPMIN,DPMAX,IMAX
      DOUBLE PRECISION MEDIAN,SHAPE,STEP,KPOKS
      PARAMETER (STEP=10.0,DPMIN=10,DPMAX=80000,IMAX=8000,
     *MEDIAN=335.300,SHAPE=1.1231,KPOKS=200.0)
C
C
```

```
      INTEGER I,J
      DOUBLE PRECISION FDP(1:IMAX),DP(0:IMAX),PI,PPL(0:IMAX),
     *DFDP(1:IMAX),SF,SFDP,SFDPS,DPN,DPW,PD,DSF,DSFDP,DSFDPS,DDPN,
     *DDPW,DPD,NYIELD,WYIELD,EOF,KSOKP,D,FMOD,DPMOD,DFMOD,DDPMOD,
     *FPK,DPPK,DFPK,DDPPK
      PI=3.141592654
      KSOKP=1/KPOKS
      DP(0)=0.00
      EOF=9999.
      OPEN (UNIT=1,STATUS='NEW')
C FILE1 WILL CONTAIN MWD DATA FOR PLOTTING
      OPEN (UNIT=2,STATUS='NEW')
C FILE2 WILL CONTAIN TABLE OF RESULTS
C
C ****************************************************************
C
C ROUTINE TO GENERATE A LOGNORMAL MOLECULAR WEIGHT DISTRIBUTION
C WITH MEDIAN=MEDIAN AND SHAPE PARAMETER=SHAPE. FDP(I)=RELATIVE
C NUMBER FRACTION OF MOLECULES OF DP(I).  EVERY (STEP)TH DP IS
C CONSIDERED. DPMOD IS DP WITH LARGEST RELATIVE FRACTION OF MOLECULES.
C
      DO 10 I=1,IMAX,1
        DP(I)=DBLE(I)*STEP
        D=DP(I)
        FDP(I)=(1/(D*SHAPE*(2*PI)**0.5))*DEXP(-(DLOG(D/MEDIAN)**2/
     *  (2*SHAPE**2)))
        CALL MAXMUM(FDP(I),DP(I),FMOD,DPMOD)
   10 CONTINUE
C
C ****************************************************************
C
C CALCULATE GEOMETRIC DISTRIBUTION OF PEELING LENGTHS. KSOKP=
C STOPPING CONSTANT/PEELING CONSTANT. PPL(I)=PROBABILITY THAT
C I*STEP UNITS ARE PEELED FROM A MOLECULE
C
C
      DO 20 I=0,IMAX,1
        PPL(I)=KSOKP*(1-KSOKP)**DP(I)
   20 CONTINUE
C
C ****************************************************************
C
C CALCULATE NON-NORMALIZED MWD FOR DEGRADED POLYMER BY FIGURING
C THE NUMBER OF MOLECULES OF EACH DEGRADED DP (DFDP) FORMED FROM
C EACH DP ORIGINALLY PRESENT IN THE STARTING DISTRIBUTION (FDP).
C
      DO 40 I=IMAX,1,-1
        DO 30 J=1,I,1
          DFDP(J)=DFDP(J)+FDP(I)*PPL(I-J)
   30   CONTINUE
   40 CONTINUE
```

```
C
C ****************************************************************
C
C CALCULATE DPN, DPW, PD=POLYDISPERSITY, NYIELD=YIELD BASED ON
C NUMBER OF MOLECULES LOST, WYIELD=YIELD BASED ON WEIGHT LOST
C
      DO 50 I=1,IMAX,1
        SF=SF+FDP(I)
C                                SF IS SUM OF FDP
        SFDP=SFDP+FDP(I)*DP(I)
C                                SFDP IS SUM OF FDP*DP
        SFDPS=SFDPS+FDP(I)*DP(I)**2
C                                SFDPS IS SFDPS+FDP*DP**2
          CALL MAXMUM(DFDP(I),DP(I),DFMOD,DDPMOD)
C DDPMOD IS DP WITH LARGEST RELATIVE NUMBER OF MOLECULES.
        DFDP(I)=DFDP(I)*STEP
C MULTIPLIED DEGRADED DISTRIBUTION BY STEP BECAUSE ONLY CONSIDERED
C PEELING LENGTHS THAT WERE MULTIPLES OF STEP
        DSF=DSF+DFDP(I)
        DSFDP=DSFDP+DFDP(I)*DP(I)
        DSFDPS=DSFDPS+DFDP(I)*DP(I)**2
   50 CONTINUE
      DPN=SFDP/SF
      DPW=SFDPS/SFDP
      PD=DPW/DPN
      DDPN=DSFDP/DSF
      DDPW=DSFDPS/DSFDP
      DPD=DDPW/DDPN
      NYIELD=(DSF/SF)*100
      WYIELD=(DSFDP/SFDP)*100
C
C ****************************************************************
C
C CONVERT MWDS TO WEIGHT FRACTION BASIS BY MULTIPLYING EACH
C FDP(I) BY DP(I). CONVERT LINEAR SCALING TO LOGARITHMIC BY
C MULTIPLYING BY AN ADDITIONAL FACTOR OF DP. NORMALIZE SO
C THAT AREA UNDER LINEAR WEIGHT CURVE (AND HENCE LOG CURVE) IS
C UNITY. FACTOR OF STEP NEEDED IN THE DENOMINATOR BECAUSE THE LINEAR
C WIDTH BETWEEN DPS CONSIDERED IS STEP. NOTE THAT DEGRADED MWD
C CAN BE NORMALIZED TO REFLECT THE YIELD LOSS BY MULTIPLYING
C THE DFDP'S BY WYIELD/100. DPPK IS PEAK DP ON LOG AND WEIGHT
C SCALE.  DDPPK IS PEAK DP FOR DEGRADED MWD.
C
      DO 60 I=1,IMAX,1
        FDP(I)=FDP(I)*DP(I)**2/(SFDP*STEP)
        CALL MAXMUM(FDP(I),DP(I),FPK,DPPK)
        DFDP(I)=DFDP(I)*DP(I)**2/(DSFDP*STEP)
        CALL MAXMUM(DFDP(I),DP(I),DFPK,DDPPK)
   60 CONTINUE
```

```
C
C ***************************************************************
C
C OUTPUT FILE FOR GRAPHING BY MARK VAN ZUMMEREN'S PLOT/1 PROGRAM
C
      WRITE (1,1)
    1 FORMAT ('MWD OF STARTING MATERIAL')
      DO 70 I=1,10,1
        WRITE (1,2) LOG(DP(I)),FDP(I)
   70 CONTINUE
      DO 75 I=11,IMAX,8
        WRITE (1,2) LOG(DP(I)),FDP(I)
   75 CONTINUE
    2 FORMAT (E15.8,','E15.8)
      WRITE (1,3) EOF,EOF
    3 FORMAT (F8.0,',',F8.0)
      WRITE (1,4) KPOKS
    4 FORMAT ('FINAL MWD FOR Kp/Ks =',F8.0)
      DO 80 I=1,10,1
        WRITE (1,2) LOG(DP(I)),DFDP(I)
   80 CONTINUE
      DO 85 I=11,IMAX,8
        WRITE (1,2) LOG(DP(I)),DFDP(I)
   85 CONTINUE
      WRITE (1,3) EOF,EOF
C
C ***************************************************************
C
C OUTPUT TABLE OF RESULTS
C
      WRITE (2,5) DPN, DPW, PD,DPMOD,STEP/2,DPPK,STEP/2
    5 FORMAT (1X,'DATA FOR STARTING MATERIAL',//,1X,'DP(N) =',
     *F12.2,/,1X,'DP(W) =',F12.2,/,1X,'POLYDISPERSITY =',F12.8,
     */,5X,'MODAL DP (LINEAR) =',F6.0,1X,'+/-',F6.0,/,5X,
     *'PEAK DP (LOGARITHMIC) =',F6.0,1X,'+/-',F6.0)
      WRITE (2,6) KPOKS,DDPN,DDPW,DPD,DDPMOD,STEP/2,
     *DDPPK,STEP/2,WYIELD,NYIELD
    6 FORMAT (////,1X,'DATA FOR DEGRADED POLYMER IF KP/KS =',
     *F8.0,//,1X,'DP(N) =',F12.2,/,1X,'DP(W) =',F12.2,/,1X,
     *'POLYDISPERSITY =',F12.8,/,5X,'MODAL DP (LINEAR) =',F6.0,
     *1X,'+/-',F6.0,/,5X,'PEAK DP (LOGARITHMIC) =',F6.0,'+/-',F6.0,
     */,1X,'YIELD (WEIGHT PERCENT) =',
     *E15.8,/,1X,'YIELD (NUMBER PERCENT) =',E15.8)
C
C ***************************************************************
C
      END
C
C ***************************************************************
C
C SUBROUTINE FOR FINDING PEAK AND MODE LOCATIONS
C
```

```
SUBROUTINE MAXMUM(F,DP,MAXF,MAXDP)
  DOUBLE PRECISION F,DP,MAXF,MAXDP
  IF (F.GT.MAXF) THEN
    MAXF=F
    MAXDP=DP
  END IF
END
```

B. Probabilistic Modeling of the Effect of Peeling and Stopping on a High DP Amylose

Listed below are the computer files used to model the effect of peeling and stopping on the substrate amylose used in degradation experiments. The FORTRAN77 program PEEL/MODEL/HIDP actually implements the model. The file WFL/DECK sets operating parameters and inputs the k_P/k_S ratio to the program as the variable KPOKS.

The input file INITIAL/MWD contains the tabulated MWD [in a weight fraction versus log(DP) format] for the starting material. When required, values between these tabulated points are interpolated using a cubic spline. The program outputs two files, one containing the MWDs and one containing a table comparing the properties of the degraded and starting amyloses.

Sample Job File WFL/DECK:

```
BEGIN JOB PEEL;
 QUEUE = 95;
 PRIORITY = 45;
?RUN OBJECT/PEEL/MODEL/V3;
 FILE FILE1 = PL3000;
 DATA
 2500
?END JOB.
```

Computer Program PEEL/MODEL/HIDP:

```
$RESET FREE
FILE  1(KIND='DISK',MYUSE='OUT',STATUS='NEW')
FILE  2(KIND='PRINTER')
FILE  3(TITLE='INITIAL/MWD.',KIND='DISK',MYUSE='IN',STATUS='OLD',
     *FILETYPE=8)
FILE  4(KIND='READER')
C
C FILE1 WILL CONTAIN MWD DATA FOR PLOTTING
C FILE2 WILL PRINT TABLE OF RESULTS
C FILE3 CONTAINS TABULATED INITIAL DISTRIBUTION AS LOG(DP) VS WT FRACTIO
C FILE4 READS DATA FROM WFL DECK
```

```
C
      INTEGER I,J,IMAX
      DOUBLE PRECISION FDP(1:4000),DP(0:4000),PI,PPL(0:4000),
     *DFDP(1:4000),SF,SFDP,SFDPS,DPN,DPW,PD,DSF,DSFDP,DSFDPS,DDPN,
     *DDPW,DPD,NYIELD,WYIELD,EOF,KSOKP,D,FMOD,DPMOD,DFMOD,DDPMOD,
     *FPK,DPPK,DFPK,DDPPK,STEP,KPOKS


      REAL KLOGDP(100),KWF(100),SECDER(100),WFLOG
      STEP=10.0
      IMAX=4000
C IMAX * STEP = MAXIMUM DP CONSIDERED
      READ (4,*) KPOKS
      KSOKP=1/KPOKS
      DP(0)=0.00
C
C ****************************************************************
C
C ROUTINE TO GENERATE THE INITIAL MOLECULAR WEIGHT DISTRIBUTION
C BASED ON GPC DATA. FRACTIONS ARE INTERPOLATED USING A CUBIC SPLINE
C FUNCTION.  EVERY (STEP)TH DP IS CONSIDERED. DPMOD IS DP WITH LARGEST
C RELATIVE FRACTION OF MOLECULES.
C
      READ (3,*,END=10) (KLOGDP(I),KWF(I),I=1,100)
   10 NUMBER=I
      CALL FITSPL(KLOGDP,KWF,NUMBER,0.,0.,SECDER)
      DO 12 I=1,IMAX,1
        DP(I)=DBLE(I)*STEP
        CALL SPEVAL(KLOGDP,KWF,SECDER,NUMBER,REAL(LOG10(DP(I))),WFLOG)
C CONVERT DISTRIBUTION FROM WEIGHT BASIS ON LOG SCALE TO NUMBER BASIS ON
C LINEAR SCALE BY DIVIDING BY THE DP TWICE. FIRST MAKE SURE WFLOG
C RETURNED IS NOT NEGATIVE DUE TO WIGGLES IN SPLINE.
        IF (WFLOG . LT . 0.0) WFLOG=0.0
        FDP(I)=WFLOG/(DP(I)*DP(I))
        CALL MAXMUM(FDP(I),DP(I),FMOD,DPMOD)
   12 CONTINUE
C
C ****************************************************************
C
C CALCULATE GEOMETRIC DISTRIBUTION OF PEELING LENGTHS. KSOKP=
C STOPPING CONSTANT/PEELING CONSTANT. PPL(I)=PROBABILITY THAT
C I*STEP UNITS ARE PEELED FROM A MOLECULE
C
C
      DO 20 I=0,IMAX,1
        PPL(I)=KSOKP*(1-KSOKP)**DP(I)
   20 CONTINUE
C
C ****************************************************************
C
C CALCULATE NON-NORMALIZED MWD FOR DEGRADED POLYMER BY FIGURING
C THE NUMBER OF MOLECULES OF EACH DEGRADED DP (DFDP) FORMED FROM
```

```
C EACH DP ORIGINALLY PRESENT IN THE STARTING DISTRIBUTION (FDP).
C
      DO 40 I=IMAX,1,-1
        DO 30 J=1,I,1
          DFDP(J)=DFDP(J)+FDP(I)*PPL(I-J)
   30   CONTINUE
   40 CONTINUE
C
C ****************************************************************
C
C CALCULATE DPN, DPW, PD=POLYDISPERSITY, NYIELD=YIELD BASED ON
C NUMBER OF MOLECULES LOST, WYIELD=YIELD BASED ON WEIGHT LOST
C


      DO 50 I=1,IMAX,1
        SF=SF+FDP(I)
C                                SF IS SUM OF FDP
        SFDP=SFDP+FDP(I)*DP(I)
C                                SFDP IS SUM OF FDP*DP
        SFDPS=SFDPS+FDP(I)*DP(I)**2
C                                SFDPS IS SFDPS+FDP*DP**2
          CALL MAXMUM(DFDP(I),DP(I),DFMOD,DDPMOD)
C DDPMOD IS DP WITH LARGEST RELATIVE NUMBER OF MOLECULES.
        DFDP(I)=DFDP(I)*STEP
C MULTIPLIED DEGRADED DISTRIBUTION BY STEP BECAUSE ONLY CONSIDERED
C PEELING LENGTHS THAT WERE MULTIPLES OF STEP
        DSF=DSF+DFDP(I)
        DSFDP=DSFDP+DFDP(I)*DP(I)
        DSFDPS=DSFDPS+DFDP(I)*DP(I)**2
   50 CONTINUE
      DPN=SFDP/SF
      DPW=SFDPS/SFDP
      PD=DPW/DPN
      DDPN=DSFDP/DSF
      DDPW=DSFDPS/DSFDP
      DPD=DDPW/DDPN
      NYIELD=(DSF/SF)*100
      WYIELD=(DSFDP/SFDP)*100
C
C ****************************************************************
C
C CONVERT MWDS TO WEIGHT FRACTION BASIS BY MULTIPLYING EACH
C FDP(I) BY DP(I). CONVERT LINEAR SCALING TO LOGARITHMIC BY
C MULTIPLYING BY AN ADDITIONAL FACTOR OF DP. NORMALIZE SO
C THAT AREA UNDER LINEAR WEIGHT CURVE IS 2.3025 AND HENCE AREA UNDER
C LOG10 CURVE IS UNITY.
C FACTOR OF STEP NEEDED IN THE DENOMINATOR BECAUSE THE LINEAR
C WIDTH BETWEEN DPS CONSIDERED IS STEP. NOTE THAT DEGRADED MWD
C CAN BE NORMALIZED TO REFLECT THE YIELD LOSS BY MULTIPLYING
C THE DFDP'S BY WYIELD/100. DPPK IS PEAK DP ON LOG AND WEIGHT
C SCALE.  DDPPK IS PEAK DP FOR DEGRADED MWD.
C
```

```
      DO 60 I=1,IMAX,1
        FDP(I)=FDP(I)*DP(I)**2/(SFDP*STEP)*2.302585093
        CALL MAXMUM(FDP(I),DP(I),FPK,DPPK)
        DFDP(I)=DFDP(I)*DP(I)**2/(DSFDP*STEP)*2.302585093
        CALL MAXMUM(DFDP(I),DP(I),DFPK,DDPPK)
   60 CONTINUE
C
C ***************************************************************
C
C OUTPUT FILE FOR GRAPHING BY EXPORT TO LOTUS 1-2-3. MAKE POINTS
C APPROXIMATELY EQUALLY SPACED ON LOG SCALE.
C
      WRITE (1,1) KPOKS
    1 FORMAT ('" MWD OF STARTING MATERIAL"' ,'"FINAL MWD FOR Kp/Ks ="',
     *F8.0)
      DO 70 I=1,10,1
        WRITE (1,2) LOG10(DP(I)),FDP(I),DFDP(I)
   70 CONTINUE
      DUMMY=10.
      ICHECK=10
   75 IF (DUMMY.LT.IMAX) THEN
        DUMMY=ANINT(DUMMY*1.1)
        I=INT(DUMMY)
        IF (I.LE.ICHECK) I=I+1
        IF (I.GT.IMAX) I=IMAX
        WRITE (1,2) LOG10(DP(I)),FDP(I),DFDP(I)
        ICHECK=I
      GOTO 75
      END IF
    2 FORMAT (E15.8,','E15.8,',',E15.8)
C
C ***************************************************************
C
C OUTPUT TABLE OF RESULTS TO PRINTER
C
      WRITE (2,5) DPN, DPW, PD,DPMOD,STEP/2,DPPK,STEP/2
    5 FORMAT (1X,'DATA FOR STARTING MATERIAL',//,1X,'DP(N) =',
     *F12.2,/,1X,'DP(W) =',F12.2,/,1X,'POLYDISPERSITY =',F12.8,
     */,5X,'MODAL DP (LINEAR) =',F6.0,1X,'+/-',F6.0,/,5X,
     *'PEAK DP (LOGARITHMIC) =',F6.0,1X,'+/-',F6.0)
      WRITE (2,6) KPOKS,DDPN,DDPW,DPD,DDPMOD,STEP/2,
     *DDPPK,STEP/2,WYIELD,NYIELD
    6 FORMAT (////,1X,'DATA FOR DEGRADED POLYMER IF KP/KS =',
     *F8.0,//,1X,'DP(N) =',F12.2,/,1X,'DP(W) =',F12.2,/,1X,
     *'POLYDISPERSITY =',F12.8,/,5X,'MODAL DP (LINEAR) =',F6.0,
     *1X,'+/-',F6.0,/,5X,'PEAK DP (LOGARITHMIC) =',F6.0,'+/-',F6.0,
     */,1X,'YIELD (WEIGHT PERCENT) =',
     *E15.8,/,1X,'YIELD (NUMBER PERCENT) =',E15.8)
C
C ***************************************************************
C
      END
```

```
C
C ***************************************************************
C
C SUBROUTINE FOR FINDING PEAK AND MODE LOCATIONS
C
      SUBROUTINE MAXMUM(F,DP,MAXF,MAXDP)
        DOUBLE PRECISION F,DP,MAXF,MAXDP
        IF (F.GT.MAXF) THEN
          MAXF=F
          MAXDP=DP
        END IF
      END
C ***************************************************************
C
C CUBIC SPLINE FITTING ROUTINE BASED ON "NUMERICAL RECIPES" ROUTINE "SPLINE"
C PRESS, ET. AL., (1986)
C D. GEDDES   12/4/86
C
      SUBROUTINE FITSPL(X,Y,NUM,D1,D2,Y2)
C GIVEN TABULATED FUNCTION Y=F(X) SORTED BY INCREASING X FIT A CUBIC SPL
C X, Y ARE ARRAYS CONTAINING THE TABULATED FUNCTION POINTS
C N IS THE NUMBER OF POINTS TABULATED
C D1, D2 ARE THE INITIAL AND FINAL FIRST DERIVATIVES FOR THE SPLINE
C      (IF GREATER THAN .99E30 THEN A NATURAL SPLINE IS FIT)
C Y2 IS ARRAY WHICH CONTAINS THE SECOND DERIVS OF THE INTERPOLATED FUNCT
C
      PARAMETER (NMAX=100)
      DIMENSION X(NUM),Y(NUM),Y2(NUM),U(NMAX)
      IF (D1.GT..99E30) THEN
        Y2(1)=0.
        U(1)=0.
      ELSE
        Y2(1)=-0.5
        U(1)=(3./(X(2)-X(1)))*((Y(2)-Y(1))/(X(2)-X(1))-D1)
      ENDIF
      DO 11 I=2,NUM-1
        SIG=(X(I)-X(I-1))/(X(I+1)-X(I-1))
        P=SIG*Y2(I-1)+2.
        Y2(I)=(SIG-1.)/P
        U(I)=(6.*((Y(I+1)-Y(I))/(X(I+1)-X(I))-(Y(I)-Y(I-1))
     *      /(X(I)-X(I-1)))/(X(I+1)-X(I-1))-SIG*U(I-1))/P
   11 CONTINUE
      IF (D2.GT..99E30) THEN
        QN=0.
        UN=0.
      ELSE
        QN=0.5
        UN=(3./(X(NUM)-X(NUM-1)))*(D2-(Y(NUM)-Y(NUM-1))/
     *(X(NUM)-X(NUM-1)))
      ENDIF
      Y2(NUM)=(UN-QN*U(NUM-1))/(QN*Y2(NUM-1)+1.)
      DO 12 K=NUM-1,1,-1
        Y2(K)=Y2(K)*Y2(K+1)+U(K)
```

```
   12 CONTINUE
      RETURN
      END
C ***************************************************************************
C
C SPLINE EVALUATION ROUTINE BASED ON "NUMERICAL RECIPES" ROUTINE "SPLINT"
C PRESS, ET. AL. (1986)
C D. GEDDES 12/4/86
C
      SUBROUTINE SPEVAL(X,Y,Y2,NUM,PX,PY)
C GIVEN ARRAYS X AND Y WHICH TABULATE A FUNCTION, AND GIVEN ARRAY Y2
C (CALCULATED BY BY FITSPL ROUTINE) RETURNS AN INTERPOLATED VALUE OF PY
C AT ANY X=PX
C
      DIMENSION X(NUM),Y(NUM),Y2(NUM)
      KLO=1
      KHI=NUM
    1 IF (KHI-KLO.GT.1) THEN
        K=(KHI+KLO)/2
        IF(X(K).GT.PX)THEN
          KHI=K
        ELSE
          KLO=K
        ENDIF
      GOTO 1
      ENDIF
      H=X(KHI)-X(KLO)
      IF (H.EQ.0.) PAUSE 'Bad X input.'
      A=(X(KHI)-PX)/H
      B=(PX-X(KLO))/H
      PY=A*Y(KLO)+B*Y(KHI)+((A**3-A)*Y2(KLO)+(B**3-B)*Y2(KHI))*(H**2)/6.
      RETURN
      END
```

Data File INITIAL/MWD:

1.0,0.0
1.576118,4.165233E-04
1.607464,7.383126E-04
1.638811,7.820898E-04
1.670162,3.975145E-04
1.701517,1.156186E-03
1.732876,1.665223E-03
1.76424,2.310422E-03
1.79561,3.525824E-03
1.826987,4.52281E-03
1.858372,4.83609E-03
1.889764,6.491223E-03
1.921164,7.984649E-03
1.952572,9.645442E-03
1.98399,1.122682E-02
2.015418,1.330747E-02
2.046855,1.484628E-02
2.078303,1.806453E-02
2.10976,2.135653E-02
2.14123,2.427975E-02
2.17271,2.885969E-02
2.204202,3.386233E-02
2.235704,.0390295
2.267219,4.478393E-02
2.298746,5.108868E-02
2.330285,5.757217E-02
2.361837,6.546274E-02
2.393401,7.367105E-02
2.44867,8.962919E-02
2.48027,9.965879E-02
2.511882,.110043
2.543508,.1211364
2.575148,.1323915
2.606801,.1437204
2.638468,.1550578
2.670148,.166432
2.701842,.1787141
2.733551,.1902784
2.765272,.203247
2.797009,.2157957
2.828759,.2289543
2.860523,.2418633
2.892301,.2565709
2.924094,.2707793
2.9559,.2865875
2.987722,.3016611
3.019557,.3189899
3.091239,.3588579
3.123122,.3778662
3.155019,.3978787
3.18693,.4182941
3.218856,.439813
3.250796,.4628185
3.282752,.4861983
3.314722,.5111329
3.346706,.5357015
3.378705,.5616459
3.410719,.5882967
3.442747,.6153986
3.474791,.6442991
3.506849,.6726264
3.538921,.7009227
3.571008,.7307707
3.603111,.758301
3.635227,.7864581
3.667359,.8136934
3.699505,.8382988
3.731667,.861046
3.763843,.8799636
3.796034,.8947336
3.828239,.9029306
3.86046,.9037375
3.892695,.89836
3.924946,.8835555
3.957211,.8603512
3.989491,.8288943
4.021786,.7894034
4.054095,.7441905
4.08642,.6941266
4.118759,.6403492
4.151114,.5852413
4.183483,.5298497
4.215866,.4739844
4.248265,.4184907
4.280679,.3629317
4.313108,.3077359
4.345551,.2524918
4.37801,.1977386
4.410483,.1455158
4.442971,9.836815E-02
4.475474,.0596262
4.507992,3.174944E-02
4.540525,1.439468E-02
4.573072,.004047
4.6021,0

C. Comprehensive Model of Effect of Alkaline Degradation on a Monodisperse Amylose

The files listed below implement the comprehensive model, which includes the peeling, stopping, and random chain cleavage reactions. The file SAMPLE/WFL/DECK is an example batch file which shows how the programs are run. The batch file contains a DATA statement which supplies to the model, in order, the peeling rate constant (KP), the stopping rate constant (KS), the cleavage rate constant (KCC), the starting DP (MAXDP), the size of the time step (DELTAT), the number of time steps for which the calculation is to be carried out (NUMSTP), and the number of time steps between outputting the results (REPINT).

The FORTRAN77 program MAKE/EMPTY creates an empty output file to which the results of the simulations are appended.

The file DIFMOD/DECLARATIONS contains the type and dimension declarations for all variables that are held in common blocks.

The actual calculation is performed by the FORTRAN77 program DIFMOD. To ensure the accuracy of the solution, the size of the time step input to the program was limited so that KCC*DELTAT*MAXDP was always less than 0.02. This limits the fraction of molecules cleaved to 2% at most, so that the chance of a given molecule cleaving twice in one time step is very small. The size of the time step also was adjusted so that (KP+KS)*DELTAT is always less than unity, otherwise the model tries to react more reducing ends than actually exist. Selected simulations were duplicated after halving DELTAT, and showed that further reductions in DELTAT do not improve the solutions obtained.

Sample job file WFL/DECK1:

```
BEGIN JOB DIFJOB(STRING A);
 QUEUE  = 30;
STRING NAME0;
NAME0 := A;
RUN OBJECT/MAKE/EMPTY;
 FILE FILE6=#NAME0;
?RUN OBJECT/DIFMOD;
 FILE FILE6=#NAME0;
 DATA
1.0,0.01,.00001,1600,0.5,2000,50
?END JOB.
```

Computer Program MAKE/EMPTY:

```
$RESET FREE
FILE  6(KIND='DISK',MYUSE='OUT',STATUS='NEW')
      WRITE(6,99)
   99 FORMAT(80X)
      END
```

Declarations File DIFMOD/DECLARATIONS:

```
      INTEGER DP, TSTEP, MAXDP, DPMAX, NUMSTP, REPINT
      REAL DPN, DPW, NYIELD, WYIELD
      DOUBLE PRECISION NA(5000), NI(5000), KP, KS, KCC, OLDNI, SUMA,
     *OLDNA, SUMI, STORNI, STORNA, TOTALN, SUMN, SUMNDP, SUMND2, MAXN,
     *DELTAT
      LOGICAL FLAG, ERROR
      COMMON/BLOCK1/ DP, TSTEP, MAXDP, DPMAX, DPN, DPW, ERROR,
     *NYIELD, WYIELD, KP, KS, KCC, OLDNI, OLDNA, SUMI, SUMA,
     *STORNI, STORNA, TOTALN, SUMN, SUMNDP, SUMND2, MAXN, FLAG,
     *NUMSTP, REPINT, DELTAT
      COMMON/BLOCK2/ NA
      COMMON/BLOCK3/ NI
C**********************************************************************
C
C DEFINITIONS OF VARIABLES IN COMMON BLOCKS
C
C NAME    TYPE     DESCRIPTION
C ------  -------  ---------------------------------------------------
C DP      INTEGER  CURRENT DEGREE OF POLYMERIZATION
C TSTEP   INTEGER  CURRENT ITERATION NUMBER
C MAXDP   INTEGER  STARTING DEGREE OF POLYMERIZATION
C DPMAX   INTEGER  MODAL DP
C NUMSTP  INTEGER  NUMBER OF ITERATIONS
C REPINT  INTEGER  REPORTING INTERVAL (OUTPUT RESULTS AFTER EVERY REPINT)
C DPN     REAL     NUMBER AVERAGE DP
C DPW     REAL     WEIGHT AVERAGE DP
C NYIELD  REAL     NUMBER YIELD (RELATIVE TOTAL END CONC. * 100)
C WYIELD  REAL     WEIGHT YIELD
C NA(i)   DOUBLE   NUMBER OF MOLECULES OF DP=i WITH ACTIVE ENDS (ARRAY)
C NI(i)   DOUBLE   NUMBER OF MOLECULES OF DP=i WITH INACTIVE ENDS (ARRAY)
C KP      DOUBLE   RATE CONSTANT - PEELING
C KS      DOUBLE   RATE CONSTANT - STOPPING
C KCC     DOUBLE   RATE CONSTANT - CHAIN CLEAVAGE
C OLDNI   DOUBLE   NI FROM PREVIOUS DP
C SUMA    DOUBLE   SUM OF ACTIVE MOLECULES LONGER THAN DP
C OLDNA   DOUBLE   NA FROM PREVIOUS DP
C SUMI    DOUBLE   SUM OF INACTIVE MOLECULES LONGER THAN DP
C STORNI  DOUBLE   TEMP STORAGE OF PREV DP's NI
C STORNA  DOUBLE   TEMP STORAGE OF PREV DP's NA
C TOTALN  DOUBLE   TOTAL NUMBER OF ENDS
C SUMN    DOUBLE   SUM OF TOTAL ENDS
C SUMNDP  DOUBLE   SUM OF NUMBER * DP
C SUMND2  DOUBLE   SUM OF NUMBER * DP * DP
C MAXN    DOUBLE   TEMP - SEARCH FOR PEAK
C DELTAT  DOUBLE   TIME STEP WIDTH
C FLAG    LOGICAL  TEST WHETHER REPORT IS REQUIRED
C ERROR   LOGICAL  TEST WHETHER ERROR ON INPUT
C **********************************************************************
```

Computer Program DIFMOD:

```
$RESET FREE
FILE  6(KIND='DISK',MYUSE='IO',
     *   STATUS='OLD')
FILE  4(KIND='READER')
C
C ***************************************************************************
C
C MAIN PROGRAM
C
      PROGRAM DIFMOD
$     INCLUDE "DIFMOD/DECLARATIONS"
      CALL ENDFIL()
      CALL INPDAT()
      CALL PRHEAD()
      IF (ERROR) GO TO 999
      CALL ZERVAR()
      NA(MAXDP) = 1.0
      DO 10 TSTEP = 1, NUMSTP
        IF (MOD(TSTEP, REPINT) .EQ. 0) THEN
          FLAG = (.TRUE.)
        ELSE
          FLAG = (.FALSE.)
        END IF
        CALL ONESTP()
        IF (FLAG) THEN
          CALL REPORT()
        END IF
   10 CONTINUE
      CALL TWOLIN()
  999 END
C
C ***************************************************************************
C
C POSITION OUTPUT FILE POINTER TO END OF FILE
C
      SUBROUTINE ENDFIL()
      CHARACTER*80, DUMMY
      READ (6,51,END=50) (DUMMY, I= 1, 3000)
   51 FORMAT (A80)
   50 END
C ***************************************************************************
C
C INPUT DATA
C
      SUBROUTINE INPDAT()
$     INCLUDE "DIFMOD/DECLARATIONS"
      READ (4,*) KP, KS, KCC, MAXDP, DELTAT, NUMSTP, REPINT
C
      IF (KCC*DELTAT*MAXDP .GT. 0.02001) THEN
        WRITE(6,15)
```

```
   15   FORMAT(1X,'"KCC * DELTA T * MAXIMUM DP > 0.02"')
        ERROR = (.TRUE.)
      END IF
C
      IF ((KP+KS)*DELTAT .GE. 1.0) THEN
        WRITE(6,16)
   16   FORMAT(1X,'"(KP+KS) * DELTA T > 1.0"')
        ERROR = (.TRUE.)
      END IF
C
      IF (ERROR) WRITE(6,17)
   17 FORMAT(/,1X,'"********PROGRAM TERMINATED. RECHECK PARAMETERS.*****
     **"')
C
      END
C ***********************************************************************
C
C PRINT HEADER FOR REPORT
C
      SUBROUTINE PRHEAD()
$     INCLUDE "DIFMOD/DECLARATIONS"
      WRITE (6,99) KP, KS, KCC, MAXDP, DELTAT, NUMSTP, REPINT
   99 FORMAT (1X,'"KP  ="',G12.4,/,1X,'"KS  ="',G12.4,/,1X,
     *'"KCC ="',G12.4,/,1X,'"STARTING DP ="',I4,/,
     *1X,'"DELTA T ="',G12.4,/,1X,'"NUMBER OF STEPS ="',I7,/,1X,
     *'"REPORT INTERVAL ="',I7,/)
      IF (ERROR) THEN
        CALL TWOLIN()
        GO TO 998
      END IF
      WRITE (6,98)
      WRITE (6,97)
   98 FORMAT('" "','"WT."','"NUM"','" "','" "','"TOTAL"','"ACTIVE"',
     *'"STOPPED"','"MODAL"')
   97 FORMAT('"STEP"','"YIELD"','"YIELD"','"DPn"','"DPw"','"ENDS"',
     *'"ENDS"','"ENDS"','"DP"','"TIME"')
      WRITE (6,95) 0,100.,100.,MAXDP,MAXDP,1.,1.,0.,MAXDP,0
   95 FORMAT (1X,I5,1X,F5.1,1X,F7.1,1X,F9.1,F9.1,F9.5,F9.5,
     *F9.5,I6,1X,F7.1)

  998 END
C ***********************************************************************
C
C ZERO THE VARIABLES
C
      SUBROUTINE ZERVAR()
$     INCLUDE "DIFMOD/DECLARATIONS"
      SUMN = 0
      SUMNDP = 0
      SUMND2 = 0
      MAXN = 0
      DPMAX = 0
      END
```

```
C ***************************************************************************
C
C PERFORM ONE ITERATION
C
      SUBROUTINE ONESTP()
$     INCLUDE "DIFMOD/DECLARATIONS"
      OLDNI = 0.0  % NO. OF STOPPED MOLECULES FOR PREVIOUS DP
      OLDNA = 0.0  % NO. OF ACTIVE  MOLECULES FOR PREVIOUS DP
      SUMI  = 0.0  % SUM OF STOPPED MOLECULES BIGGER THAN DP
      SUMA  = 0.0  % SUM OF ACTIVE  MOLECULES BIGGER THAN DP
C
      DO 20 DP = MAXDP, 1, -1
        STORNI = NI(DP)
        STORNA = NA(DP)
        NA(DP) = NA(DP)+((-KS-KP-KCC*(DP-1))*NA(DP)+KP*OLDNA+KCC*
     *  (2*SUMA+SUMI))*DELTAT
        NI(DP) = NI(DP)+(KS*STORNA-KCC*(DP-1)*NI(DP)+KCC*SUMI)*DELTAT
        OLDNI=STORNI
        OLDNA=STORNA
        SUMA = SUMA + STORNA
        SUMI = SUMI + STORNI
C
        IF (FLAG) THEN
          TOTALN = NA(DP) + NI(DP)
          SUMN = SUMN + TOTALN
          SUMNDP = SUMNDP + TOTALN * DP
          SUMND2 = SUMND2 + TOTALN * DP * DP
          IF (TOTALN .GT. MAXN) THEN
            MAXN = TOTALN
            DPMAX = DP
          END IF
C
        END IF
C
   20 CONTINUE
      END
C
C ***************************************************************************
C
C OUTPUT A REPORT OF RESULTS FOR DESIRED ITERATIONS
C
      SUBROUTINE REPORT()
$     INCLUDE "DIFMOD/DECLARATIONS"
      WYIELD = 100 * SUMNDP / MAXDP % ASSUMES ORIG FRACT MAXDP = 1.0
      NYIELD = 100 * SUMN
      DPN = SUMNDP / SUMN
      DPW = SUMND2 / SUMNDP
      TIME = TSTEP * DELTAT
      WRITE (6,95) TSTEP, WYIELD, NYIELD, DPN, DPW, SUMA+SUMI, SUMA,
     *SUMI, DPMAX, TIME
   95 FORMAT (1X,I5,1X,F5.1,1X,F7.1,1X,F9.1,F9.1,F9.5,F9.5,
     *F9.5,I6,1X,F7.1)
      CALL ZERVAR()
      END
```

```
C
C ***************************************************************************
C
C ADD TWO BLANK LINES TO OUTPUT FILE
C
      SUBROUTINE TWOLIN()
      WRITE(6,88)
   88 FORMAT (/)
      END
```

APPENDIX III

ENZYMATIC SYNTHESIS OF AMYLOSE

Linear amyloses have been synthesized previously by several researchers,[54-58] using enzymatic techniques. The enzyme phosphorylase, which normally depolymerizes polyglucans in vivo,[59] can under the proper reaction conditions be used to build up chains of amylose from an oligosaccharide primer substrate and glucose 1-phosphate. The reaction scheme is shown in Fig. 29. Because the number of growing chains throughout the reaction is fixed by the initial concentration of the primer substrate, the polymerization process is analogous to other "living" polymerization reactions. Flory[60] has shown mathematically that such "living" polymerizations result in products which have molecular weight distributions conforming to the Poisson distribution. The polydispersity index (the ratio of the weight average to the number average molecular weight) for such a polymer is given by

$$\frac{M_W}{M_N} = 1 + \frac{(\overline{DP}_N - 1)}{\overline{DP}_N{}^2} \qquad (24)$$

where $\overline{DP}_N$ is the number average degree of polymerization, and so very low polydispersities are attainable.

Equation (24) holds strictly only for an irreversible polymerization process. The action of phosphorylase is reversible, and reaction in the direction of amylose depolymerization becomes more important as the initial supply of glucose 1-phosphate is depleted. If too high a conversion of glucose 1-phosphate to amylose is attempted, a broad distribution will result.[56] Too low a conversion makes the synthesis expensive, as starting material is wasted. A balance must therefore be struck between the desire

for the narrowest distribution and the desire for a high conversion. Acceptably narrow distributions can be obtained with conversions up to about 50%.[56]

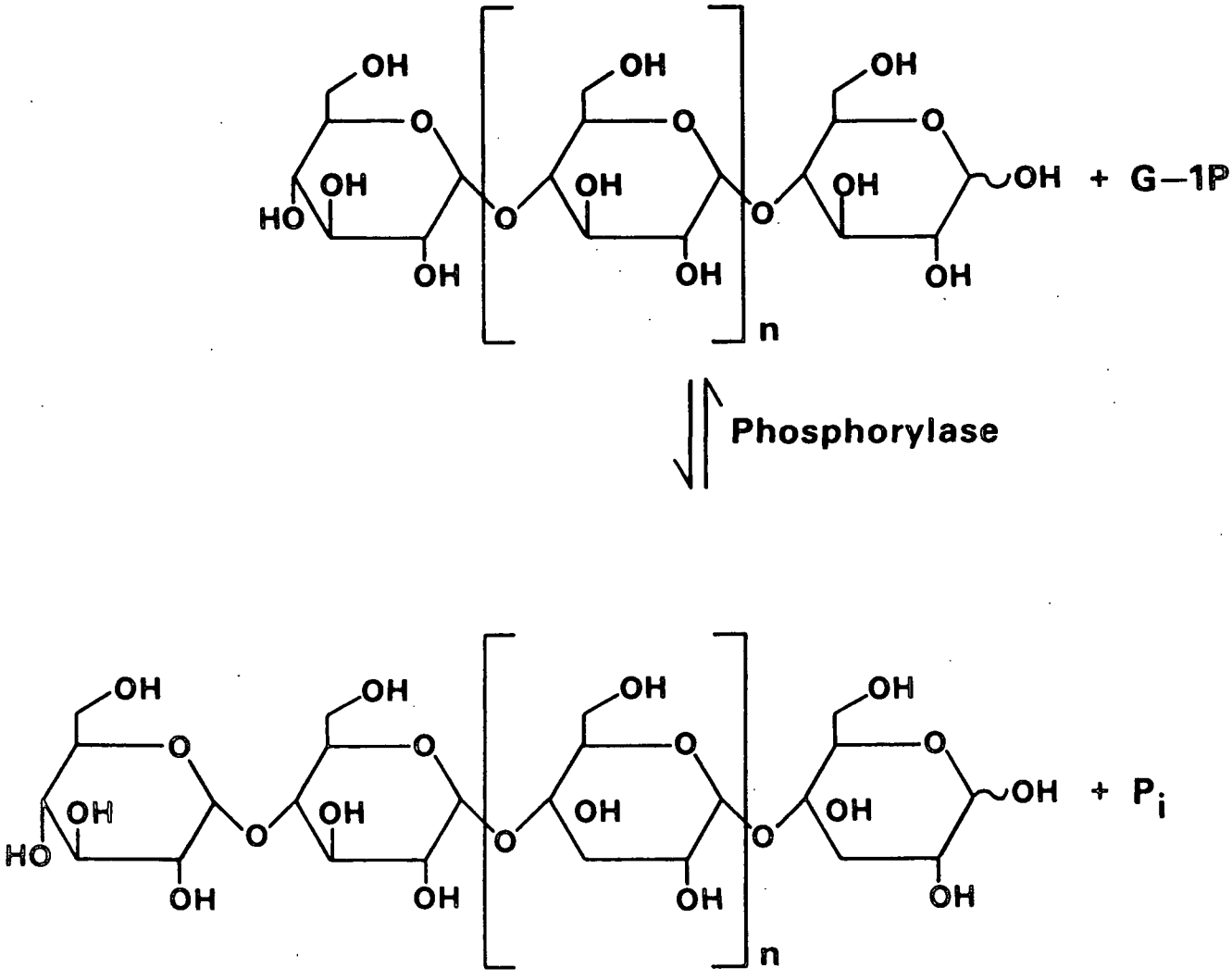

Figure 29. Phosphorylase-catalyzed lengthening of an amylose chain.

The objective was to develop a means of synthesizing amyloses with DPs up to several thousand in quantities approaching a gram or more using commercially available reagents, to be used as molecular weight standards in the calibration of a gel permeation chromatography column. The previously reported enzymatic amylose synthesis procedures[54-58] could not be used to meet these objectives because they produced milligram-sized quantities at the most, and typical DPs extended only into the hundreds. Furthermore, phosphorylase isolated from potatoes was used exclusively, but the potato enzyme is not widely available commercially and is difficult to store.

The approach taken was to scale up the reactions to increase the yields obtained, to find suitable reaction conditions for producing high DPs, and to investigate alternate sources of phosphorylase. Rabbit muscle phosphorylase is widely available in lyophilized form, and so it was a logical choice for the source of enzyme.

The nature of the primer substrate required to initiate the synthesis varies with the type of phosphorylase used. For the potato enzyme, several references[59,61-63] state that a linear maltooligosaccharide containing at least three or four glucose units can function as the primer. Banks et al.[54] used a mixture of maltohexaose and maltoheptaose in their synthesis using potato phosphorylase, and Bailey and Whelan[55,58] used maltohexaose. The literature is unclear and conflicting on what length of primer molecule is needed for the muscle-derived enzyme. Bourne[62] states that muscle phosphorylases cannot be primed by maltooligosaccharides containing fewer than eight glucose units. More recently, however, Madsen and coworkers[64,65] studied the kinetics of the action of rabbit phosphorylase and the binding of maltoheptaose to the enzyme. These

workers report that they were able to get the reaction to proceed in the direction of synthesis using maltoheptaose as the primer, although no product was isolated.

The first experiments conducted in working toward a practical synthesis used glycogen as the primer substrate. Muscle phosphorylase is primed most efficiently by glycogen, its native substrate.[61] Reaction conditions such as pH, temperature, and reagent concentration could thus be optimized without worrying about the effectiveness of the primer. Reactions with glycogen also served as a quick test of the activity of the enzyme used in other reactions. Measurement of the phosphate liberated during synthesis proved to be an effective means of monitoring the progress of the reactions.

One problem that became apparent in the early experiments was that over the long course of the synthesis reactions (sometimes spanning weeks) the enzyme tended to denature and precipitate out of solution. Degradation of the enzyme by oxidation was kept to a minimum in subsequent reactions by addition of the antioxidant dithiothreitol[66] and by blanketing the reaction vessels with argon. The temperature of the reactions was limited to 30°C and EDTA was added as a chelating agent to further stabilize the enzyme. Even with these precautions, it was sometimes necessary to add additional enzyme during the course of a synthesis to make up for that lost by degradation.

It was discovered that maltoheptaose could function as the primer substrate, if careful attention was paid to the order of addition of reagents to the reaction vessel. The reaction proceeded most rapidly when the enzyme was first mixed with the maltoheptaose before being added to the glucose 1-phosphate. In contrast, when the enzyme solution was added to an existing mixture of maltoheptaose and glucose 1-phosphate, no reaction took place.

After appropriate reaction conditions were found, four amyloses were successfully synthesized. Details of the procedure are covered in the Experimental section of this thesis. The amyloses produced ranged in DPN from 41 to 6100. The synthetic amyloses, as well as maltoheptaose, were analyzed by gel permeation chromatography (GPC) as their tricarbanilate derivatives. The chromatograms are shown in Fig. 30. With the exception of Product 4, the chromatograms demonstrate that the molecular weight distributions of the products are very narrow.

The molecular weight of the products could theoretically be calculated from the final inorganic phosphate concentration and the initial maltoheptaose concentration. This method failed to give accurate results, however. In particular, the $\overline{DP}_N$ calculated in this way for Product 4 was much higher than indicated by the gel permeation chromatogram. Since this product also had the widest distribution of any of the synthetic amyloses, it may be speculated that during the long reaction time involved (9 days) there was some hydrolysis of the product. A reducing end group analysis was therefore used to characterize the size of the synthetic amyloses.

Examination of gel permeation chromatograms before and after treatment with isoamylase was used to check the synthetic amyloses for α-(1,6) branches. The analysis verified that the products were completely free of branching.

When a later attempt was made to produce thirty grams of a single material at one time, the resulting product was highly contaminated with a branched polysaccharide. Figure 31 shows that the largest peak of this product's trimodal molecular weight distribution was composed of a branched material which was degraded by isoamylase. The branching was probably initiated by contamination

of the reactor vessel with a small amount of amylopectin or glycogen, which acted as an efficient primer substrate.

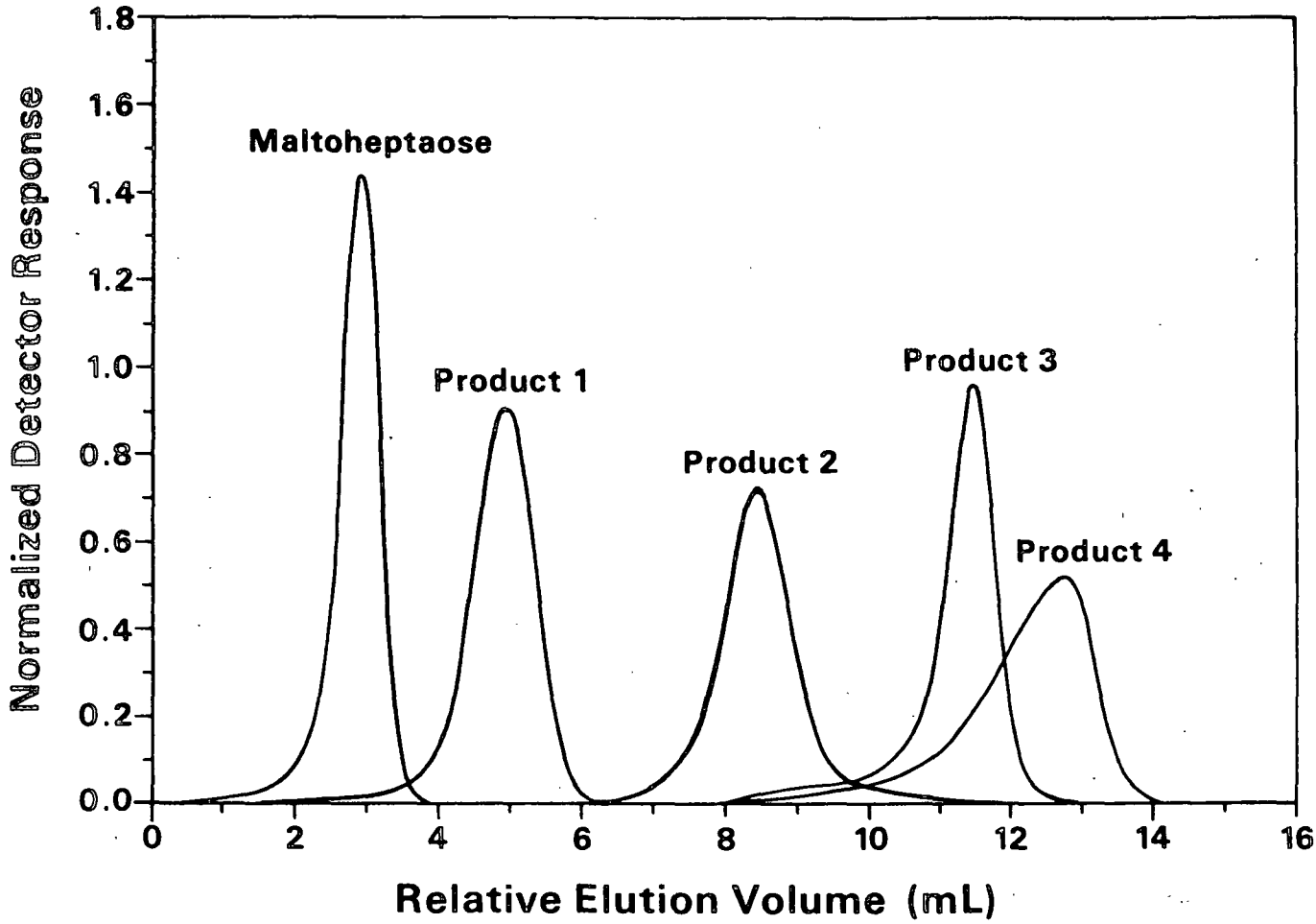

Figure 30. Gel permeation chromatograms of enzymatically synthesized amyloses and maltoheptaose (peak areas have been normalized to a constant value).

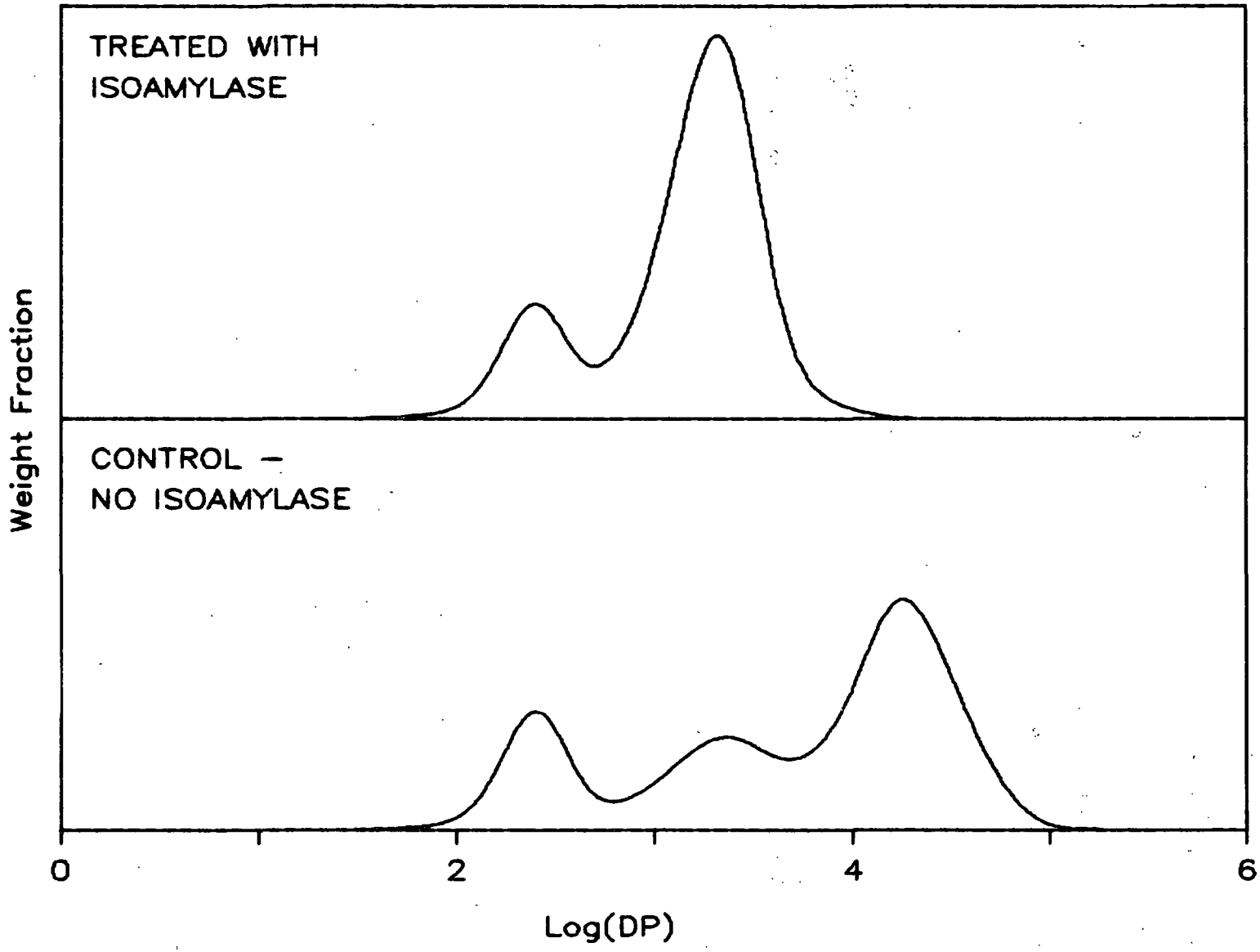

Figure 31. MWD of "amylose" produced by a very large scale enzymatic synthesis before and after treatment with isoamylase.

APPENDIX IV

EXPERIMENTAL DATA

This section contains the complete experimental data for the amylose degradation reactions conducted at 60, 80, and 100°C. The reactions were conducted under anaerobic conditions in 1M sodium hydroxide, and the amylose concentration was 1%, on a weight per volume of alkali basis.

Table 5. Yield,[a] $\overline{DP}_N$, and end group[b] results for amylose degradation in 1.0M sodium hydroxide at 60°C.

Reaction Time, min	Yield[c]	Smoothed Yield	$\overline{DP}_N$	Relative Total End Group Concentration	Relative Reducing End Group Concentration	Relative Acid End Group Concentration
0	100.0	100.0	1835	1.00	1.00	0.00
60	94.4	98.8	1080	1.68	--	--
120	96.5	97.7	750	2.39	1.00	1.39
240	96.3	95.5	632	2.77	--	--
480	94.1	91.2	560	2.99	1.12	1.87
720	90.1	87.1	393	4.07	1.20	2.87
1020	84.8	82.2	302	4.99	1.72	3.27
1320	76.5	77.6	258	5.52	--	--
1620	73.9	73.2	191	7.03	1.63	5.40
1920	67.8	69.1	183	6.93	1.46	5.47
2280	62.8	64.5	178	6.65	0.91	5.74
2820	57.1	58.1	168	6.35	--	--
3600	50.6	50.0	146	6.28	0.74	5.54

[a]Yield = percent by weight of the initial amylose concentration.
[b]End group concentrations = mole fraction of end groups present at zero time.
[c]Average of four determinations.

Table 6. Yield,[a] $\overline{DP_N}$, and end group[b] results for amylose degradation in 1.0M sodium hydroxide at 80°C (reaction 80-4).

Reaction Time, min	Yield[c]	Smoothed Yield	$\overline{DP_N}$	Relative Total End Group Concentration	Relative Reducing End Group Concentration	Relative Acid End Group Concentration
0	100.0	100.0	1861	1.00	1.00	0.00
60	95.8	96.4	875	2.05	--	--
120	93.9	93.0	687	2.52	1.08	1.44
180	90.1	89.9	531	3.15	--	--
240	86.8	87.1	485	3.34	1.23	2.11
300	84.4	84.5	435	3.62	--	--
360	82.1	82.0	413	3.69	0.77	2.92
420	79.9	79.8	367	4.05	--	--
480	77.6	77.8	353	4.10	0.64	3.46
720	70.6	71.0	344	3.84	--	--
960	67.1	66.2	308	4.00	0.27	3.73
1320	60.9	61.3	226	5.05	--	--
1680	58.3	58.3	193	5.62	0.26	5.36

[a]Yield = percent by weight of the initial amylose concentration.
[b]End group concentrations = mole fraction of end groups present at zero time.
[c]Average of four determinations.

Table 7. Yield,[a] $\overline{DP_N}$, and end group[b] results for amylose degradation in 1.0M sodium hydroxide at 80°C (reaction 80-5).

Reaction Time, min	Yield[c]	Smoothed Yield	$\overline{DP_N}$	Relative Total End Group Concentration	Relative Reducing End Group Concentration	Relative Acid End Group Concentration
0	100.0	100.0	1842	1.00	1.00	0.00
60	94.5	96.2	884	2.00	--	--
120	94.4	92.7	588	2.90	1.26	1.64
180	90.3	89.4	546	3.02	--	--
240	87.0	86.5	462	3.45	1.33	2.12
300	84.2	83.8	474	3.26	--	--
360	80.9	81.3	447	3.35	0.60	2.75
420	77.6	79.1	412	3.54	--	--
480	76.3	77.0	366	3.88	0.50	3.38
720	71.3	70.7	354	3.68	--	--
960	65.0	65.6	315	3.84	0.25	3.59
1320	62.4	61.0	253	4.44	--	--
1680	57.5	58.3	235	4.57	0.22	4.35

[a]Yield = percent by weight of the initial amylose concentration.
[b]End group concentrations = mole fraction of end groups present at zero time.
[c]Average of four determinations.

Table 8. Yield,[a] $\overline{DP_N}$, and end group[b] results for amylose degradation in 1.0M sodium hydroxide at 100°C.

Reaction Time, min	Yield[c]	Smoothed Yield	$\overline{DP_N}$	Relative Total End Group Concentration	Relative Reducing End Group Concentration	Relative Acid End Group Concentration
0	100.0	100.0	1835	1.00	1.00	0.00
15	99.4	98.4	838	2.15	--	--
30	98.7	96.8	568	3.13	2.02	1.11
45	95.7	95.2	539	3.24	--	--
60	93.1	93.7	607	2.83	0.54	2.29
75	92.1	92.3	723	2.34	0.41	1.93
90	89.6	90.9	659	2.53	0.37	2.16
120	87.0	88.2	592	2.73	0.24	2.49
180	82.3	83.5	565	2.71	0.35	2.36
240	78.5	79.2	522	2.78	0.12	2.66
360	72.8	72.3	435	3.05	0.20	2.85
600	65.4	62.7	316	3.64	--	--
1320	50.6	51.7	219	4.33	0.03	4.30

[a]Yield = percent by weight of the initial amylose concentration.
[b]End group concentrations = mole fraction of end groups present at zero time.
[c]Average of four determinations.